UiT The Arctic University of Norway

Faculty of Biosciences, Fisheries and Economics (BFE)

Norwegian College of Fishery Science

The effect of climate related stressors on liver in Atlantic Salmon (*Salmo salar*)

Mina Bjerke Kleiv

Master's thesis in Aquamedicine | BIO-3955 | May 2023

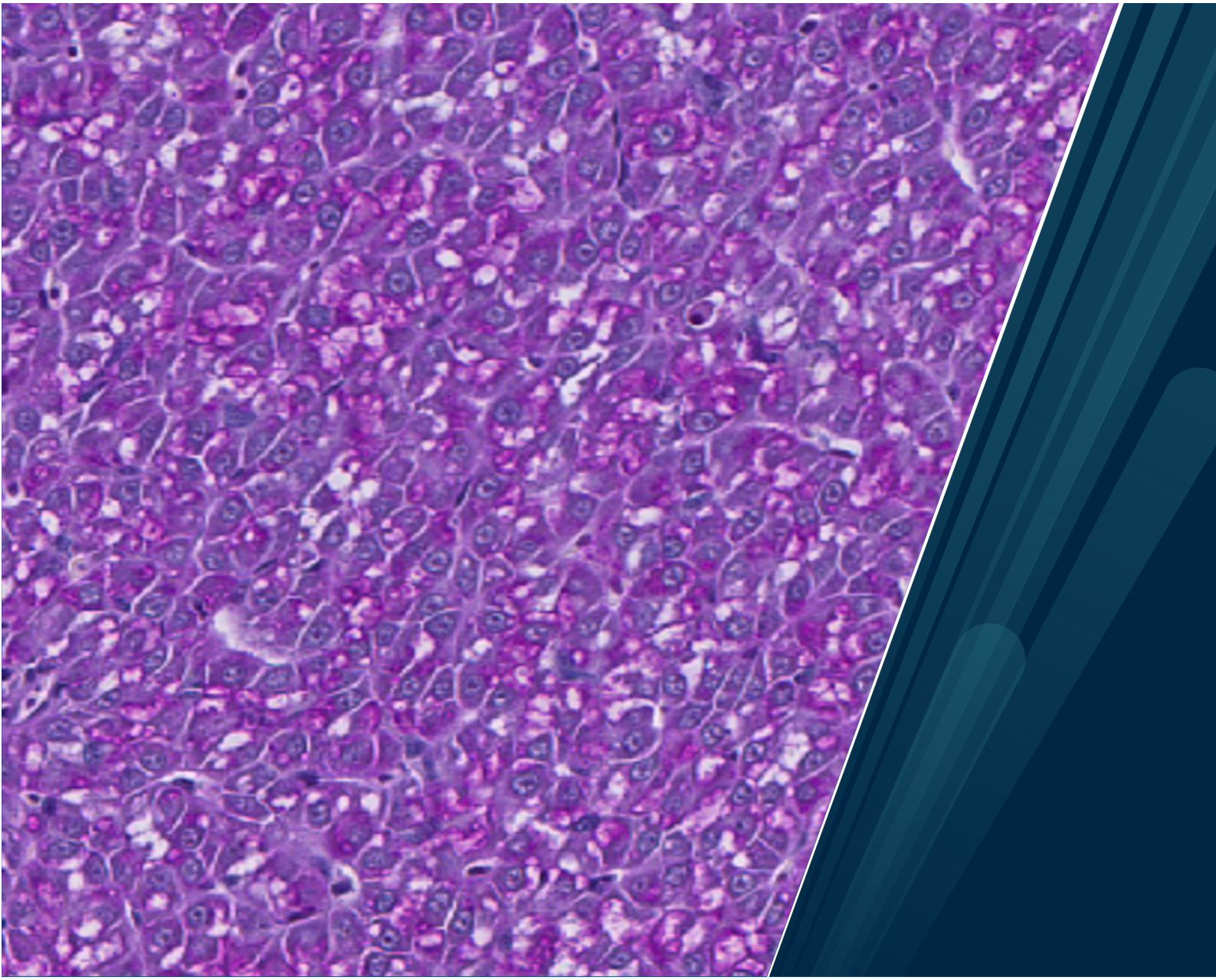

Liver tissue by Mina B. Kleiv.

Acknowledgments

This thesis was written for my master´s degree in Aquamedicine, at the Artic University of Tromsø (UiT). The study was a part of a bigger project, "*Insight*", by Nofima, focusing on climate change and the effect these changes might have on fish health- and welfare. This thesis specifically involved liver. The study is relevant in the process of generating a deeper understanding on how today's climate changes affect the Atlantic salmon farming.

Firstly, I want to thank my supervisors, Elisabeth and Carlo, for giving me the opportunity to be a part of this exciting project. You have provided me great knowledge on how to work as a researcher, and have been available when I needed your expertise, both within working hours and on your leisure time. I am truly grateful for that.

I would also like to thank Mira, for having us and taking you time in showing us how your high-quality histological slides, used in this thesis, were made. Ragnhild and Hanne, for all your help and guidance on the lab work. Gunhild, for sharing your expertise in how to cope with Aiforia®, as well as your guidance connected to all histology within this thesis. Gerrit, for your help connected to the statistical part of this thesis. Jelena, for your assistance in administration, as well as your academic guidance.

A huge thank you to Anne-Marja, for pushing and supporting me through this year. We did it.

To my family, friends, and boyfriend, thank you for comforting me at times when I felt overwhelmed, and thank you for constantly filling my everyday life with sunshine throughout this whole process. I love you to the moon and back!

Moving to Tromsø five years ago, still feels like yesterday. Five years shared with friends, fellow students, and professors at The Norwegian College of Fishery Science have come to an end. I am forever grateful for what these years have given me, both socially and academically. A new era is now about to start, as I am moving to Vesterålen, to continue creating memories in the astonishing North.

Tromsø, May 2023

Table of Contents

List of Tables

List of Figures

Abstract

Climate change impacts the average temperature in the world's oceans, as well as other environmental parameters, such as oxygen levels. These changes are threatening and challenging animals living there, including farmed species. In this trial Atlantic salmon (*Salmo salar*) were exposed to fluctuating temperature (12-17C°) as a single stressor, and in combination with lowered level of dissolved oxygen (~70%), to evaluate how combined environmental stressors affect the fish health- and welfare. The two groups exposed to environmental stressors were compared to a control group (12°C). In earlier studies, both elevated temperature and lower levels of oxygen have resulted in signs of reduced fish health- and welfare. Combining these stressors, as well as exposing salmon to a fluctuating temperature regime, can provide important knowledge connected to the affect climate related stressors may have on caged salmon, when, for example, a heatwave occurs. In this study the salmon liver was major focus, because this organ can provide important information regarding the overall health- and welfare of the fish. The parameters studied were metabolism, stress, apoptosis, and immune response, as well as growth, scale loss, and gill score. The methods used were histology and gene transcription. In addition, development of a new digital histopathological tool for salmon liver was commenced. Exposing fish to conditions simulating heatwaves, as well as lowered level of dissolved oxygen, resulted in cellular differences and morphological changes in the liver, such as reduction in lipid storage, increased amount of connective tissue, and higher occurrence of melanin spots. Further, these changes may affect the homeostatic balance in the fish, thus causing reduced health and welfare. The fish exposed to environmental stressors combined had the lowest growth-related indicators, as well as the highest score of examined welfare parameters, indicating reduced fish welfare compared to the control group. However, there is a need for further studies in order to generate more knowledge on how climate related stressors affect the Atlantic salmon, and to understand the biological effects of the changes observed in this study. Regarding the development of the digital histopathological tool for salmon liver, results from the final version showed several errors, indicating that the algorithm needs additional training. In this trial, approximately 80 hours of drawing was done in the training of the algorithm, resulting in increased accuracy in detecting the different components, and for some features, such as melanin, there were no errors in detection. Continuing developing tools like this may be useful in the evaluation on how climate change effect the liver of the fish, as changes may be difficult to observe using traditional histology.

1 Introduction

Seafood has throughout history been an important part of human consumption, and different marine species have fed and nourished an uncountable number of people (Pitcher & Lam, 2015). Through decades, people have developed methods to catch and gather different types of fish, and today the world is enriched with fisheries and aquaculture. Norway is a country with a long coastline, and this has given the people easy access to this exceptional food source.

Aquaculture is stated to have a crucial role in global food security. The Food and Agriculture Organization of the United Nations (FAO) is convinced that the methods involved in aquaculture will provide the population of the world with an increase in food supply, if handled in sustainable ways (FAO, 2020). Production of fish is essential to the fight against hunger and poverty but is now under a threat. Climate change affects and threatens the world's food production (FAO, 2021). There is no doubt that the impacts of climate change will affect today´s- and future aquaculture. Effort in knowledge development and exchange connected to this great challenge is now highly important in facilitating new adaptation methods, so that aquaculture can continue to respond to the world´s demand for food.

1.1 Salmon aquaculture in Norway

In 1969 the great "salmon farming adventure" began, with the establishment of Atlantic salmon (*Salmo salar*) farming in Norway. The Grøntvedt Brothers, located in Hitra, and Mowi A/S in Bergen, were the first to place smoltified salmon in constructed facilities in the sea (Webb et al., 2007). Two years later, the fish had grown significantly, and they could sell food that people previously had limited access to. Since then, the industry has exploded. Today, Atlantic salmon is the dominating aquaculture species in Norway, providing food and local workspaces. Further, with approximately 500 million farmed salmon spread out in cages by the Norwegian coast, salmon is the greatest livestock production in the country (Grefsrud et al., 2022). This reflects the importance of salmon farming in Norway.

In year 2021, the salmon, together with the closely related rainbow trout (*Oncorhynchus mykiss*), stood for 72% of the total value of export of seafood in Norway, at 85,42 billions NOK

(Sjømatråd, 2021). These numbers show the enormous impact the Norwegian salmon industry has on the country's economic market. Sushi is one example of a worldwide utilization of the Atlantic salmon, and this Japanese dish has provided Norway some large costumers, preferring this fish of high quality and health advantages (Rembold, 2004).

Salmon farming is established, not only in Norway, but also in other counties around the world, such as Chile, Canada and Faroe Islands (Iversen et al., 2020). Salmon farming went from being a niche industry to producing a million tons of fish worldwide as early as in 2003 (Webb et al., 2007).

Today's salmon farming usually consists of land-based facilities and open sea cages. The land-based facilities often have the ability to provide both freshwater and marine water, where salmon is kept from hatching to smoltification (physiologically developed the ability to survive in seawater). Some land-based farms also have broodstock fish, kept providing eggs for new generations. When the fish undergo smoltification, they are transferred to the sea, most commonly to open sea cages. The sea cages are constructed to give the salmon an area to develop and grow. They have multiple imposed routines and functions to provide good welfare and health for the fish. Here, the fish gets fed and taken care of until it is ready for slaughter, usually until they are 4-6 kg (Kristjánsson et al., 2020).

Atlantic salmon farming requires well-established routines to prevent diseases and ensure good animal welfare. At the beginning of salmon farming (1960s-1970s), the salmon seemed to be easily reared in cages, but only a few years later with upscaled production, diseases started to occur and limit the growth of the industry (Tilseth et al., 1991). Antibiotics were commonly used until the first vaccine was developed in 1987 (Tilseth et al., 1991). Since this breakthrough, vaccines against several pathogens have been developed with success. Unfortunately, the efficiency of the vaccines varies, and it is challenging and costly to produce (Adams, 2019). One example is the disease "winter ulcers", caused by the bacteria *Moritella viscosa.* In year 2022, there were reported several cases where the efficiency was reduced (Veterinærinstituttet, 2023). It has been suggested that this is due to a different variant of the bacteria than today's vaccine is based on. A new vaccine is under development (Veterinærinstituttet, 2023).

Today, the salmon industry is still facing problems that affect health and welfare. Diseases are still the major cause of welfare issues in the salmon industry, and an increase in bacterial, viral and parasitic have been observed in the last decades (Veterinærinstituttet, 2023). Several of

these microorganisms are expected to continue increasing, and one factor that substantiates this is higher temperatures in both fresh and marine water (Veterinærinstituttet, 2023). Salmon lice (*Lepeophtheirus salmonis*) and the amoeba *Paramoeba perurans* are examples of parasites that have a higher infection pressure in increased seawater temperature, and therefore might develop into an even bigger problem in the future (Veterinærinstituttet, 2023). Thus, parasitic and bacterial diseases are expected to increase with climate change and the warming of the ocean (Burge et al., 2014).

1.2 Climate changes and aquaculture

Humans and our existence have made an impact on the climate in the last decades, and the world is now experiencing environmental changes (Scheffers et al., 2016). The global average temperature has increased by 1°C from preindustrial levels, impacting every ecosystem on the planet, including terrestrial, marine, and freshwater systems. Record high concentrations of greenhouse gases have been detected in the atmosphere, mainly caused through burning of fossil fuels. It is not only the increased average temperature that is a detected effect of climate change. Changes in seasonal weather patterns and more extreme weather like precipitation regimes, stronger winds and storms, and heatwaves are also documented (Scheffers et al., 2016; Verspoor et al., 2007). The earth experiences more extreme weather and variations in weather, such as stronger winds or extreme temperatures. It is highly unlikely that we will manage to reduce global warming to 1.5 degrees as agreed upon in the Paris Agreement ((IPCC), 2023), and it is, therefore, necessary to prepare for the coming changes. Especially when it comes to how the impact from climate change will affect our food production system.

Documenting the effects of climate changes has become a prominent research niche in aquaculture in the last years. Climate changes, as for example increased seawater temperatures and reduced concentrations of dissolved oxygen in the water, will have an impact on all stages of salmon production (Falconer et al., 2022). Since salmon mainly is held in open net-pens and in direct contact with the environment, the fish will be directly impacted by climate changes. The environmental changes may stress the fish, as both temperature and oxygen are vital factors for good salmon growth, health, and welfare (Breitburg et al., 2018; Veterinærinstituttet, 2023). Decreased levels of oxygen might lead to hypoxia (McBryan et al., 2013). Additionally, a high

number of biological and biogeochemical cycles are depending on a certain level of oxygen to function. Increasing temperatures are for example correlated with increased rate of oxygen consumption through respiration for fish (Breitburg et al., 2018). A study implemented on wild fish, has shown that declining oxygen levels lead to noticeable changes in, for example migration, bioenergetics, and habitat compression for pelagic fish (Rabalais et al., 2014). Wild fish species can move and migrate if environmental conditions change, but farmed fish do not have this possibility. Farmed aquatic animals are kept in closed cages, without the ability to move away if conditions get unfavorable, for example if the temperature gets too high.

Marine heatwaves (HWs) are a phenomenon that brings anomalous warm seawater to an area for a limited period of time and can affect marine ecosystems (Oliver et al., 2021). Mounting evidence shows that climate change leads to more frequent and more intense HWs on land (Frölicher et al., 2018). On the other hand, there is still lack of evidence and documentation on how global warming affects HWs (Frölicher et al., 2018). We do know that there have been documented an increase in the frequency and duration of HWs over the past years (Mills et al., 2023; Oliver et al., 2018). Literature and news articles link several incidences of mortality at salmon farms, to increased temperature. One example is an event that took place on the south coast of Newfoundland and Labrador, where a sudden and prolonged increase in seawater temperature occurred (Newfoundland, 2020). This increase in temperature further led to hypoxia, which eventually caused mass mortality of farmed Atlantic salmon. The fish had gone through therapeutic treatments for sea lice before the incident took place and the condition of the fish was already reduced. Before the temperature reached 18°C, all fish died. The temperature in this trial is determined with justification in this occurrence.

How changes in environmental parameters affect the farmed fish as single stressor and in combination, is important in order to know how to adapt and respond to climate change. The stressors might affect the fish on a small scale independent of each other, but together they can cause devastating impacts on the fish (McBryan et al., 2013)

1.3 Liver tissue and its responses to temperature and oxygen saturation

1.3.1 Liver

The liver is described as the central metabolic organ in fish and is located cranially of the abdominal cavity, with the cranial part next to septum transversum. The external appearance is a large reddish-brown organ (Bruno et al., 2013). The hepatic artery and the portal vein both enter the liver (Bruno et al., 2013). The liver mainly consists of hepatocytic cells, erythrocytes, adipocytes, and bile duct. The tissue is called hepatocytic tissue and plays an important role in the regulation of nutrient metabolism and detoxification (Nuez-Ortín et al., 2018).

1.3.2 Cellular organization

The cellular organization in the liver includes tubular glands, which are built up by hepatocytes. These hepatocytes are structured around a central lumen called bile capillaries, and sinusoids are on the outer side of the hepatocytes (figure 1). There is a small space called Space of Disse between the sinusoids and hepatocytes. The sinusoids are small, thin, fenestrated blood channels that can provide the hepatocytes with substances (etc. gas exchange and nutrients absorption) (Wake & Sato, 2015). Additionally, sinusoids are involved in excretion in the liver, such as detoxifying substances (Wake & Sato, 2015). The tubular glands extend into complex networks, and these go in different directions, forming a "web" where they connect to each other in several parts. The different bile capillaries in the tubular glands assemble into bile ducts. The bile ducts are constructed with single-layered cubic/cylindrical epithelium which is surrounded by loose connective tissue and smooth muscle (Kryvi & Poppe, 2016). Connective tissue mainly consists of fibroblasts but might also hold pigment cells (such as melanin spots), macrophages, eosinophilic granulocytes, lymphocytes and adipocytes (Kryvi & Poppe, 2016).

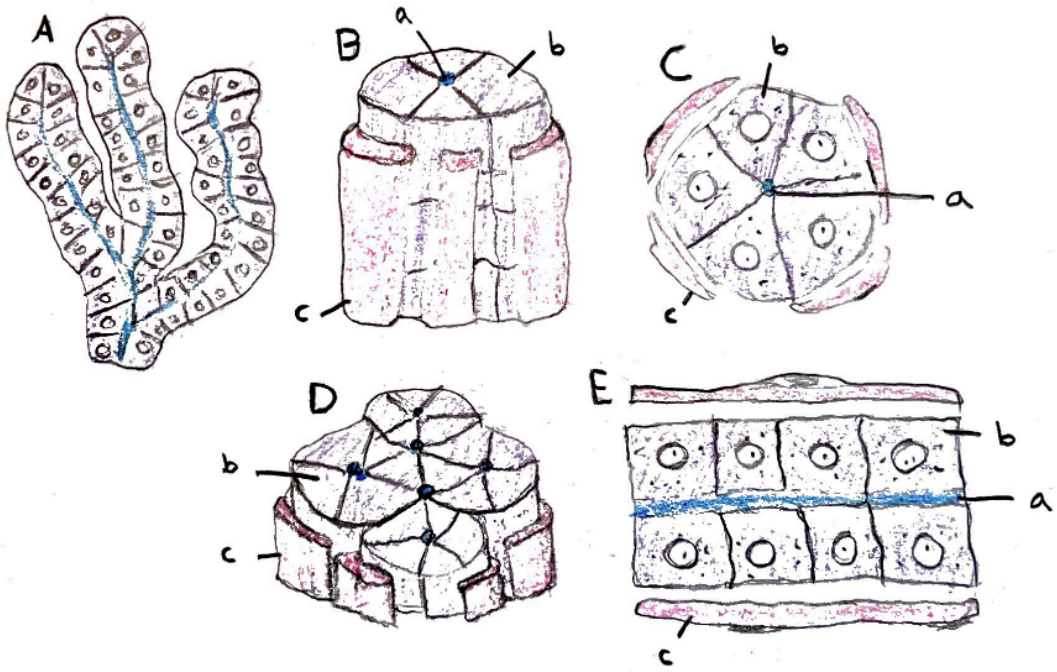

Figure 1: Drawing of cellular organization in liver. Within all figures a = bile capillaries, b = hepatocytes, c = sinusoid. A: Network of tubular glands. B: Sideview of tubular gland with hepatocytes. C: Cross-section of tubular gland with hepatocytes. D: Several tubular glands gathered in a complex. E: Longitudinal section of tubular gland. Inspiration from "Fiskeanatomi" (Kryvi & Poppe, 2016).

The hepatocytes vary in appearance, depending on the amount of fat in the liver. The Atlantic salmon has a low level of fat in the liver, resulting in hepatocytes with a spherical and centralized nucleus. The cytoplasm surrounds the nucleus and contains granular endoplasmic reticulum and glycogen (Kryvi & Poppe, 2016). Differences in liver parenchyma occur due to changes in the hepatic energy storage, consisting of lipids and glycogen (Bruslé & Anadon, 1996). The amounts of lipid and glycogen varies depending on the nutritional status of the fish or general variation (Bruno et al., 2013). Feeding activity and quality of the food are suggested as the main factors of the variations in liver energy storage (Bruslé & Anadon, 1996). In histology with Alcian blue/Periodic Acid Schiff (AB/PAS) staining, glycogen is recognized by PAS-positive affinity, while lipids are detected as empty vacuoles (Bruslé & Anadon, 1996) (figure 2). Figure 3 presents liver tissue with Martius-Scarlet Blue (MSB) staining.

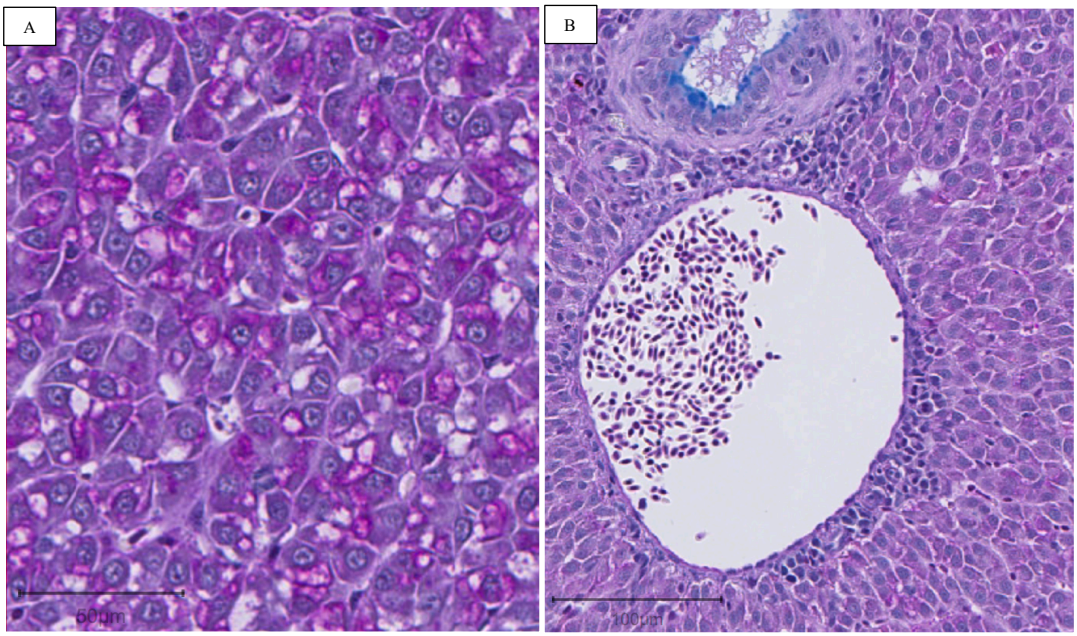

Figure 2: A: Histological picture of liver tissue, AB/PAS staining, scale bar 50µm. B: Histological picture of liver tissue, AB/PAS, scale bar 100µm, with bile duct supreme and vein with erythrocytes.

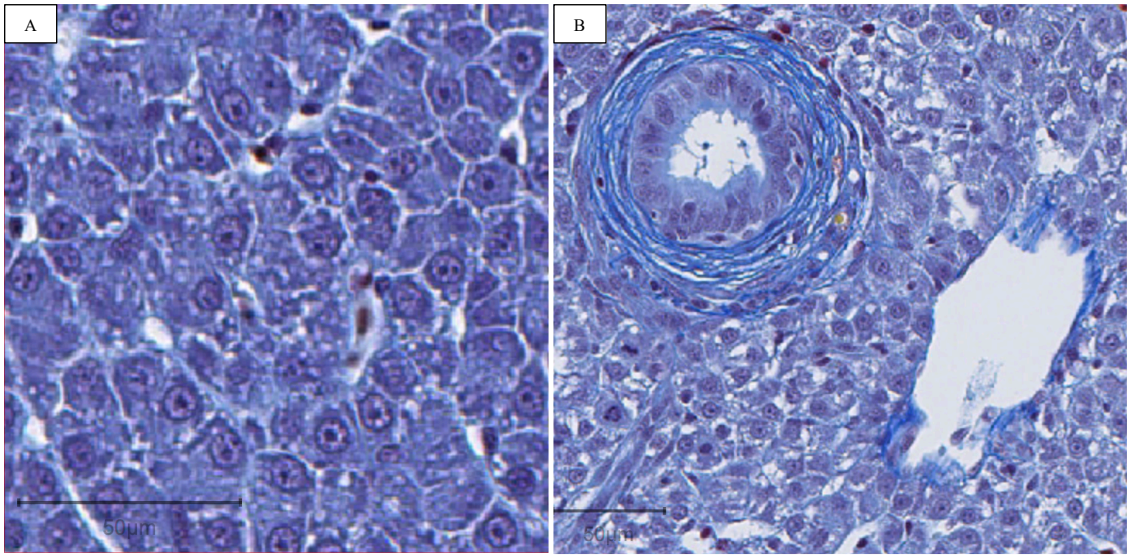

Figure 3: Scale bar on 50µm. A: Histological picture of liver tissue, MSB staining. B: Histological picture of liver tissue, MSB, with bile duct in upper left corner, and vein to the right.

1.3.3 Function

The liver is important for the metabolism in fish, and its biochemical functions can be connected to amino acid-, carbohydrate-, and lipid metabolism. Storing is another important function of the liver, and significant amount of vitamins, fat and glycogen can be found (Kryvi & Poppe, 2016). In addition, the liver produces bile fluids. Bile has the ability to emulsify fat in the intestine, and is therefore important for absorption and transport of lipids (Chiang, 2009). Detoxification also takes place in the liver, mainly involving environmental toxins (Kryvi & Poppe, 2016). The main functions in fish liver are presented in figure 4.

The human liver is known to be involved in the immune response and is described as the largest lymphoid organ (Chentoufi et al., 2014; Selmi et al., 2007). In fish, the liver often has melano-macrophage centers, which are pigment-containing cells with high density in a defined area (Agius & Roberts, 2003). They can develop in association with chronic inflammatory lesions and can contain both macrophages and lymphocytes. In the liver, phagocytosis and particular antigens play an important role in the immune system of the fish (Bruno et al., 2013). This includes specialized cells, such as the macrophages, carrying out phagocytosis (Guillot & Tacke, 2019). Additionally, lysozyme can be synthesized in the liver (Kiron, 2011). Lysozyme is an enzyme important in the innate immune system of a fish, due to the anti-inflammatory and antiviral properties (Paulsen et al., 2003), together with, for example, *il8* (Jin et al., 2010). Lysozyme also participates in activation of the complement system and phagocytes (Saurabh & Sahoo, 2008).

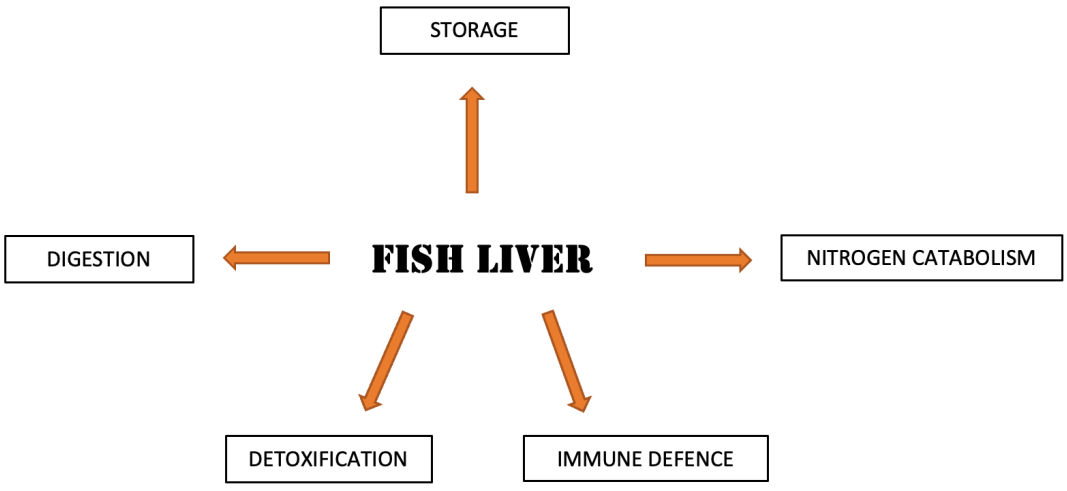

Figure 4: Illustration of main functions in fish liver. Literature from (Bruslé & Anadon, 1996).

1.3.4 Responses to stress

Salmonoid fish are ectotherms, which means that their physiology and metabolism are directly controlled by water temperature (Thorstad et al., 2021). Thus, liver is an interesting organ to study at different temperatures. An earlier study on salmon exposed to higher temperature and lower oxygen saturation resulted in liver cell metabolic decline (Olsvik et al., 2013). In the same study, heat as a stressor down-regulated genes connected to protection against oxidative stress, such as *CuZn sod* and *mnsod* (Olsvik et al., 2013). Another study on the liver in Atlantic salmon exposed to higher temperature and hypoxia showed increased gene expression of heat shock-, apoptosis-relevant and immune-relevant genes, and same as the other study, genes associated with general metabolic responses were largely suppressed (Beemelmanns, Zanuzzo, Xue, et al., 2021).

In an experiment executed on redheaded bunting (*Emberiza bruniceps*), liver was exposed to higher temperatures (38°C), resulting in increased expression of genes involved in the gluconeogenesis and lipolysis (Sur et al., 2019). Gluconeogenesis involves provision of glucose when there is limited access to carbohydrates, for example during starvation, to provide energy (Exton, 1972). Lipolysis catabolism of stored fat in liver tissue provides tissues with fatty acids, which can be used as metabolites and energy substrates (Zechner et al., 2005). Greater than 95% of oxygen consumed by fish is used in ATP production, aerobic catabolism (Richards, 2009). Lack of oxygen will lead to anaerobic catabolism, and ATP can only be generated through glycolysis yielding lactate production (further to gluconeogenesis as gluconeogenic precursor) or through direct phosphate transfer from phosphorylated intermediates (etc. creatine phosphate) (Emhoff et al., 2013; Richards, 2009).

There are several studies on changes in liver, however there is still a need for further understanding on how fish liver responds to environmental changes, such as temperature and oxygen. In earlier studies, research on heat-shock and oxidative stress responses in liver have been limited to transcriptional changes (Beemelmanns, Zanuzzo, Xue, et al., 2021; Olsvik et al., 2013). Taking advantage of other methods in addition, such as histology, can result in greater knowledge on how these stressors affect the fish. Further, acute heat stress and constant heat exposure have been the most common exposure through studies (Nuez-Ortín et al., 2018; Shi et al., 2019). Studies with exposure to fluctuating temperatures are available (Raina et al., 2015), but the amount is limited compared to acute- or chronic heat stress. The liver is highly

important for the metabolism in fish and can provide important information on the health and welfare, when exposed to climate related stressors (Bruslé & Anadon, 1996). Thus, responses should be better documented.

1.4 Aim of study

The aim of this study was to get a better insight into how climate related stressors affect the health of Atlantic salmon, with specific focus on the liver. Many studies have explored prolonged exposure of salmon to higher temperature and the effect of single stressor, while few studies include fluctuating temperature conditions or the effect of combined stressors. With increasing occurrence of heatwaves in the ocean, there is a need for a better understanding of how these environmental changes affect the fish health- and welfare.

The objective of this study was to generate new knowledge on how fluctuating temperatures affect the salmon liver alone, and in combination with lowered levels of dissolved oxygen. This study had three sub-objectives:

- Evaluate how different temperature regimes and oxygen levels affect liver status and chosen welfare operational welfare indicators
- Evaluate if there is a difference between effect of single and multiple stressors after returning from high temperatures
- Develop a new digital histopathological tool for salmon liver

The main hypothesis of this study was that fluctuating temperatures and reduced oxygen levels have compounding effects on Atlantic salmon, and that cellular differences and morphological changes can be observed in the liver.

2 Materials and Methods

Climate-related factors were emphasized when this trial was designed. The importance to not only expose fish to constant higher temperatures but illustrate other protentional threats and multiple stressors that can affect fish welfare and health, such as marine heatwaves and decreasing oxygen. This experiment was designed to give an insight on the impact climate change, and the potential cascading effects, can have on farmed Atlantic salmon, by exposing fish to optimal (12°C) and fluctuating (12-17°C) thermal condition. One group were additionally exposed to water with reduced concentration of dissolved oxygen.

To evaluate the impact caused by different stressors in fish health, it is important to use a wide specter of different approaches in order to capture molecular and cellular changes. To detect comprehensive changes, looking at both transcriptional- and histological levels gives a greater understanding of the effects. Research on transcriptional level with qPCR (quantitative polymerase chain reaction) is an effective way of detecting genes, while looking at histological slides detect changes in tissue. Today, analysis of histological slides can be done both physically in microscope and software's for bioimage analysis (etc. QuPath (Bankhead et al., 2017)), but also digitally with trained algorithms. Aiforia® (aiforia.com) is a digital pathology company, who provide artificial intelligence software that can be trained to detect changes in tissue, as well as present quantitative cell-data. Studies on fish health and welfare can use this platform, and it will provide the research with several new possibilities.

2.1 Ethical statement

The described study was approved by the Norwegian Food Safety Authority (FOTS ID 29728) and conducted in accordance with the regulations controlling experiments and procedures for live animals in Norway.

2.2 Fish trial

Post-smolt Atlantic salmon (Salmo salar) from NRS Settefisk Dåfjord, located on Ringvassøya (Tromsø, Norway) were used in the trial. In the hatchery, the temperature was 6-8°C during first-feeding, and then 12°C until smolt. All fish were vaccinated with Alfa Ject 6-2 (Pharmaq, Norway) before being transferred to the Tromsø Aquaculture Research Station (Havbruksstasjonen) in Indre Kårvika, owned by Nofima and UiT (The Artic University of Tromsø). At transfer to seawater, they had a starting weight of 70-80 grams (g). At Kårvika, the fish were divided into six 500 liters (L) tanks, flow through, with 100 individuals in each tank, and acclimatized for three weeks before the trial started. All fish were continuously fed with Skretting feed, type Olympic 3 millimeter (mm).

The fish were divided into three groups, with duplicated tanks of fish in each group. Group one was the control group and had a stable temperature on 12°C with optimal oxygen-level (>90%). Group two and three were exposed to fluctuating temperatures (to mimic HWs), where the temperature was raised from 12°C to 17°C with an interval of five days at 12°C: five days to reach 17°C, 10 days stable at 17°C and five days to reach 12°C again. In the second group, oxygen level was held optimal (>90%), in the third group, reduced level of dissolved oxygen (DO) (~70%) was introduced each time the temperature reached 17°C. Hereafter referred to as "Control/12°C", "HW/17°C" and "HW+DO/17+DO".

Five fish from each tank were sampled at every sampling point, illustrated in figure 5.

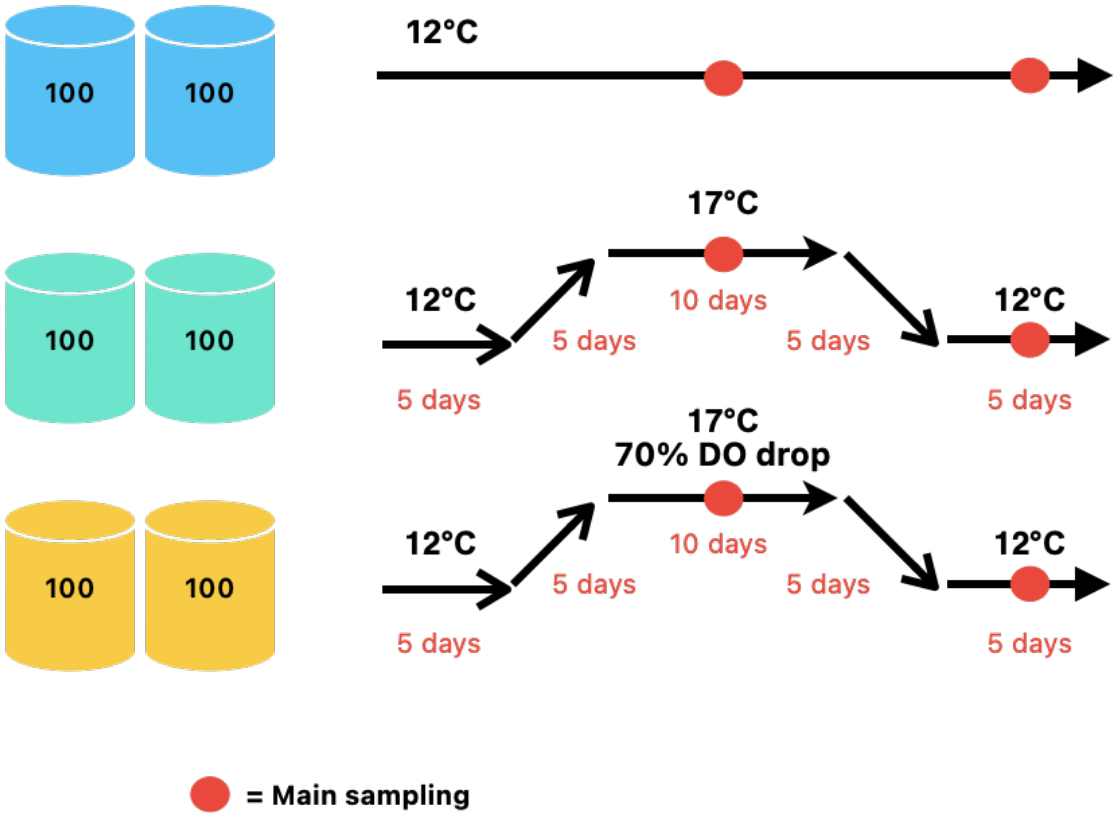

Figure 5: Overview of the trial, with sampling points (red dot). Illustration created in Apple Freeform.

2.3 Tissue sampling

The tissue sampling took place at Tromsø Aquaculture Research Station (Havbruksstasjonen), where the fish were held. It was sampled tissue for both histological and gene transcription analyses.

During sampling, five random fish from each tank were first placed in a bucket filled with water and an overdose of Benzocaine, according to the manufacturers protocol (ACD PHARMA, Norway). In order to maintain good quality of the samples, it was important to work quickly after the fish was killed. Length and weight were measured for each fish. Additionally, left-side scale loss, right-side scale loss, and gills, were scored on a scale 0-3, where 3 was the worst. The scoring system on scale loss was from FISHWELL (Noble et al., 2018), where fish with loss of several single scales or a few spots of scale loss was given Score 1, several small spots of scale loss or a few larger areas of scale loss was Score 2, and Score 3 was great scale loss where comprehensive areas of the fish had clear scale loss. The scoring system of gills was from H2Salar project, modified from the Laksvel scoring manual (Nilsson et al., 2022). Score 1 indicated signs of change on gills that might could give some reduction in gill function, Score 2 indicates clear changes on up to 50% of the gill tissue, and Score 3 was given gills with great changes (>50% of gill tissue affected).

Tissue sampling was done by placing the fish with the right side down on a cutting board, with the dorsal part pointing away from the sampler. The cranial part was placed on a piece of paper, so that the fish would not be so slippery during the cutting. The tissues that got sampled were skin, gills, olfactory organ, liver, spleen, head kidney, heart, and intestine, in the written order, and all the different tissues were sampled for RNA extraction. Skin, gills, olfactory, liver, heart and intestine were sampled for histology in addition. Only the sampled liver is relevant for this master´s thesis, while the other samples are a part of a bigger project, *Insight* (Norwegian Research Council, grant agreement #194050).

Samples for RNA extraction were placed in a 2.0 milliliter (ml) micro tube (SARSTEDT, Germany) filled with 1 ml RNAlater solution (Invitrogen, Waltham, MA, USA). Samples in RNAlater were kept at 4°C overnight, before being stored at -80°C until use. Samples for histology were carefully placed in pre-labeled 20-mL pots containing 10% buffered formalin (CellStor, CellPath, Newtown, UK) and stored at 4 °C until use.

The abdominal cavity of the fish was opened by a scalpel (PARAGON®, Sigma-Aldrich, St. Louis, MU, USA) and scissor, and it was important not to damage any of the organs on the inside. Especially the pyloric caeca and the intestine were important not to puncture, because of danger of contamination due to degrading enzymes and bacteria present in these organs. The liver was sampled by using the scalpel to cut a small part off the tissue for RNAlater fixation, and a bigger part (approximately 0,5 centimeters (cm)) for histological fixation (figure 6).

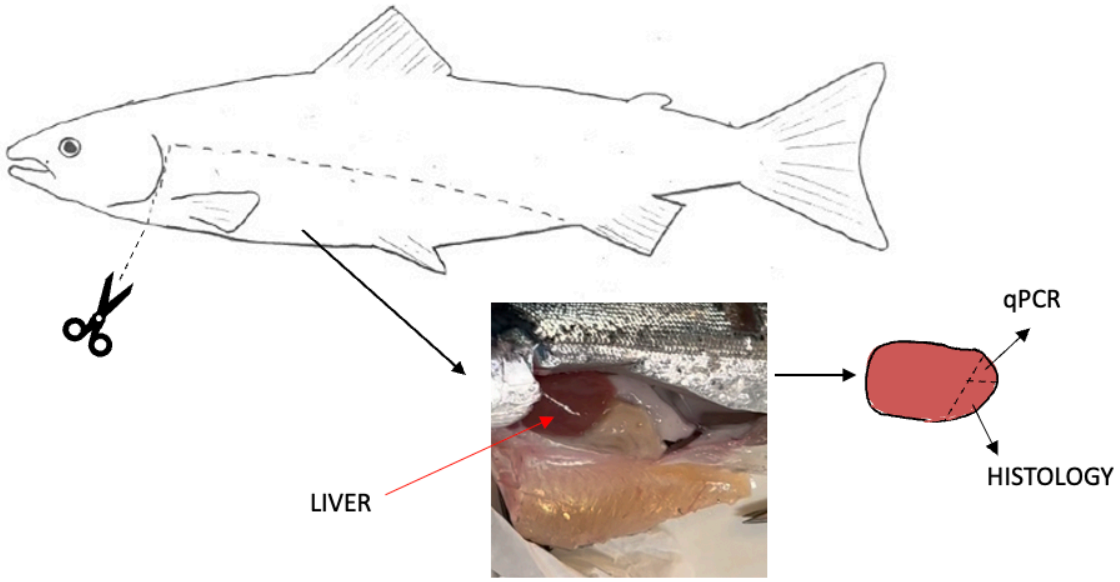

Figure 6: Sampling of liver for transcriptional analysis and histology. The part of tissue for histological fixation was approximately 0,5 cm.

During the sampling gloves and scalpel-blade were changed between each fish, and the other equipment was cleaned with 70% Ethanol (Merck, Rahway, NJ, USA) including the cutting board. This was done to prevent contamination.

There were two sampling days with nine days apart. Sampling 1 was from Peak, where the fish were exposed to a higher temperature (17°C). This was done 1. November 2022. Sampling 2 was from Return, where the temperature was regulated back to 12°C. This sampling was done 11. November 2022.

2.4 Histology

The process from tissue to histological slide involved trimming of tissue, dehydration, wax-infiltration, embedding of samples, sectioning, and staining, and this was done at Norwegian Veterinary Institute (Harstad, Norway).

Tissue preparation and embedding

The process started with the cassettes (Simport™ Scientific Histosette™, Quebec, Canada) being labeled with a Signature® Cassette Printer (Primera, Plymouth, MN, USA). Prior to embedding, tissue was prepared for histology through several steps. First, samples were taken out of the formalin, trimmed to appropriate size, and placed in a labeled embedding cassette. Before the sample could be prepared in a wax-block, the tissue needed to go through a dehydration process to remove formalin, followed by getting infiltrated with paraffine wax (HISTOWAX®, Histolab Products AB). This was done with the machine Logos Microwave Hybrid Tissue Processor (MILESTONE, Italy).

The program was finished during the night, and the steps and chemicals that were included in the process were 10% formalin, 70% ethanol, absolute alcohol, 99% isopropanol, and paraffin wax. The chemicals and time exposed are illustrated in table 1.

Table 1: Steps and time exposed, Logos Microwave Hybrid Tissue Processor

Chemical	Time
10% Formalin	Adapted machine
70% Ethanol	3-5 minutes
Absolute alcohol	55-60 minutes
Isopropanol	1,55-2,25 hours
Paraffin wax	2,3-4,0 hours

Embedding samples in paraffin wax was the next step in preparation of histology samples, and for this a heated paraffine embedding module (Leica EG1160) was used. The wax used was from HISTOWAX® (Histolab Products AB, Gothenburg, Sweden) and metallic trays were used in the making of blocks. The sample was first placed in the metallic tray and wax was added to the tray. Then the sample was gently pressed down in the tray with a metallic plate and the cassette was placed on top. Extra wax was added to fill up. The temperature held through this process was 60°C, but the metallic tray with sample, wax, and cassette, was quickly moved to a cooling plate when finished. This was to prevent the tissue from changing position in the wax and to avoid the wax spreading. When the blocks were congealed (after approximately 15 minutes), the paraffin blocks were taken out of the metallic tray and redundant wax was trimmed.

Sectioning of the blocks were done with a microtome (Leica RM2255, Germany). This process was done with the blocks first placed on ice to make them easier to work with (more solid) and then the samples were trimmed down by cutting thicker slices (approximately 18 micrometer (µm)) to get to the tissue inside the paraffine wax. The microtome was then tuned to cut 2µm slices that were immediately put on a Tissue Flotation Bath (medite – medizintecknik, Germany) at 43°C. Then the slice was gently transferred to pre-marked microscope slides (Klinipath, The Netherlands). The slides were dried at 37°C over night.

Pictures from tissue preparation, embedding and sectioning are presented in figure 7.

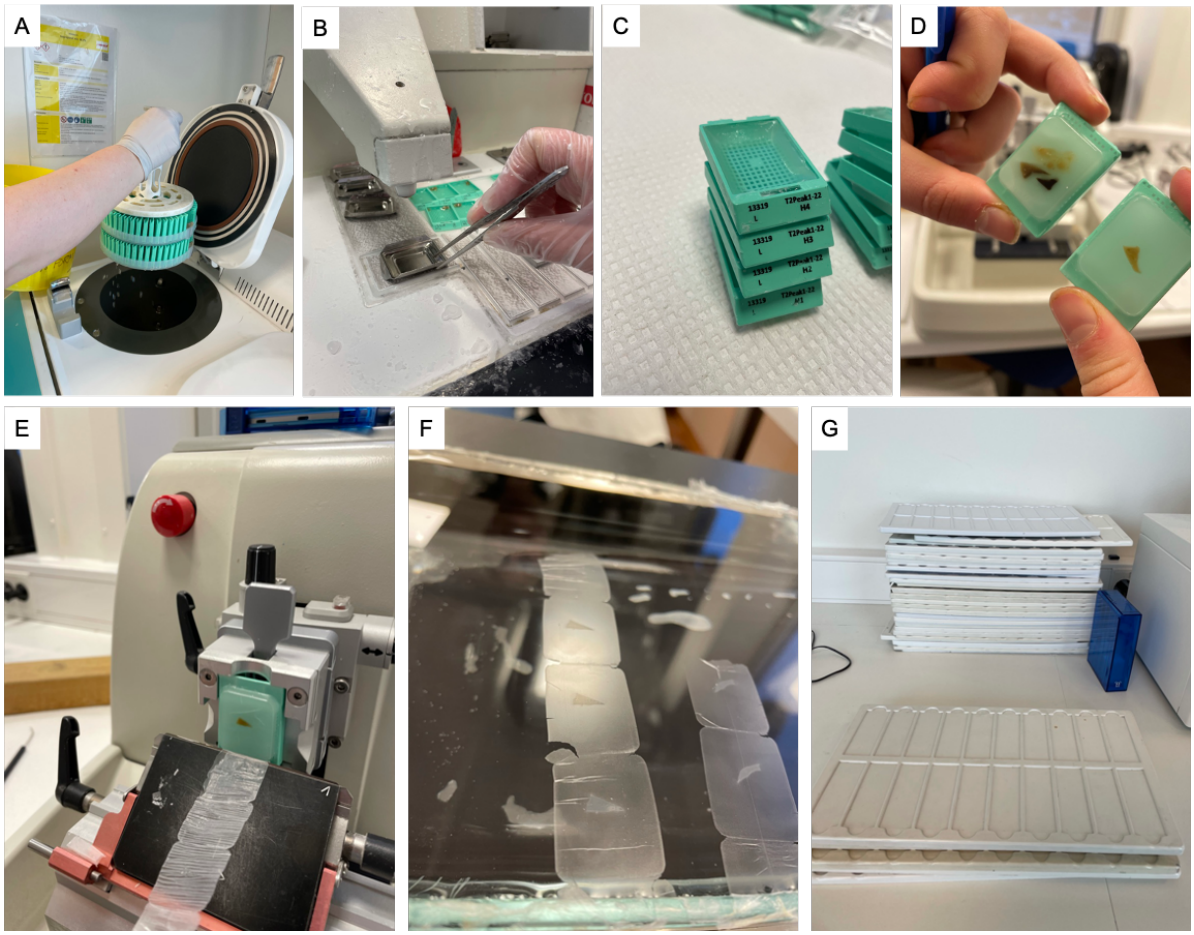

Figure 7: Pictures from tissue preparation, embedding and sectioning. A: Dehydration process in the machine Logos Microwave Hybrid Tissue Processor. B: Embedding in heated paraffine embedding module. C and D: Trimmed wax blocks with liver tissue, ready for sectioning. E: Sectioning of a block with a microtome. F: 2µm slices put on a Tissue Flotation Bath, ready for transferring to microscope slides (G).

Alcian blue/Periodic Acid Schiff (AB/PAS) staining

Staining with Alcian blue/Periodic Acid Schiff (AB/PAS, pH 2.5, Alcian Blue 8GX, Sigma-Aldrich) was done with Tissue-Tek Prisma® *Plus* (Sakura, The Netherlands), while Martius, scarlet and blue staining (MSB) was done manually. The AB/PAS staining was done by incubating the slides at 60°C, followed by a drying process to remove wax. The drying/dehydration process included xylene, absolute alcohol, 95% alcohol and 70% alcohol. The slides were rinsed in water and this was done between all the following steps: Alcian Blue, Periodic Acid, Schiff´s, Heamatoxylin, Blaaning, and Hydrochloric acid. The staining ended with wash station, alcohol 70%, alcohol 90%, absolute alcohol and xylene. The full AB/PAS program is presented in table 2, with time held in tray.

Table 2: AB/PAS staining program with steps and time. All steps were carried out at room temperature.

STEP	TIME
Xylene	10 minutes
Absolute alcohol	5 minutes
Alcohol 95%	45 seconds
Alcohol 70%	45 seconds
Wash Station	2 minutes
Alcian Blue	15 minutes
Wash Station	2 minutes
Periodic Acid	10 minutes
Wash Station	10 seconds
Schiff´s	15 minutes
Wash Station	5 minutes
Heamatoxylin	30 seconds
Wash Station	1 minute and 30 seconds
Blaaning	1 minute
Wash Station	45 seconds
Hydrochloric acid	2 seconds
Wash Station	35 seconds
Alcohol 70%	10 seconds
Alcohol 95%	10 seconds
Absolute Alcohol	10 seconds
Absolute Alcohol	15 seconds
Absolute Alcohol	15 seconds
Xylene	10 seconds

Martius-Scarlet Blue (MSB) staining

This staining was done manually, except for the deparaffinization, which was done with Tissue-Tek Prisma® *Plus* (Sakura). The technique and procedure was done as written in the book "Theory and Practice of Histological Techniques" (Bancroft & Stevens, 1990), in brief deparaffinization, Alcian blue, Celestine blue-hematoxylin, Martius yellow, Brilliant crystal blue, 1% phosphotungstic acid, Methyl blue, dehydration, and permanent mounting medium. The full MSB-staining program is presented in table 3, with time exposed and method.

Pictures from the MSB-staining are presented in figure 8.

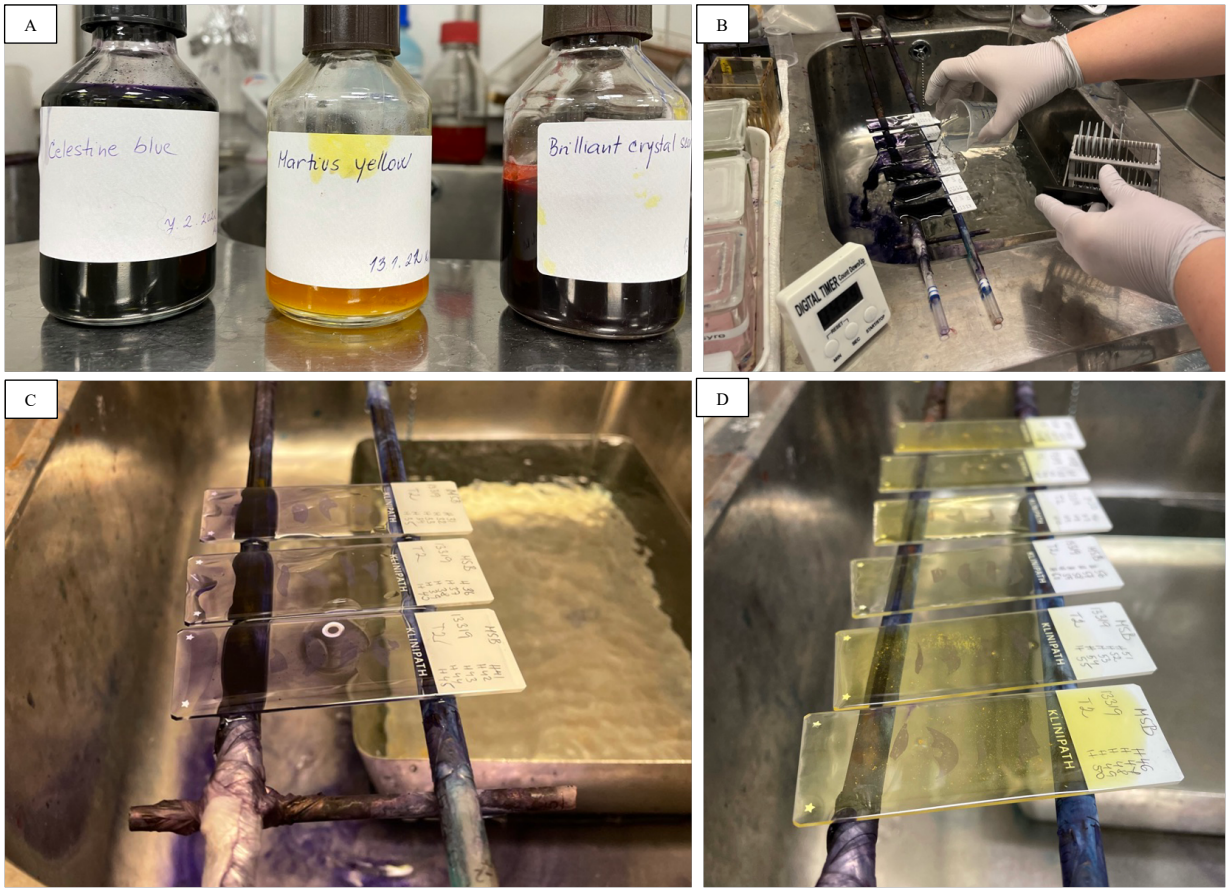

Figure 8: Pictures from MSB-staining. A: The staining colors Celestine blue, Martius yellow, and Brilliant crystal scarlet. B: Rinsing with water. C: Slides with 1% acid alcohol. D: Slides inflicted with Martius yellow.

Table 3: MSB-staining with step, time, and method

STEP	TIME	METHOD
Xylene	10 minutes	Tissue-Tek Prisma® *Plus*
Absolute alcohol	5 minutes	Tissue-Tek Prisma® *Plus*
Alcohol 95%	45 seconds	Tissue-Tek Prisma® *Plus*
Alcohol 70%	45 seconds	Tissue-Tek Prisma® *Plus*
Wash Station	2 minutes	Tissue-Tek Prisma® *Plus*
Alcian Blue	15 minutes	Tissue-Tek Prisma® *Plus*
Wash Station	2 minutes	Tissue-Tek Prisma® *Plus*
Celestine blue-hematoxylin	5 minutes	Manually
1% acid alcohol	Rinse	Manually
Water	~ 10 minutes	Manually
Alcohol 95%	Quick rinse	Manually
Martius yellow	2 minutes	Manually
Distilled water	Quick rinse	Manually
Brilliant crystal scarlet	10 minutes	Manually
Distilled water	Quick rinse	Manually
1% phosphotungstic acid	5 minutes	Manually
Distilled water	Rinse	Manually
Methyl blue	2 minutes + 2 minutes	Manually
1% acetic acid	Rinse	Manually
Dehydration through ascending grades of alcohol	Rinse	Manually
Xylene	Rinse	Manually
Permanent mounting medium		Manually

After finished staining AB/PAS and MSB, all slides were scanned to computer-format with the machine NanoZoomer S360 (Hamamatsu, Shizuoka, Japan). This gave easy access to the histological slides, via the computer program QuPath (Bankhead et al., 2017).

2.4.1 Manual histological scoring

Manual scoring was done by looking at the scanned slides with the help of the computer program QuPath (Bankhead et al., 2017), where slides could be zoomed in to simulate 40x in a physical microscope.

A scoring-system was developed for the slides stained with both AB/PAS and MSB. The slides were scored on connective tissue, adipocytes/vacuoles, steatosis, and melanomacrophage centers (melanin spots). The scale was 0-4, where 4 indicated the highest amount and 0 absence (figure 9). Vacuoles and melanin spots were scored in an area of ~35000µm, example in figure 11, where the sample was scored 1 in vacuoles and 3 in melanin spots. Connective tissue was scored on both overall view (figure 9) and thickness (figure 10). The thickness was measures on slides with MSB-staining, in Qupath (scoring system in figure 10, example illustrated in figure 12). The overall view was scored on slides with AB/PAS staining. Steatosis was scored with percentage present (%), illustrated in figure 13.

Scoring system AB/PAS

The scoring is done in an area of ~35000µm

	Connective Tissue	Vacuoles + melanin spots	Steatosis
0	None	None	None
1	Some	Few	25 %
2	Clear connective tissue formation	Several	50 %
3	Thick formation	Several on small area	75 %
4	Massive	High amount	Full

Scoring system MSB

Connective tissue, thickness

Score 1 = <6 µm
Score 2 = 6-10 µm
Score 3 = > 10 µm

Figure 9 and 10: Scoring system AB/PAS staining (9). Scoring system MSB staining (10)

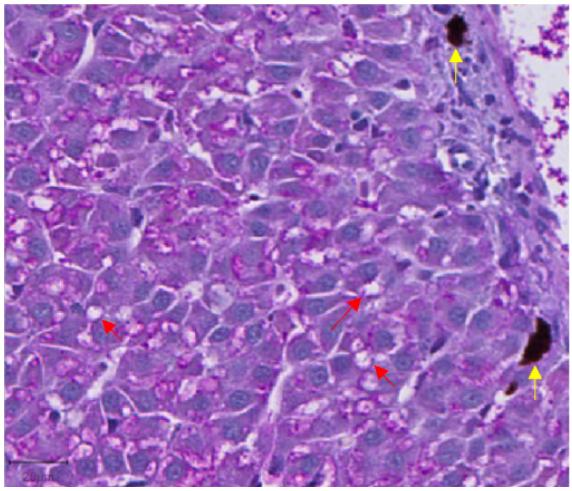

Figure 11: Histological liver sample (AB/PAS staining) given score 1 in vacuoles and 3 in melanin spots. Red arrow represents examples of vacuoles. Yellow arrow indicates example of melanin spots.

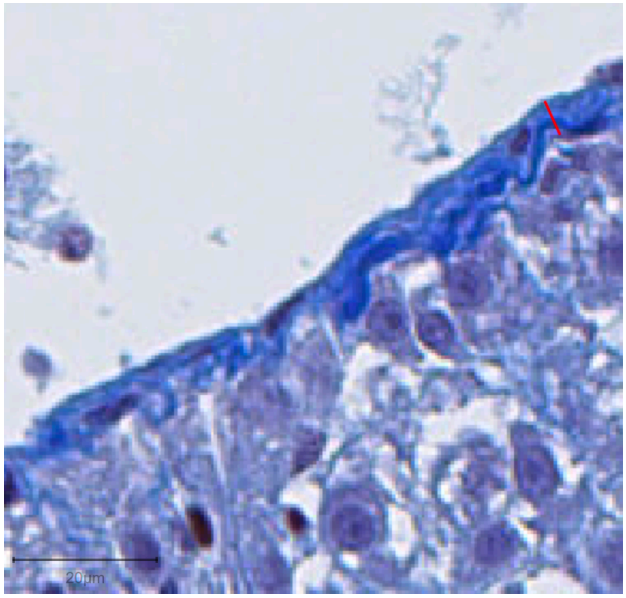

Figure 12: Histological liver sample (MSB-staining). Example on scoring of thickness on connective tissue. Red line is measured area, with the length 4,9µm, which gives score 1.

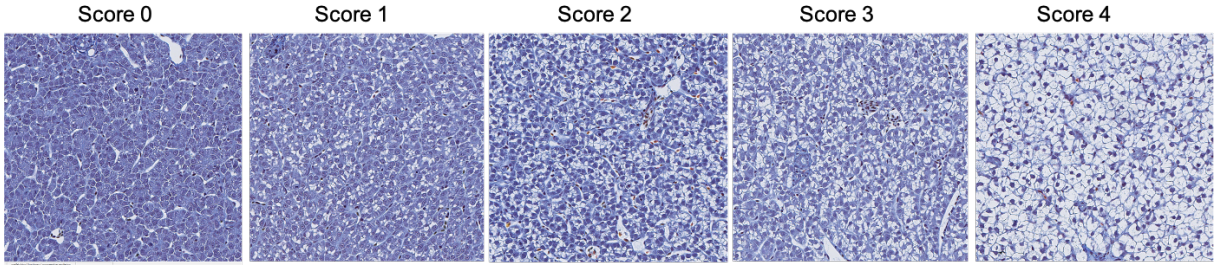

Figure 13: Histological liver samples (MSB-staining). Examples on scoring of steatosis, where it was given score 0-4. Ascending order from left to right (0, 1, 2, 3 and 4).

All scorings were controlled by an internal histopathologist, to quality check the results.

2.4.2 Development of a liver algorithm for digital histopathology

Aiforia® (AI) is a digital platform for image analysis, that gives the possibility to translate images into discoveries, decisions, and diagnoses (aiforia.com). The program includes an artificial intelligence model (AI-model) that may be trained to recognize color and pattern from images. AI was used as a digital counter and cell-estimator, where algorithms first were trained by manual drawing/marking of tissue and cells, before running all the slides with the algorithms.

Twelve out of the 60 scanned histological slides (AB/PAS) were uploaded to the Aiforia® cloud-based management platform, to train the algorithm. These slides were chosen because of a variation in fat and color, detected through manual scoring. Drawing of annotations and training regions was next step, and the focus areas through this process were to create a high repertoire of training areas, thus train the algorithm to give precise markings, thereunder differentiate between constructures and cells within the tissue and the tissue itself. Figure 14 shows liver tissue in AI where different components are pointed out with arrows (orange = melanin spots, green = glycogen, and yellow = macro vesicular fat).

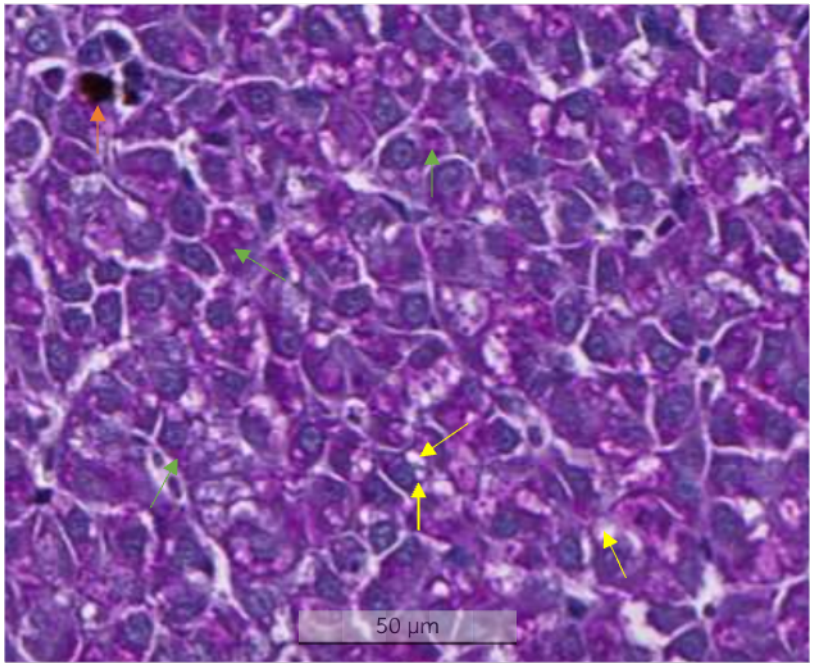

Figure 14: Screenshot of liver tissue in AI. The arrows point out examples of the different components in liver tissue, where orange = melanin spots, green = glycogen, and yellow = macro vesicular fat.

Figure 15 is a screenshot of the first step in the drawing process. This is the “first layer” (layer 1) out of three layers and these layers gave the algorithm different sections to learn. Layer 1 was for marking overall tissue, and in figure 15 the brown “boxes” is marked tissue while the black markings is the training area. The training area is where the data technology creates and trains the algorithm.

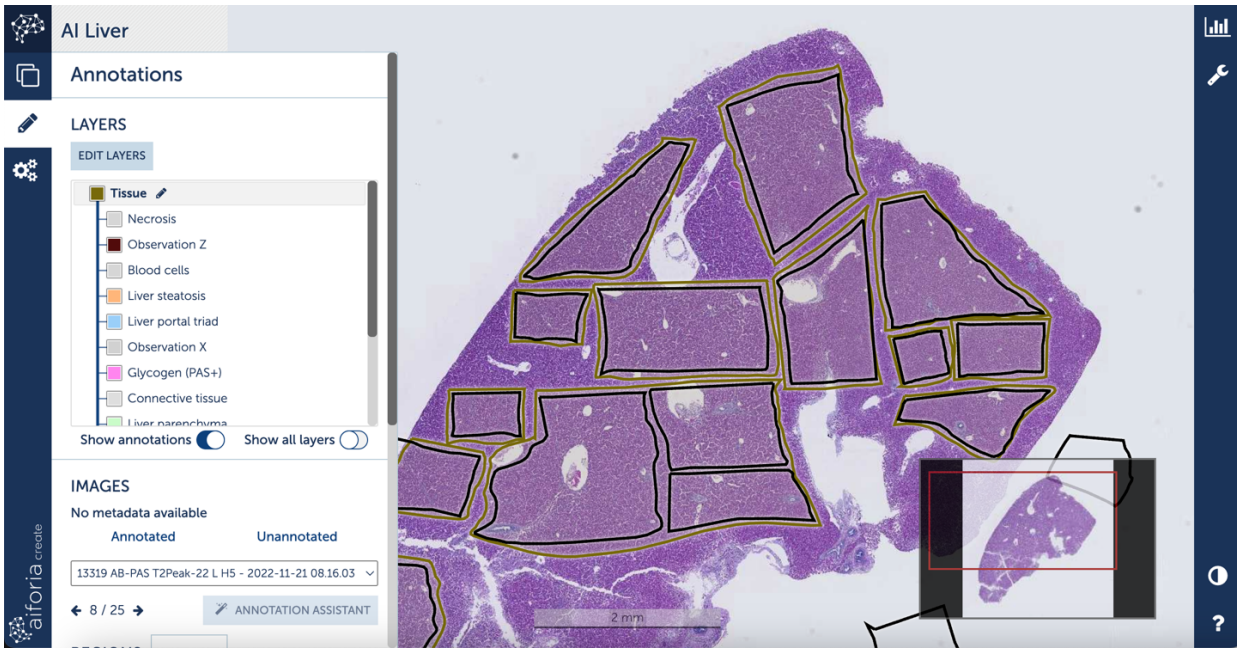

Figure 15: Layer 1, AI Liver. Marking of tissue.

Layer 2 included marking of liver parenchyma, liver portals, blood vessels, glycogen, melanin spots (Observation Z in the figures) and liver steatosis. Figure 16 and 17 shows markings on layer 2. The black markings are training areas.

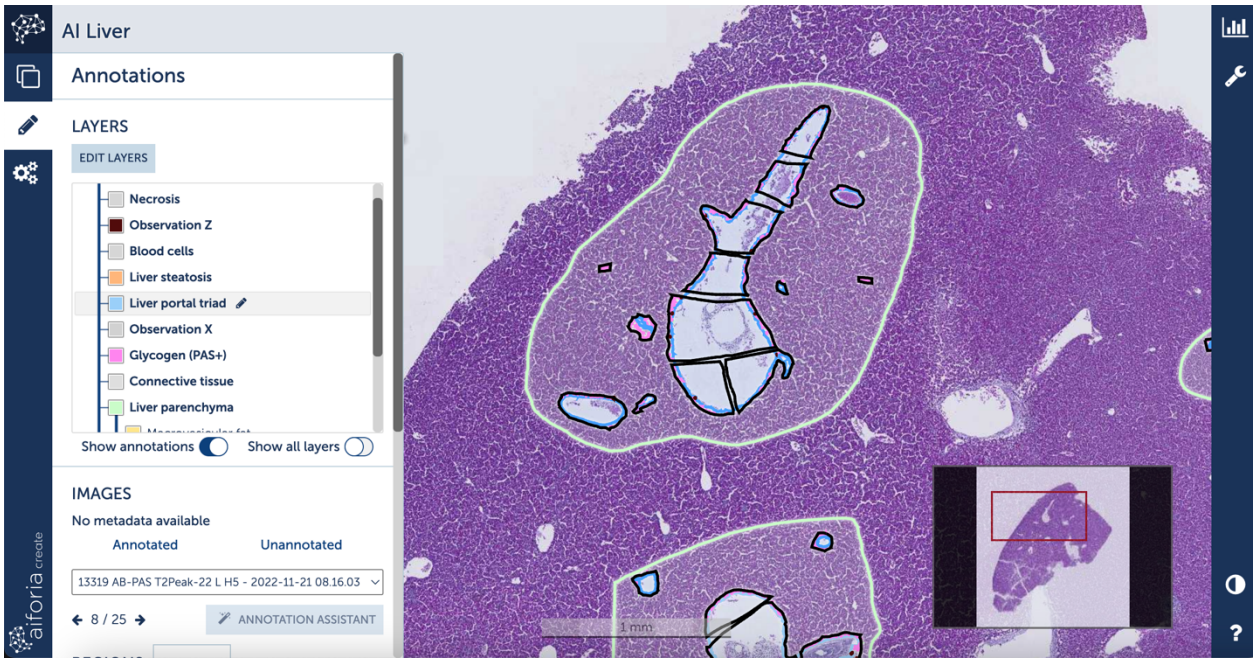

Figure 16: Layer 2, AI Liver. Marking of liver parenchyma, liver portals, blood vessels, glycogen, melanin spots (Observation Z) and liver steatosis.

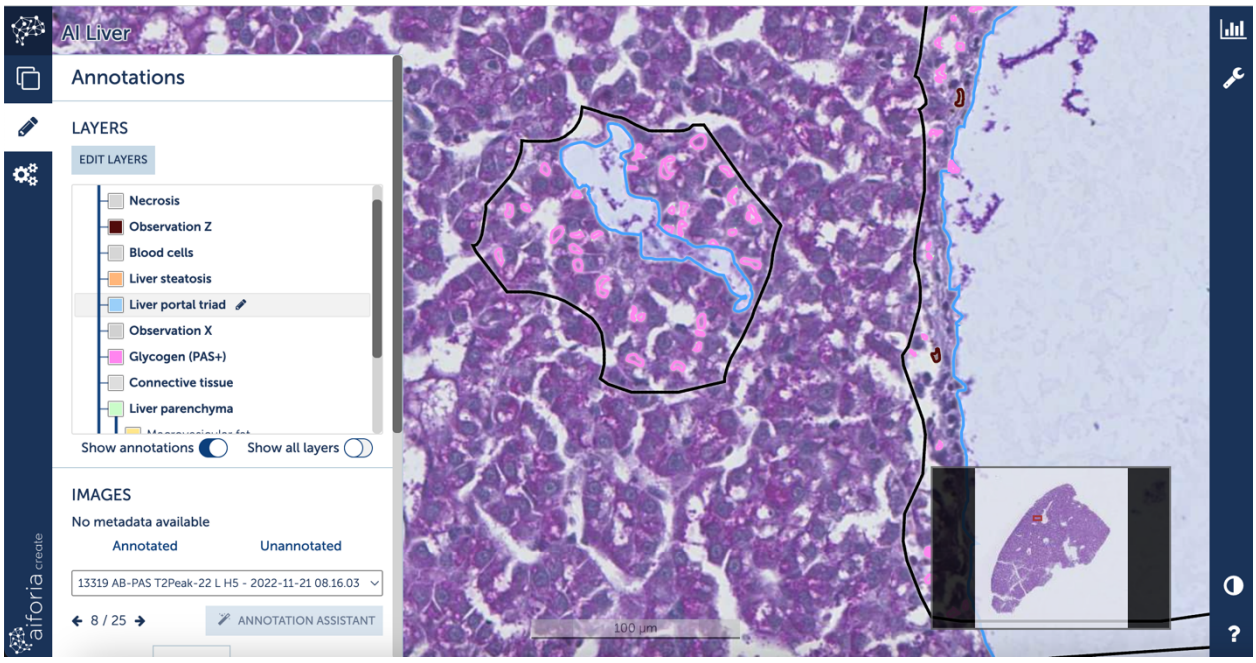

Figure 17: Layer 2 (zoomed), AI Liver. Marking of liver portals, blood vessels, glycogen, and melanin spots (Observation Z).

Layer 3 was marking of macro vesicular fat (vacuoles). In figure 18 it is drawn one training area with five markings (yellow).

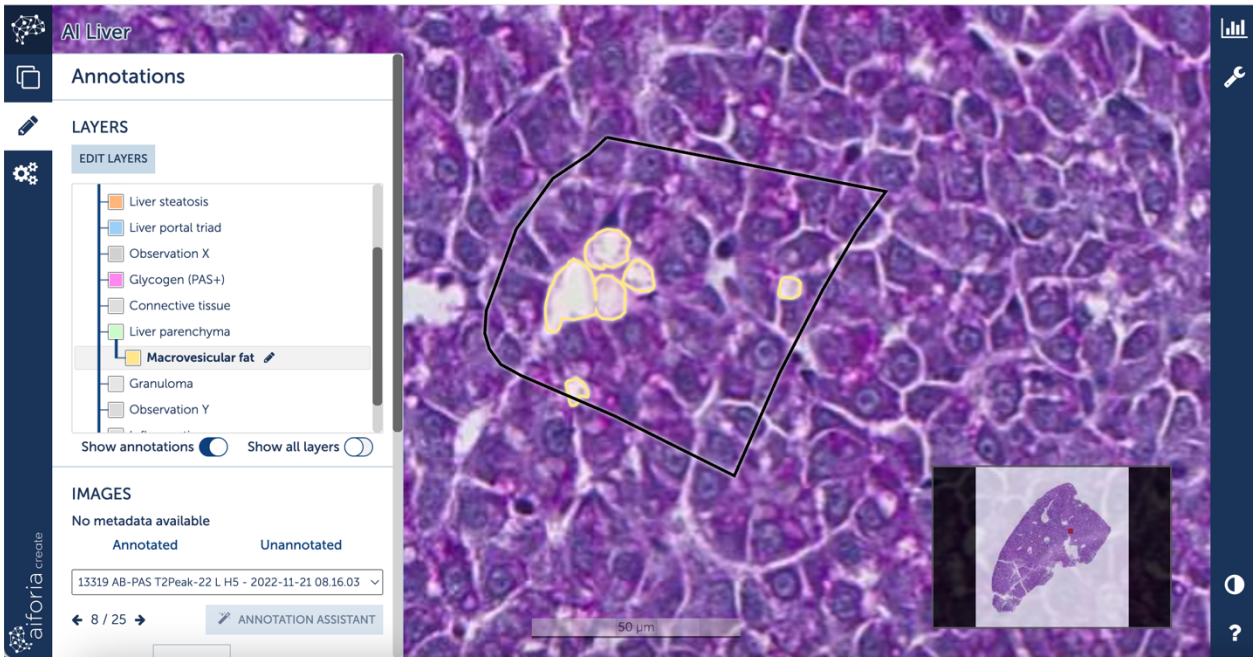

Figure 18: Layer 3, AI Liver. Marking of macro vesicular fat.

After drawing the training areas in all three layers, on all twelve slides, a test run was carried out to give an estimate on how correct the algorithms were working. This process was automatic. The results exhibited validation with a total area error (%) in the different layers, on each slide, and indicated if the drawing was approved or if it needed correction. A manual correlation/inspection was also done after each training, to evaluate where to focus on further training. Two test runs were done before the % error was low enough to run an analysis. The amount of training areas within each run is presented in table 4.

With good results on the test run, an analysis of all 60 slides could be done. Regions of interest (ROI) were manually drawn in each slide, and the analysis was done within each ROI. This analysis used the trained algorithms to detect the different components of the liver tissue, and present diagnostics that further could be used to compare the different histological slides. This was a development of a new algorithm on fish liver, and the first analysis did not exhibit results with high accuracy (assessment done by manually controlling the detections within the ROIs). To develop it further, more manually drawing of training area was done. When finished, a new test run was done (version 5, table 4), followed by a new analysis. The accuracy was evaluated

and concluded as better, and the results were to be used. Additionally, the results were inspected and validated by internal researcher. The results were transferred to a local hard drive, ready for statistical analysis (chapter 1.10). Total time of manually drawing test regions was approximately 80 hours.

AIFORIA TEST RUN	LAYER 1	LAYER 2	LAYER 3	TOTAL TRAINING AREAS
VERSION 3 (V3)	565	1323	389	2277
VERSION 4 (V4)	565	1349	744	2658
VERSION 5 (V5)	565	1369	803	2737

Table 4: The amount of training areas in each test run for the AI Liver algorithm.

Summary of the process in developing a new algorithm for salmon liver presented in figure 19.

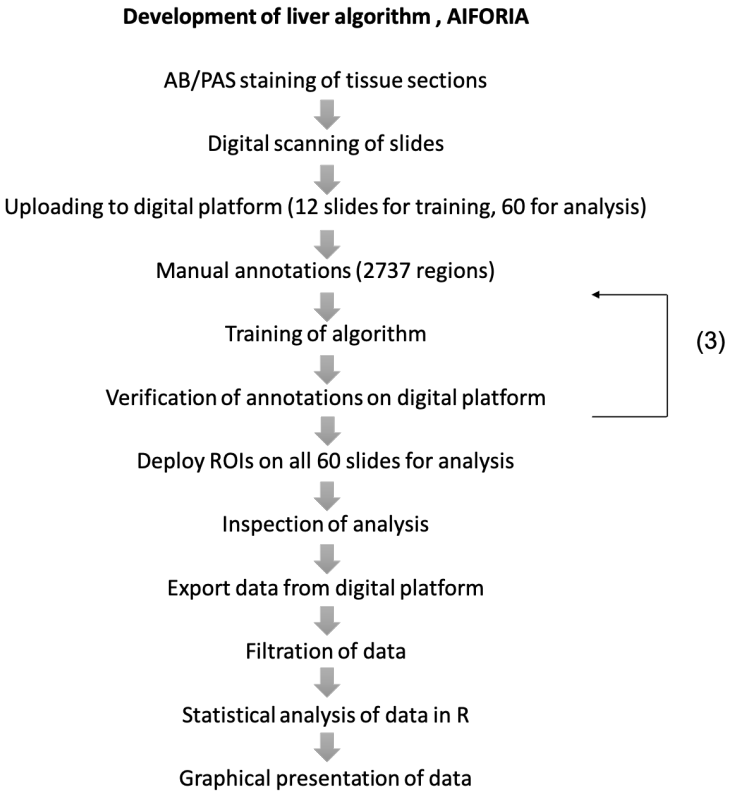

Figure 19: A summary of the process in developing a new algorithm for salmon liver, using the digital platform Aiforia®. Inspiration from "Deep neural network analysis – a paradigm shift for histological examination of health and welfare of farmed fish" (Sveen et al., 2021).

2.5 RNA-isolation, cDNA synthesis and Real time qPCR

2.5.1 Homogenization

The solution for the homogenization process, was made in an RNA-free area, where two metal beads (2,8 mm, Lysing Matrix S, Bulk, MP Biomedicals, USA) were placed in 1 ml 8-strips (Collection Microtubes, Qiagen, Germany) for each sample. 400µl of lysis buffer (LBE) from the RNA Advance Tissue kit (Beckman Coulter, USA) was added, with a pipette (Thermo Scientific, Finland), in each tube for breakdown of the proteins in the tissue. A piece of liver tissue from each fish, approximately 0,02 milligram (mg) (0,15-0,2 cm in diameter), was added to the separate tubes. This was done by taking out the liver tissue from the RNAlater and placing the piece on a sterile cutting place. With the use of the scalpel blade and a RNA free pipette tip, the right amount of tissue was cut off from the original piece. The originally piece was returned to the RNAlater tube, while the piece for homogenization was added in the tubes with beads and lysis buffer. Both the pipette tip and the scalpel were changed between each fish to avoid contamination, and scalpel holder and pincher cleaned with both RNAase inhibiting surfactant solution (RnaseZap, Invitrogen^{TM}, Lithuania) and alcohol 70%. Gloves were always used when handling the samples.

When all samples were cut and put on tubes, 20µl of protein kinase K (Beckman Coulter) was added in each tube with a multi-pipette (Eppendorf, Germany). It was important that this was done last, since after adding protein kinase K the run in the fastprep96 machine (fastprep96^{TM}, USA) needs to be done after maximum 10 minutes, because of the reaction of the protein.

Tubes were carefully sealed with strips and placed in the fastprep96 machine, and it was set to speed 1800 RPM and time 120 seconds. This was followed by a quick centrifugation (Centrifuge 5804, Eppendorf) to spin down the liquid. Samples were further placed in an incubator (TS 9053, Termaks, Norway) and incubated at 37°C for 25 minutes. The samples were stored at $-80°C$ until further analyzation.

2.5.2 RNA isolation Biomek i5

The homogenized samples thawed on ice approximately 30 minutes before starting. Biomek i5 (Beckman Coulter) was prepared using the RNAdvance Tissue program.

The following amount of chemicals were to be prepared in the robot for this sample set (8x8): 200 µL of Sample Aliquot (lysate volume) and 200µL binding buffer, 800µL Wash buffer and 800µL EtOH, and while the Dnase was 100µL Dnase for 400µL lysis buffer. This gave 50µL lysis buffer for each of the 200µL samples. The elution volume was 40µL, which should give 38µL of eluted RNA when finished. The Biomek Software (*Biomek i5*) of the robot gave instructions on where to put the different chemicals.

2.5.3 RNA quality

Nanodrop

Nanodrop (NanoDrop^{TM} 8000, Thermo Fisher Scientific) is used to measure RNA-concentration, purity and quality. Nanodrop was used by first cleaning the area of analysis with dH_2O and lens paper. This was done by adding 1,6 µl of dH_2O, with a multi-pipette, on each pedestal and then further procedure was used according to manufactures protocol (Thermo Fisher Scientific).

The results from NanoDrop were saved and further presented and sorted in an Excel file. These results were to be used in the Normalization-process. The analyzed samples were stored at $-80°C$.

Bioanalyzer

Bioanalyzer (Agilent 2100 Bioanalyzer, Agilent Technologies, Germany) is used to specific measure the quality and integrity of the isolated RNA, to prevent using degraded- or contaminated RNA in further analysis. The RNA integrity number (RIN value) was the number of interests to assess the quality of the RNA, and the samples were OK with a RIN-value >7,

indicating that RNA is not degraded. In addition to the robot, a priming-station was used in the process, where the chip was prepared for the robot. The whole procedure was done by following the manufactory protocol (Agilent Technologies, Germany), and the products used was in the package Agilent RNA 600 Nano Kit (Agilent Technologies, Germany). Measured RIN-values presented in table 5, where four samples had no RIN value (N/A).

Table 5: RIN value. N/A = no RIN value.

Sample name	**RIN value**
L7	N/A
L8	7,9
L15	6,6
L16	7,5
L23	8
L24	5,7
L31	N/A
L32	N/A
L39	5,7
L40	N/A
L47	6,1
L55	7,2

2.5.4 Normalization

Normalization was done together with a DNAse treatment. This was done by first dilute the samples with the calculated amount of RNA nuclease free water (Invitrogen, Thermo Fisher Scientific, USA) to get an RNA concentration of 33 nanogram per microliter (ng/µl). Then a DNAse mix was prepared by adding 64 µl DNAse buffer and 64 µl DNAse 1 in a 2 ml tube (Eppendorf). Calculations are illustrated in table 6. The mix was put on ice while 6 µl of each sample was added in a new 96-well plate. When this was done, 2 µl of the DNAse mix was added into each of the 60 wells with sample on the plate. Corks were put on the plate to prevent spreading of the liquid, and the plate was spun down (1000 RPM), vortexed and spun down again. The plate was then incubated at 37°C in 17 minutes in Thermocycler (2720 Thermal Cycler, Applied Biosystems, USA).

Next, 1 µl EDTA was added to each well, vortexed and spun down. When finished, the plate was placed in the Thermocycler (Applied Biosystems) and exposed for 65°C in 10 minutes.

Table 6: Calculated total amount DNAse buffer and DNAse 1.

RNA-sample	**DNAse buffer**	**DNAse 1**
6 µl	1 µl	1 µl
64 samples give:	1µlX64 = 64 µl	1µlX64 = 64 µl

2.5.5 cDNA

cDNA synthesis was done with "High-Capacity RNA-to-cDNA^{TM} kit" (Thermofisher Scientific), and it was used according to manufacturer's protocol (Thermofisher Scientific). A mastermix was prepared by mixing 640 µl RT Buffer mix with 64 µl RT enzyme mix in a tube (Eppendorf). Then 11 µl of the cDNA mix was added into each sample with a pipette. In four of the empty wells, 11 µl cDNA buffer was added in each as *no transcriptase control* (NRT-control). The plate was covered before being vortexed and spun down. After checking that the cover was properly placed on, the plate was put in a Thermocycler (Applied Biosystems) with the following program: 37°C 60 minutes, 95 °C 5 minutes, ended with 4°C.

Dilution of cDNA was done by first diluting the concentration to a 1:10 dilution in the plate from normalization, by adding 180 µl H_2O into each well. The plate was vortexed and spun down. Then the cDNA was diluted to 1:40 in a new 96-well plate, by adding 50 µl 1:10 and 150 µl H_2O in each well (60 wells). In this step a positive control was also made. The positive control was made by taking 8 µl sample out of 18 different samples and add them together as a mix in an empty well. Corks were put on the labeled plate, vortexed and spun down. The next step was to add 7 µl of each sample in 384 well plates. Seven plates were filled, since 14 primers were to be used (60 X 14). Together with the NRT and the positive control, *none template control* (NTC-control) was also made (only 7 µl H_2O and qPCR mix). The plates were stored at -20°C.

Primers used are presented in table 7, with gene name, primer sequence, accession number, and main function.

Table 7: Genes used in qPCR, with primer sequence, accession number and function.

Gene	Primer sequence	Accession numbers	Function
Elongation factor 1-Alpha (Ef1-α)	F: 5'CGC-CAA-CAT-GGG-CTG-G3' R: 5'TCA-CAC-CAT-TGG-CGT-TAC-CA3'	DQ834870	Reference gene
Beta actin (β-actin)	F: 5'CAG-CCC-TCC-TTC-CTC-GGT-AT3' R: 5'CGT-CAC-ACT-TCA-TGA-TGG-AGT-TG3'	AF012125	Reference gene

NADH: ubiquinone oxidoreductase subunit A1 (ndufa1)	F: 5'TGATGGAGAGAGACAGACGAGT3' R: 5'AGGTGAGATCTGGGATTAGTGGA3'	BT046880.1	Metabolism
NDUFA4 mitochondrial complex associated (ndufa4)	F: 5'GCCTCTTTCAACACACAACACT3' R: 5'TCACTTTAGGGTTGGAGAGGGT3'	XR_001319779.1	Metabolism
Pyruvate dehydrogenase kinase 3 (pdk3)	F: 5'AGTACATTATTTCCCGTGGTGTCA3' R: 5'CCACAGTTTCCATGGTAGCAGA3'	NM_001139694.1	Metabolism
Pyruvate kinase (pk)	F: 5'GTGACCATGATGCACTCGATC3' R: 5'GGACAGCGTGGGCGATAC3'	CK888371	Metabolism
Heat-shock protein 70a (HSP70a)	F: 5'CTG-GGA-TGA-ATG-TGC-TGA-GA3' R: 5'CTG-GAC-ATG-CCT-TTG-TCC-ATG3'	BG933934	Stress (metabolism)
Glutathione peroxidase (gp)	F: 5'GATTCGTTCCAAACTTCCTGCTA3' R: 5'GCTCCCAGAACAGCCTGTTG3'	BG934453	Stress
Catalase (cat)	F: 5'GGGCAACTGGGACCTTACTG3' R: 5'GCATGGCGTCCCTGATAAA3'	BG935638	Stress
Manganese superoxide dismutase (mnSOD)	F: 5'GTT-TCT-CTC-CAG-CCT-GCT-CTA-AG3' R: 5'CCG-CTC-TCC-TTG-TCG-AAG-C3'	DY718412	Stress (oxidative)
Copper/zinc superoxide dismutase (cu_znSOD)	F: 5'CCA-CGT-CCA-TGC-CTT-TGG3' R: 5'TCA-GCT-GCT-GCA-GTC-ACG-TT3'	BG936553	Stress (oxidative)
Bcl-2 Associated X (bax)	F: 5'TGACAGATTTCATCTACGAGCGGG3' R: 5'GCCATCCAGCTCATCTCCAATCT3'	DY722290	Apoptosis
Caspase 3A (casp3a)	F: 5'ACAGCAAAGAGCTAGAGGTCCAACAC3' R: 5'AAAGCCAGGAGAGTTTGACGCAG3'	DQ008070	Apoptosis
Interleukin-8 (Il8)	F: 5'GAAAGCAGACGAATTGGTAGAC3' R: 5'GCTGTTGCTCAGAGTTGCAAT3'	BT046706	Immune system

2.5.6 Real time PCR analyses

The pre-made 384 well plates (X7), with 7 µl sample in each well was used in Real time PCR analyses. While the plates were thawed, a qPCR mastermix was made per gene by mixing PowerUp™ SYBR™ Green Master Mix (Thermofisher, Lithuania) with Primer FW and Primer RW, and nuclease-free water. This is illustrated in figure 20, and the table to the right gave the total amount to mix per gene, with 132 samplers per gene. Each mastermix was vortexed and spun down before use.

1X reaction	
10 µl	Mastermix
1,2 µl	Primer FW (5uM)
1,2 µl	Primer RW (5 uM)
0,6 µl	Nucleasefree water
= 13 µl reaction mix + 7 µl sample	

132 reactions for full plate		
142 reactions		(m/dødvolum)
1420	µl	Mastermix
170	µl	Primer FW
170	µl	Primer RW
85	µl	Nucleasefree water

Figure 20: qPCR mastermix. m/dødvolum = with excessive volume.

When finished thawing, the plates were spun down. 13 µl of mastermix was added to each well, plates were sealed and spun down.

Plates were analyzed in the machine Quant Studio 5 (Applied Biosystems, Singapore) and the Run Method and Plate Setup was chosen in the belonging software (QuantStudio™ Design & Analysis Software) before starting the run. The chosen Run Method is shown in figure 21, and additionally SYBR® Green Reagents was set as *Chemistry* under *Experiment Properties*.

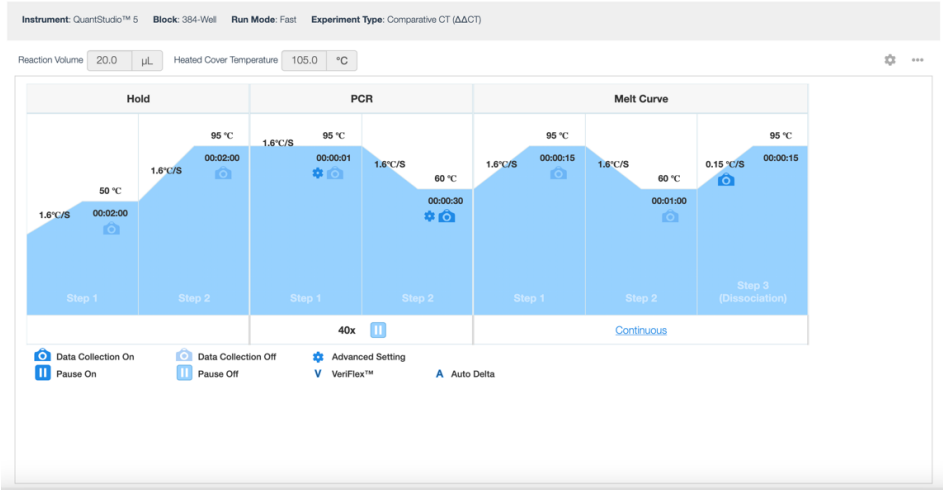

Figure 21: Run Method; QuantStudio 5 as instrument, 384-Well, fast run mode, and Comparative CT as experiment type.

The NTC controls and the positive controls were controlled when finished, to verify the quality of the qPCR reaction.

2.6 Statistical analysis

For simple statistics, such as mean and standard deviation (std), Microsoft Excel (version 16.48) was used. This was done with all data collected. Ct-data from qPCR were calculated using the 2^ΔΔCt method in Excel, and further used in SigmaPlot (version 14) to carry out statistical analysis. Fish with invalid CT-Value (>35) was excluded from the trial.

In SigmaPlot statistical differences were calculated (P=<0,05). This was used on data from growth, scale loss, and gills, as well as manual histological scores, and gene transcription. ANOVA (The analysis of variance), thereunder two-way ANOVA, was used to calculate significant differences between, and within, timepoint and treatment, when data was absolute values that were measured. Prior to this calculation, SigmaPlot calculated the normality of the data sets. Chi-square test was used to calculate the frequency of a score within the groups, thereunder the statistical difference. Chi-square test was used when the data represented a description, and the numbers were not the value itself.

The data from Aiforia® (digital histological scoring) was processed in program R (version R.4.0.2), by researcher in Nofima. Firstly, the data from Aiforia® was filtrated, where detections with higher error% that pre-sat limit, were excluded. The analysis was done group vice, where normalization of samples was done prior to statistical analysis (P=<0,05), as previously described for a similar skin algorithm (Sveen et al., 2021).

3 Results

3.1 Operational welfare scores (OWIs)

The average length of the fish within each treatment group and timepoint is presented in figure 22. There was a significant difference in the length of fish from the Control and HW groups between Peak and Return (P=<0,024, P=<0,003), but no difference between treatments within each time-point.

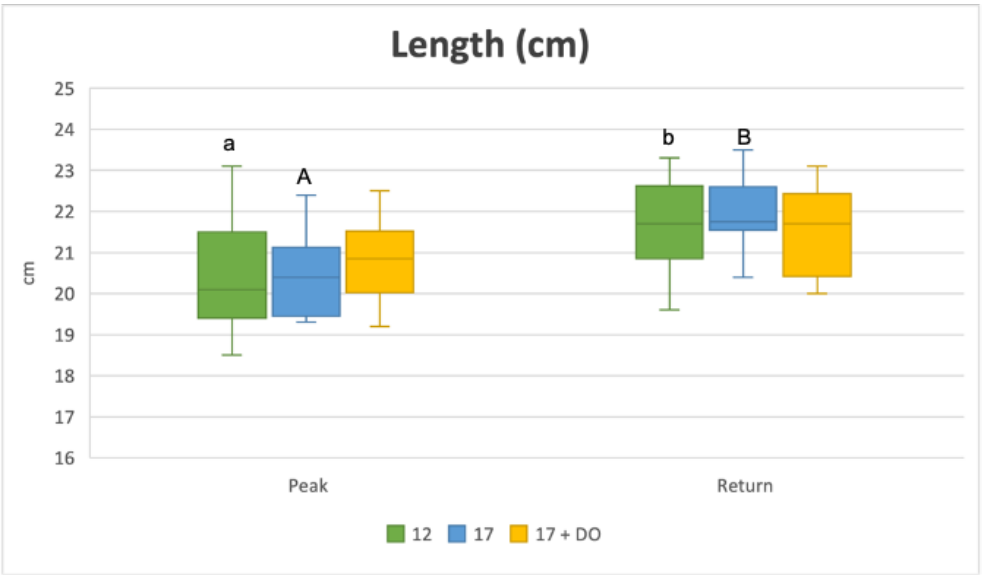

Figure 22: Average length of the fish from each of the three groups at Peak and Return presented as mean and ±std. The significant difference between the two time points in a treatment group is denoted by different letters (lowercase: Control; uppercase: HW).

The average weight of the fish within each treatment group and timepoint is presented in figure 23. There was a significant difference in the length of fish from the Control and HW groups between Peak and Return (P=<0,018, P=<0,004).

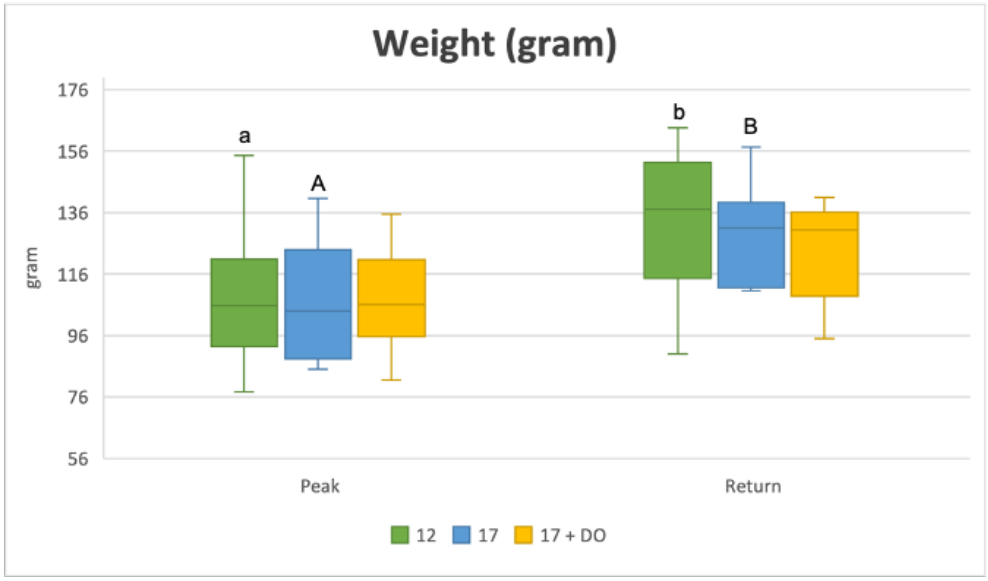

Figure 23: Average weight of the fish from each of the three groups at Peak and Return presented as mean and ±std. The significant difference between the two time points in a treatment group is denoted by different letters (lowercase: Control; uppercase: HW).

K-factor is presented in figure 24. The results showed no significant difference (P=>0,05). Within Return, Control had the highest K-factor compared to HW and HW+DO.

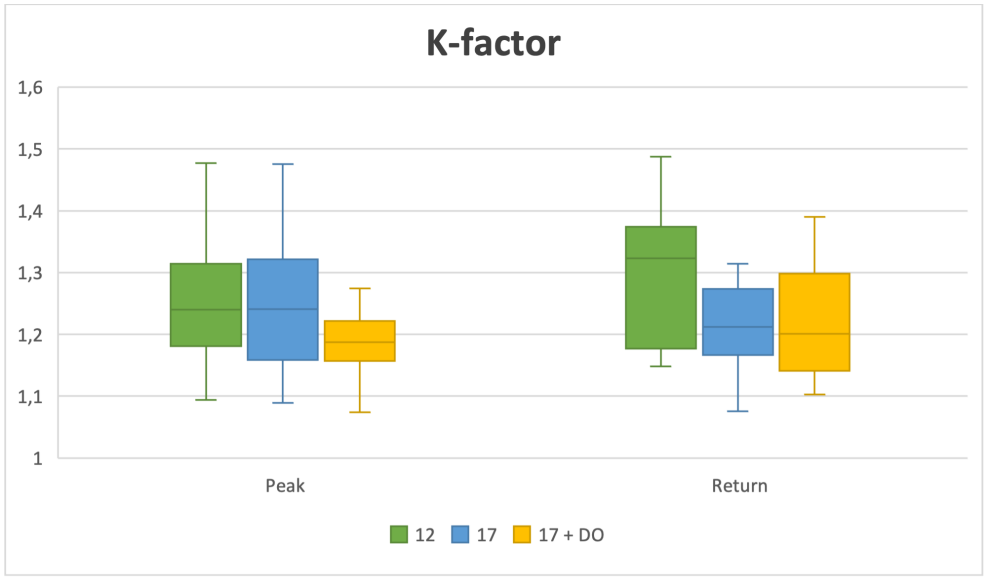

Figure 24: Average K-factor for fish from the three different groups at Peak and Return, presented as mean and ±std.

The operational welfare scores (OWIs) (Noble et al., 2018) are presented in figure 25 and 26. The results showed no significant difference between scored parameters (left scale loss; P=0,511, right scale loss; P=0,611, and gill score; P=0,244). Control had a trend with lower score than the two other groups on both scale loss and gill score. HW+DO scored the highest on all three parameters.

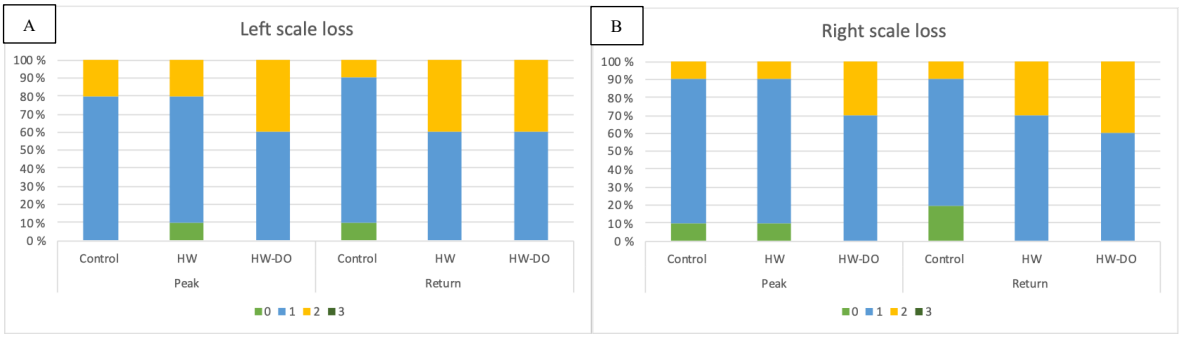

Figure 25: Score on left scale loss (A) and right scale loss (B). Each fish was given a specific score (0-3, where 0 is best and 3 worst), here sorted in percentage within each group and timepoint. Score 0 is illustrated in color green, 1 in blue, 2 in yellow, and 3 in green.

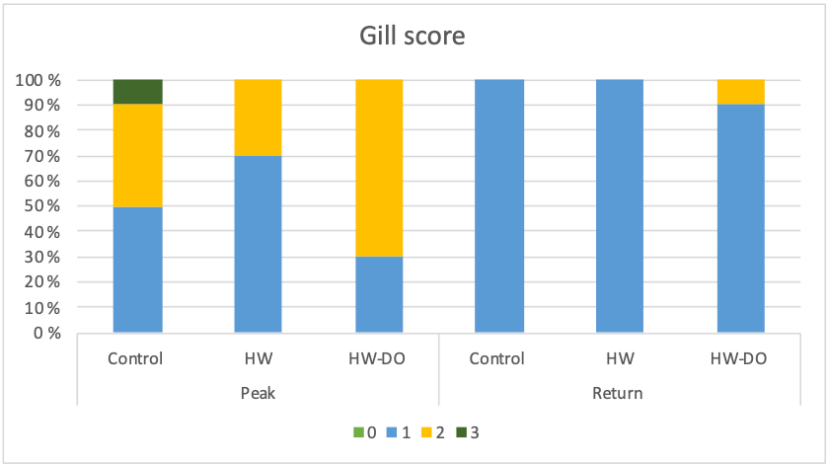

Figure 26: Gill score. Each fish was given a specific score (0-3, where 0 is best and 3 worst), here sorted in percentage within each group and timepoint. Score 0 is illustrated in color green, 1 in blue, 2 in yellow, and 3 in green.

3.2 Histology

3.2.1 Manual histology

The connective tissue was scored both on general appearance (figure 27A) and measured thickness (figure 27B). On general appearance, a significant difference was observed within Return, between all three groups; Control and HW (P=0,004), Control and HW+DO (P=0,036), HW and HW+DO (P=0,025). Livers from HW+DO group had an average of the thickest connective tissue measured at both Peak and Return. Control had the lowest score in both appearance and thickness within both Peak and Return.

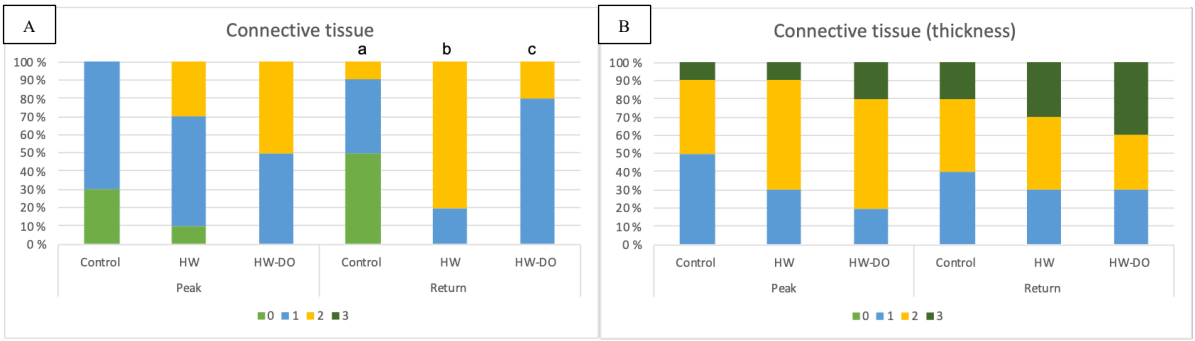

Figure 27: Manual scoring of connective tissue, overall view (A) and measured thickness (B). Each histological slide was given a specific score (0-3, where 0 is best and 3 worst), here sorted in percentage within each group and timepoint. Score 0 is illustrated in color green, 1 in blue, 2 in yellow, and 3 in green. A: The significant difference between the three treatment groups within Return is denoted by different letters (a, b, c).

.

The scoring of melanin spots is presented in figure 28. There was no significant difference within treatments nor timepoints (P=0,261). Control had the lowest score at both Peak and Return, while HW+DO had the highest score at Peak and HW the highest at Return.

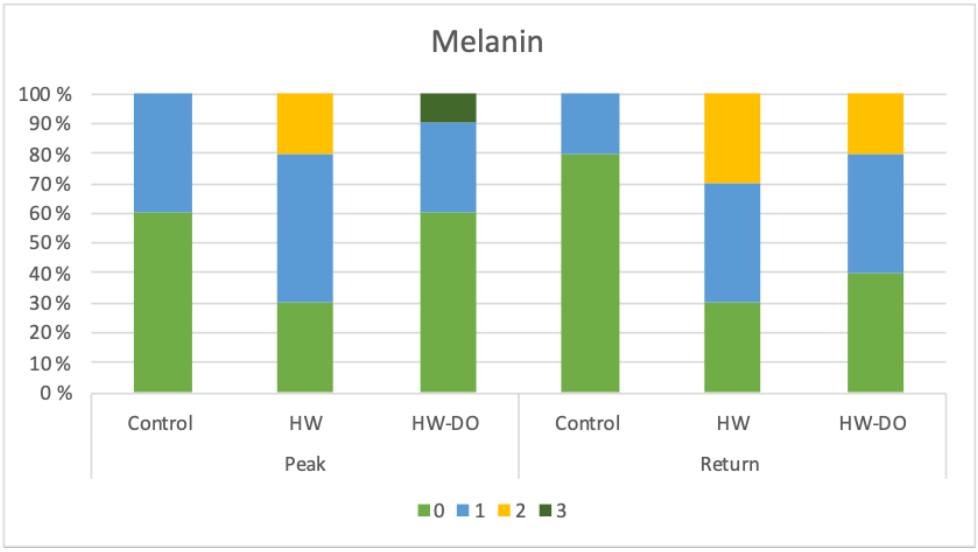

Figure 28: Manual scoring of melanin. Each histological slide was given a specific score (0-3, where 0 is best and 3 worst), here sorted in percentage within each group and timepoint. Score 0 is illustrated in color green, 1 in blue, 2 in yellow, and 3 in green.

The score of steatosis is presented in figure 29. There was a significant difference between treatments within Return, where Control differed from HW (P=0,005) and HW+DO (P=0,026).

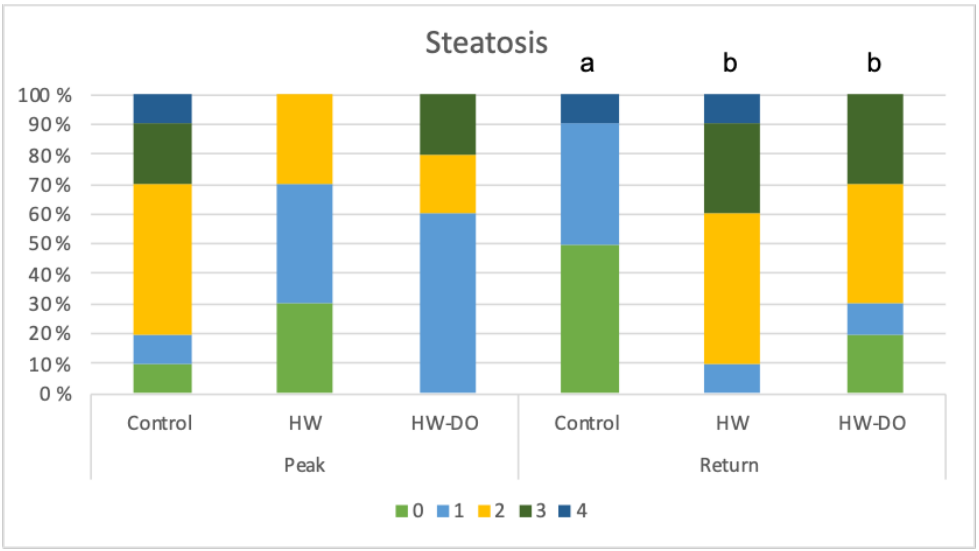

Figure 29: Manual scoring on steatosis. Each histological slide was given a specific score (0-3, where 0 is best and 3 worst), here sorted in percentage within each group and timepoint. Score 0 is illustrated in color green, 1 in blue, 2 in yellow, and 3 in green. The significant difference within Return is denoted by different letters (a, b).

The scores connected to vacuoles are presented in figure 30. There was no significant difference detected. HW had limited variation between timepoints. From Peak to Return, Control had an increase of score 1 and a reduction in score 0 and 2. HW+DO had an increase of score 1 in Return, while number of score 2 was reduced. Within both timepoints, Control had the highest score. HW+DO had the lowest.

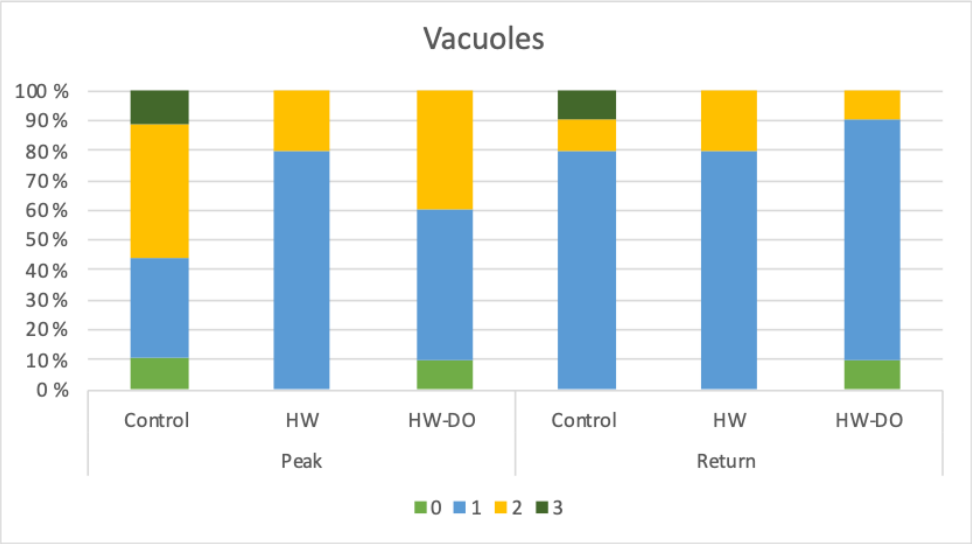

Figure 30: Manual scoring of vacuoles. Each histological slide was given a specific score (0-3, where 0 is best and 3 worst), here sorted in percentage within each group and timepoint. Score 0 is illustrated in color green, 1 in blue, 2 in yellow, and 3 in green.

3.2.2 Digital histology

The results from the digital histology, Aiforia®, is presented as screenshots directly from the program to illustrate the accuracy of the algorithm and errors in the algorithm. Further, the quantitative results, processed in Excel and R, are presented in boxplots and distribution plots.

Figure 31 precents the improvement in detection of micro vesicular fat (vacuoles) between analysis V3 and analysis V4, while figure 32 precents improvement between V4 and V5. Training the algorithm, exhibited results in higher accuracy on micro vesicular fat, illustrated in figure 31B with more precise detection, and in figure 32B with overall detection.

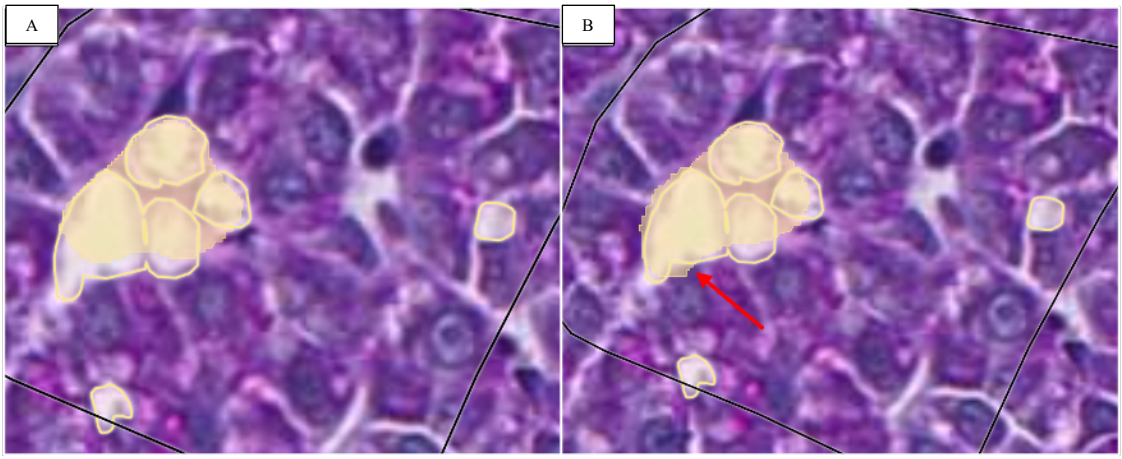

Figure 31: Training liver algorithm. Progression in detection of micro vesicular fat (marked yellow), AI (layer 3), A; analysis V3 and B; analysis V4. Red arrow points at progression.

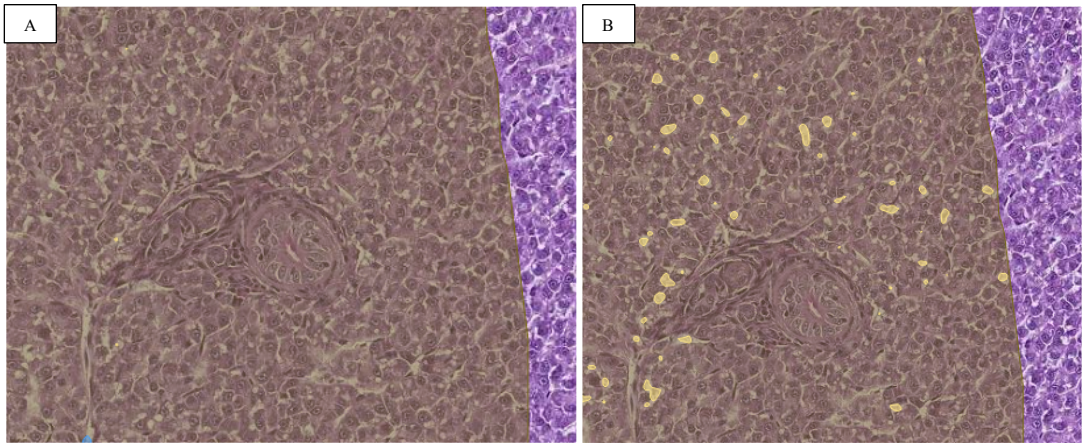

Figure 32: Training liver algorithm. Progression in detection of micro vesicular fat (marked yellow), AI (layer 3). A; analysis V4 and B; analysis V5.

The difference in detection of glycogen between V4 and V5 is presented in figure 33. The accuracy is presented as higher in V5.

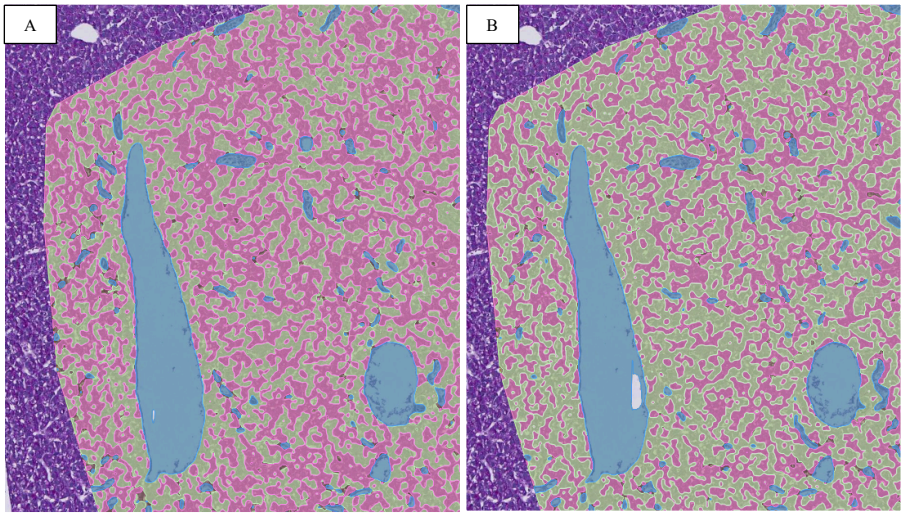

Figure 33: Training liver algorithm. Progression in detection of glycogen (marked pink), AI (layer 2). A; analysis V4 and B; analysis V5. In both figures, tissue marked blue is detected veins, and tissue marked green is liver parenchyma.

Figure 34, 35 and 36 showes ROIs, analysis V5, from three different slides. Figure 34 contains a high amount of detected glycogen, while in figure 35 there is less, illustrating differences between the slides. Figure 36 shows a slide where close to all the tissue within ROI was detected as liver steatosis. A screenshot of the tissue, zoomed in and without the markings (36B), confirms that the detection was correct.

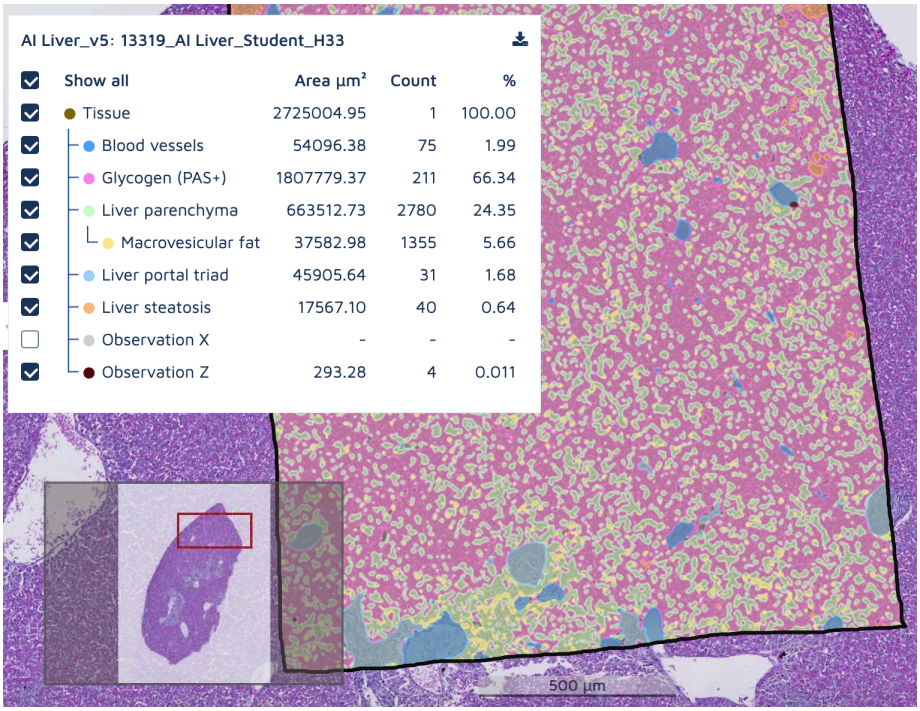

Figure 34: Screenshot from AI V5. Glycogen marked pink, blood vessels marked blue, liver portal triad marked light blue, macro vesicular fat marked yellow, liver parenchyma marked green, steatosis marked orange, and melanin spots (observation Z) marked brown. This histological slide has a high amount of glycogen (66,34% of the liver tissue).

Figure 35: Screenshot from AI V5. Glycogen marked pink, blood vessels marked blue, liver portal triad marked light blue, macro vesicular fat marked yellow, liver parenchyma marked green, steatosis marked orange, and melanin spots (observation Z) marked brown. This histological slide has a low amount of glycogen (8,13% of the liver tissue).

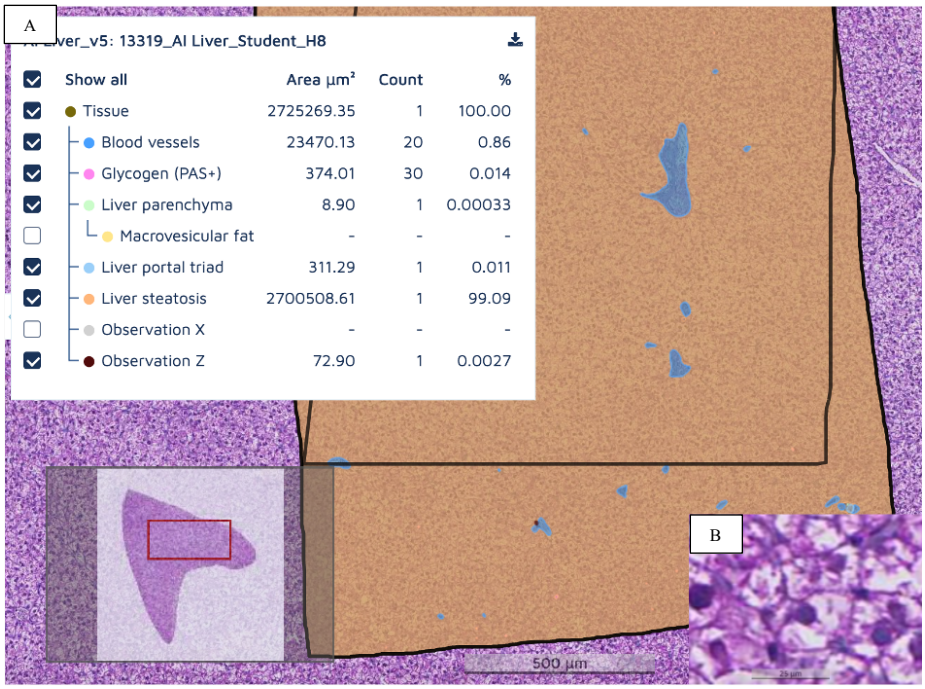

Figure 36: Screenshot from AI V5. A: Detection of steatosis by the algorithm, marked with orange. Blood vessels marked with blue. 99.09% of the liver tissue in this histological slide was detected as steatosis. B: Zoom of the tissue marked with orange, which confirms steatosis.

The precision of the algorithm (V5) is presented, with higher magnification, in figure 37. The detection of both blood vessels (blue) and liver portal triad (light blue), as well as melanin (brown), are well detected.

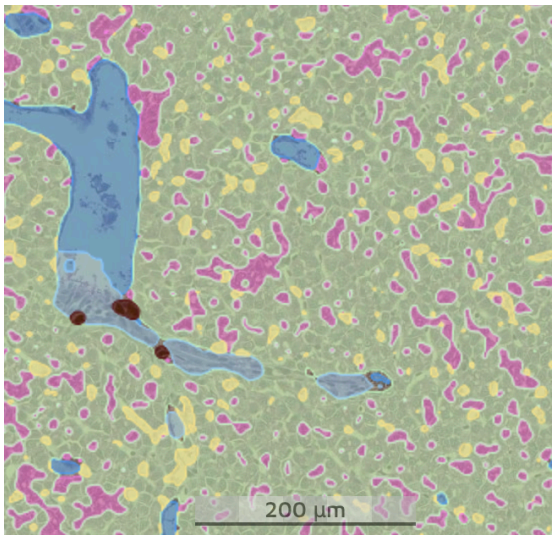

Figure 37: Screenshots from AI V5. Detection of blood vessels marked with blue by the algorithm, liver portal triad marked light blue, melanin spots marked with brown, glycogen with pink, vacuoles with yellow, and liver parenchyma marked with light green.

The detection of glycogen alone, V5, is presented in figure 38. There are several errors where vacuoles are marked as glycogen.

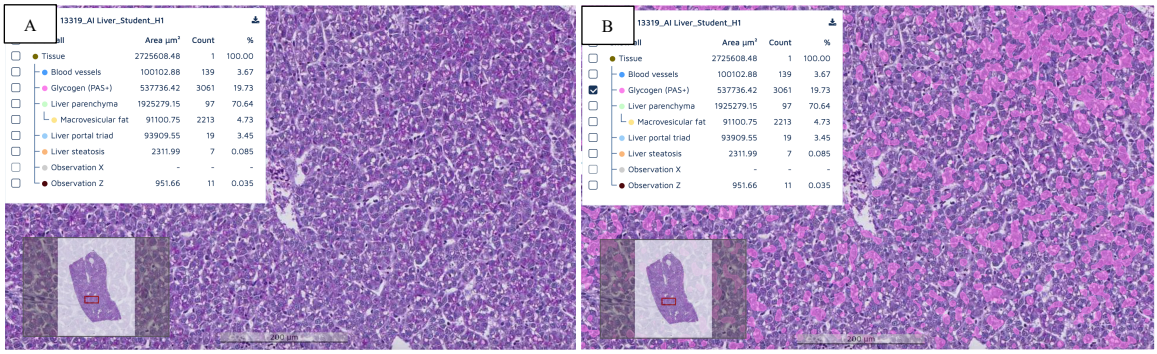

Figure 38: Screenshots from AI V5. Detection of glycogen marked pink by the algorithm. A: Liver tissue. B: Same area of liver tissue with detected glycogen.

Figure 39 illustrates the detection of melanin spots (A) and liver steatosis (B). Both components were well detected, with high accuracy.

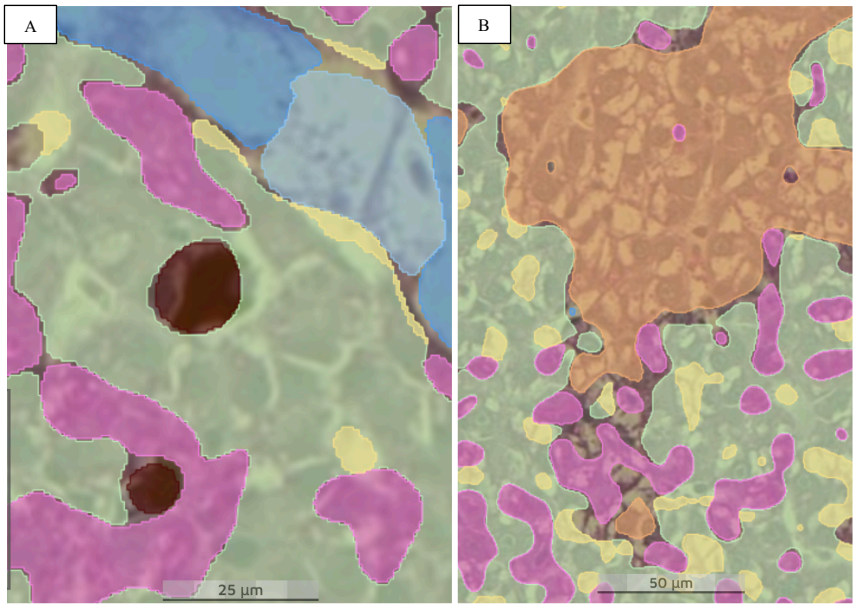

Figure 39: Screenshots from AI V5. A: Melanin spots well detected, marked with brown. B: Liver steatosis well detected, marked with orange. In both A and B, glycogen is marked pink, vacuoles are marked yellow, liver parenchyma marked green, liver portal triad marked light blue, and blood vessel marked blue.

Figures 40, 41, 42 and 43 are screenshots from AI V5, where errors are presented within both detection of vacuoles, and detection of glycogen. Figure 40 and 41 show failure in marking all vacuoles in an area, where examples of vacuoles that are not detected are presented within the red circles in 40B and 41B.

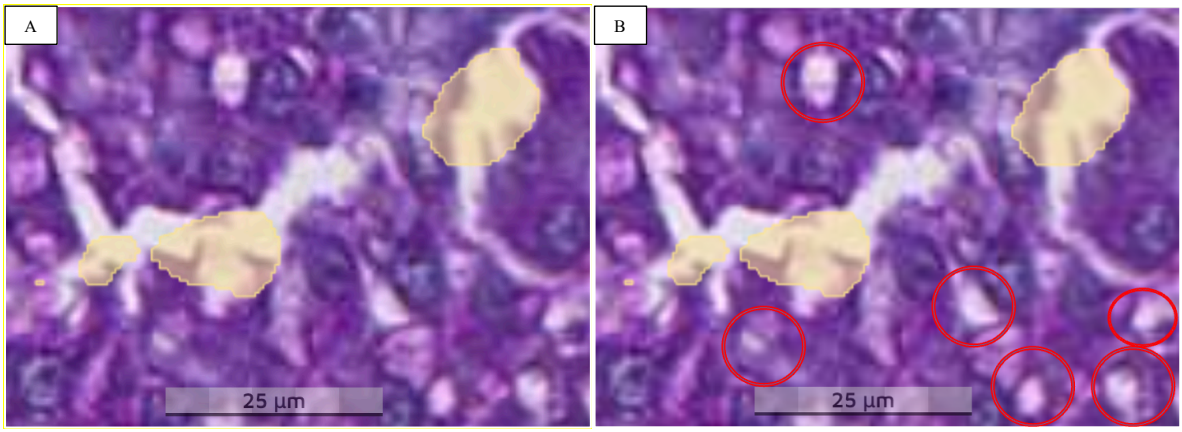

Figure 40: Screenshots from AI V5. A: Detected vacuoles by the algorithm marked with yellow. Example of errors in detection of vacuoles presented within red markings in B.

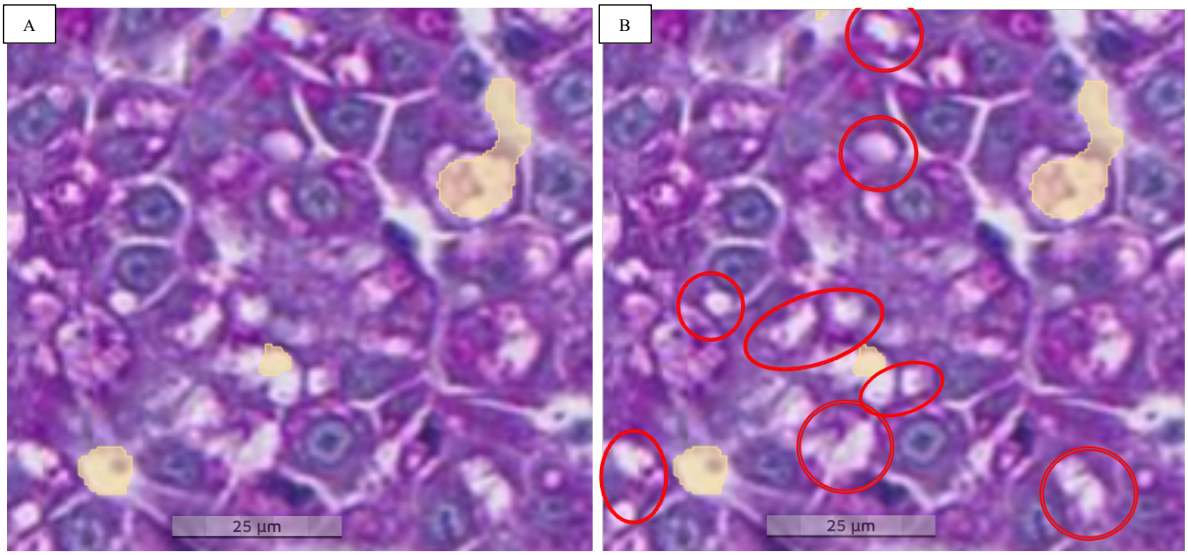

Figure 41: Screenshots from AI V5. A: Detected vacuoles by the algorithm marked with yellow. Example of errors in detection of vacuoles presented within red markings in B.

Vacuoles detected as glycogen by the algorithm, are presented in figure 42 and 43. Example of errors are marked with red circles. In figure 43, it is presented an example of a hepatocyte detected as glycogen.

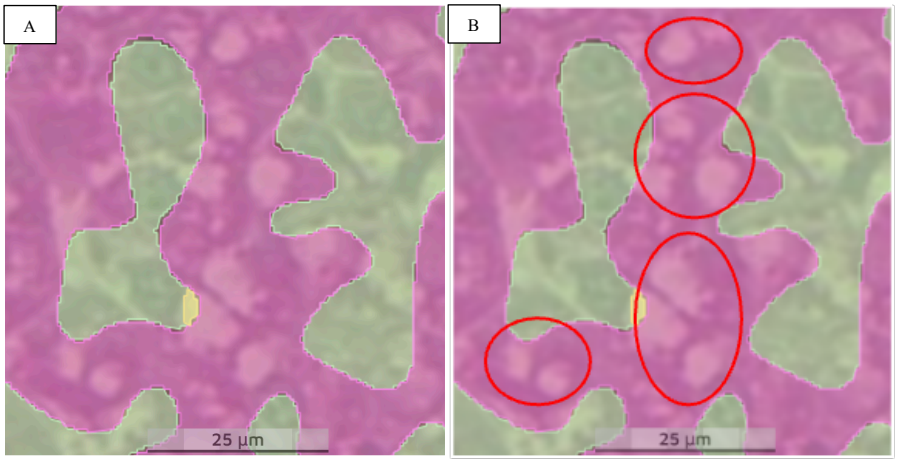

Figure 42: Screenshots from AI V5. Pink indicates detection glycogen. Green is marked liver parenchyma, yellow is marked detected vacuoles by the algorithm. Example of errors in detection of vacuoles, where vacuoles is read as glycogen by the algorithm. Errors presented within red markings (B).

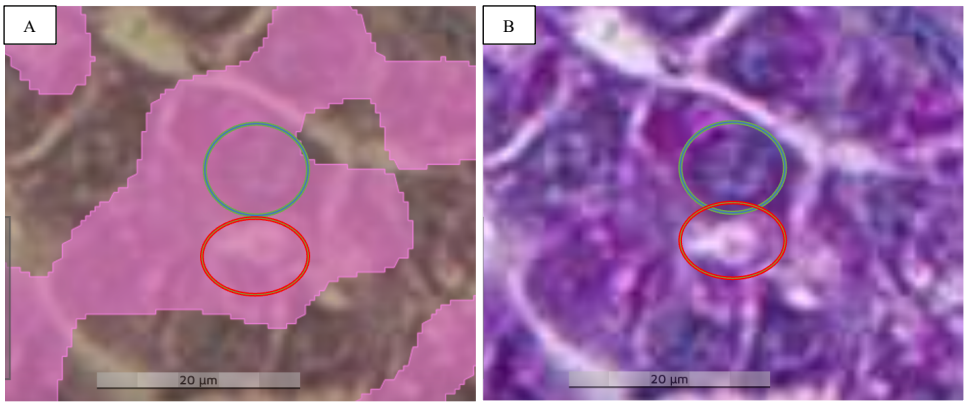

Figure 43: Screenshots from AI V5, same area with detection of glycogen (A) and without detection (B). A: Pink indicates detection of glycogen by the algorithm. Example of errors in detection of glycogen, are presented with red circle, where a vacuole detected as glycogen. The green circle presents a hepatocyte detected as glycogen by the algorithm.

The complete measured data from the AI algorithm is shown in an overview in figure 44 and 45. Figure 44 shows the distribution of the different components normalized within each fish (one ROI per fish). Four fish (8, 10, 31 and 44) had a high amount of steatosis, and few other features were detected in these fish.

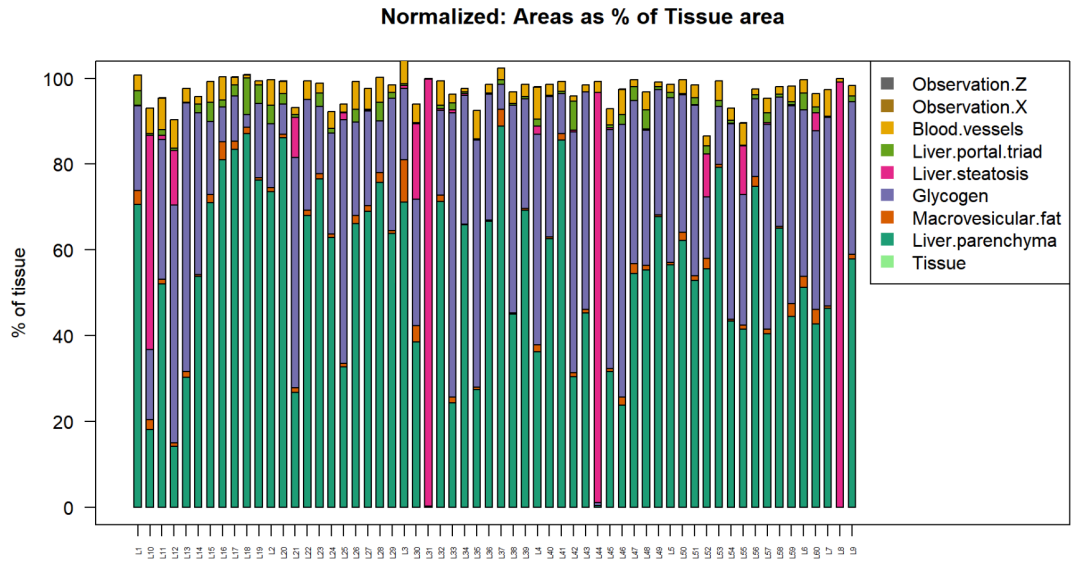

Figure 44: Distribution of the different components (normalized) within each fish (per ROI). Observation Z = melanin.

Groupwise overview of the distribution of the different components presented in figure 45.

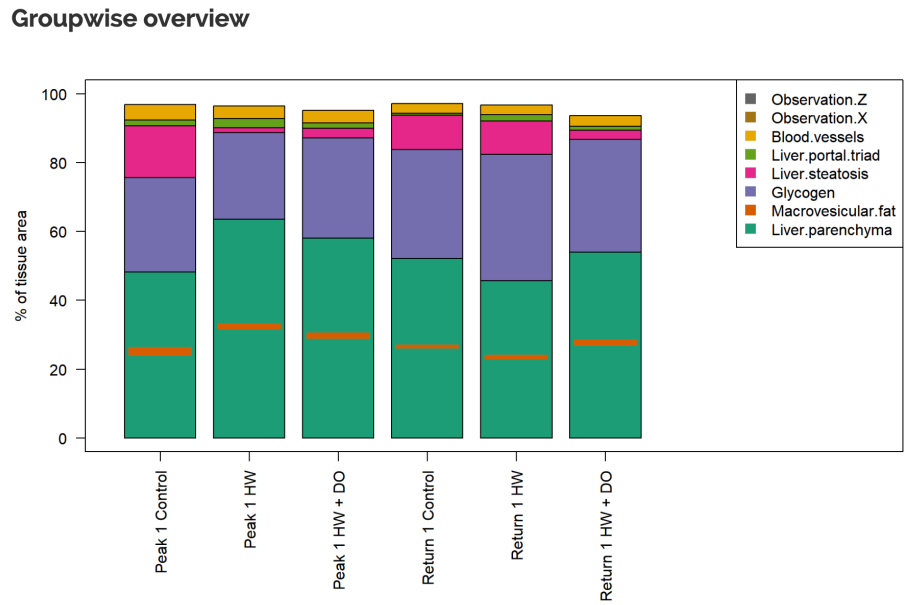

Figure 45: Groupwise overview of the distribution of the different components. Data from AI V5. Observation Z = melanin.

The results from Macro vesicular fat and Liver steatosis are presented in figure 46 and 47.

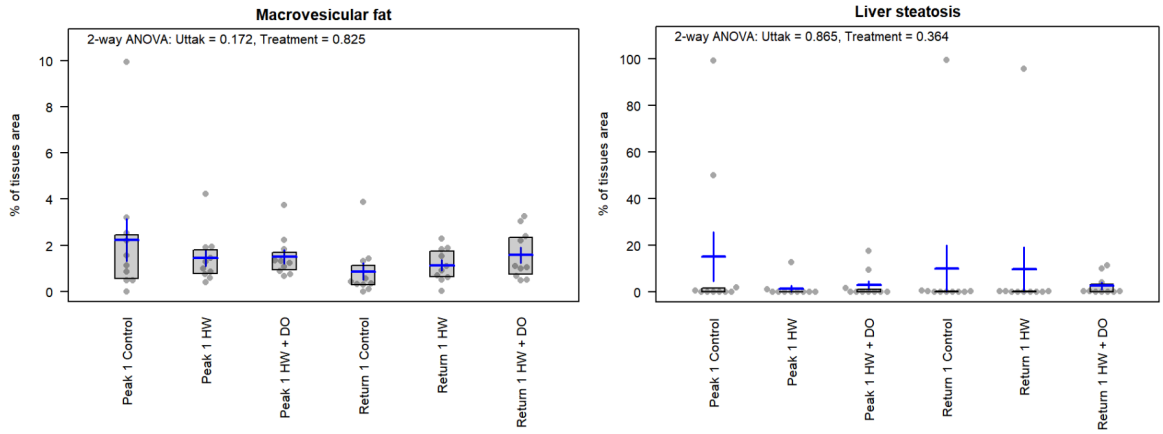

Figure 46 and 47: The data results from AI presented as mean, ±std, and outside values. Figure 46 shows macro vesicular fat, while figure 47 shows liver steatosis.

Glycogen in presented in figure 48. Within liver portal triad (figure 49), there was a trend to higher values at Peak in comparison to Return (P=0.083). In addition, HW had higher values than Control and/or HW+DO (P=0.052). The lowest variance was found within HW, while the greatest variance was found within Control.

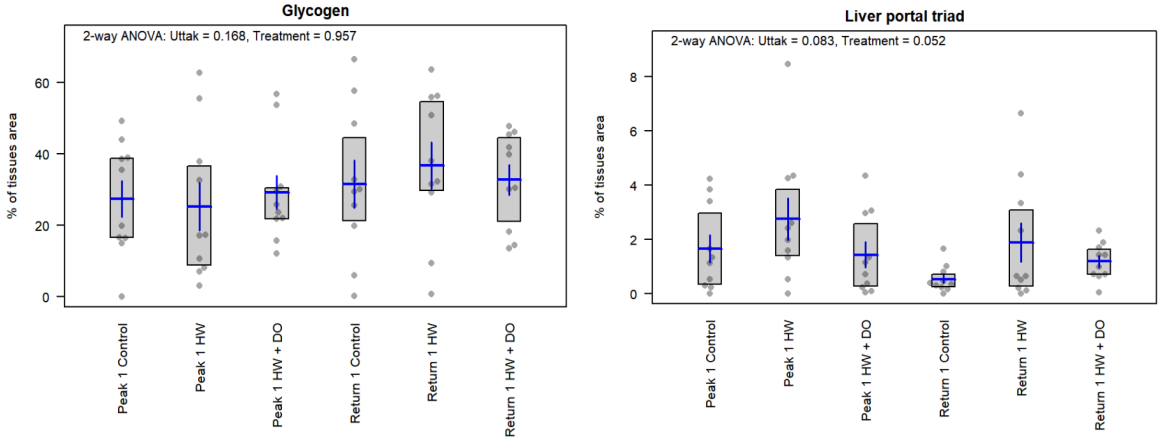

Figure 48 and 49: The data results from AI presented as mean, ±std, and outside values. Figure 48 shows glycogen, while figure 49 shows liver portal triad.

Significant difference was exhibited in blood vessels within timepoint (P=0,04), with decrease in expression within Return (figure 50).

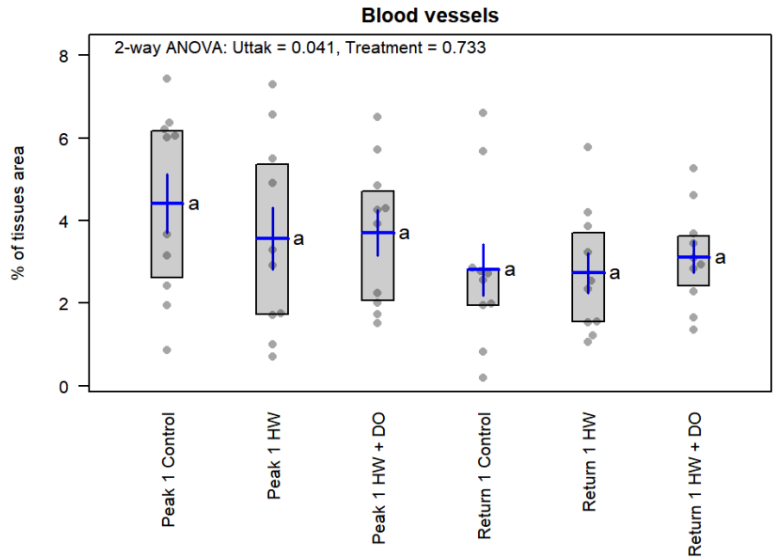

Figure 50: The data results connected to blood vessels from AI, presented as mean, ±std, and outside values. Statistical difference (2-way ANOVA test) was P=0,041 within timepoint (Uttak). Statistical difference from Tukey post-hoc test is denoted with letter a.

In melanin (figure 51), there was a trend to higher values at Peak in comparison to Return (P=0.051). Additionally, a significant difference was exhibited within treatment (P=0,016), where Control had lowest expression within both timepoints compared to HW and HW+DO.

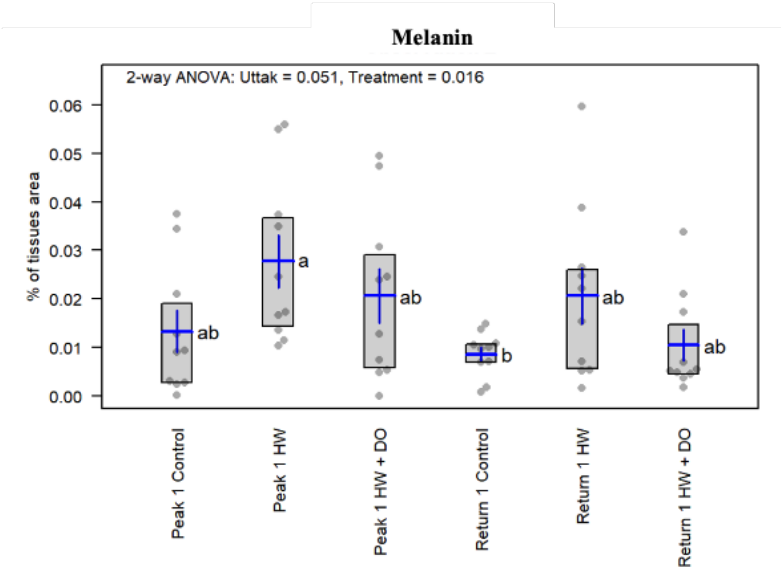

Figure 51: The data results connected to melanin spots from AI, presented as mean, ±std, and outside values. Statistical difference (2-way ANOVA test) was P=0,051 and P=0,016. Statistical difference from Tukey post-hoc test is denoted by different letters (a, b).

Since four samples showed extensive steatosis, with few other features measured (fish 8, 10, 31 and 44), a new analyze was done without these four sections (second run, figure 52) to evaluate the details of other tissue structures better. Figure 52 shows the distribution of the different components normalized within each ROI for the second run.

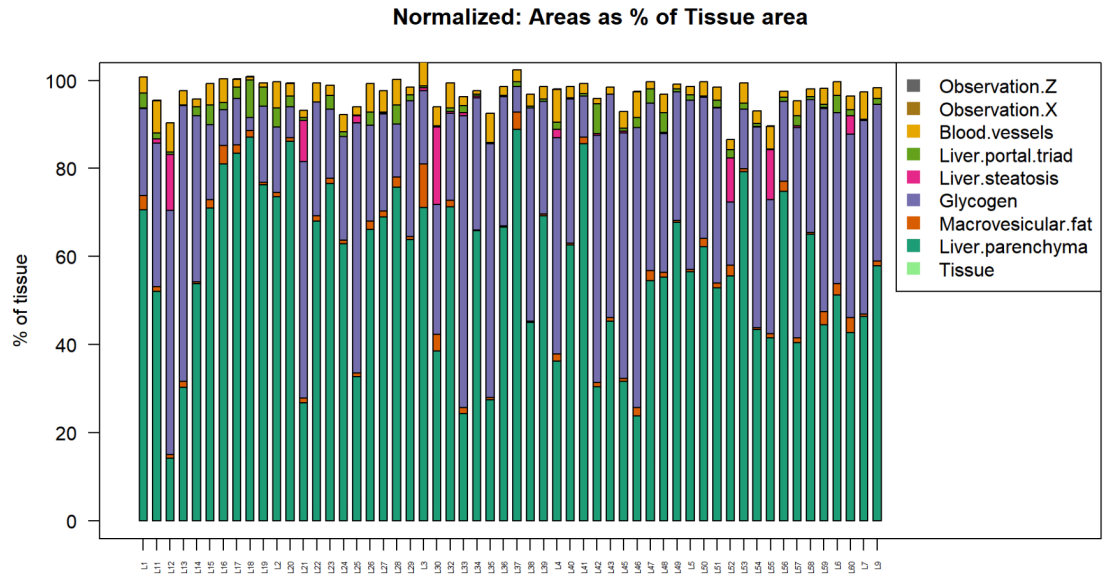

Figure 52: Distribution of the different components (normalized) within each fish (ROI). Fish 8, 10, 31 and 44 are excluded from the data, and therefore not included in the figure. Observation Z = melanin.

Groupwise overview of the distribution of the different components, second run, presented in figure 53. The highest percentage of steatosis was within HW+DO.

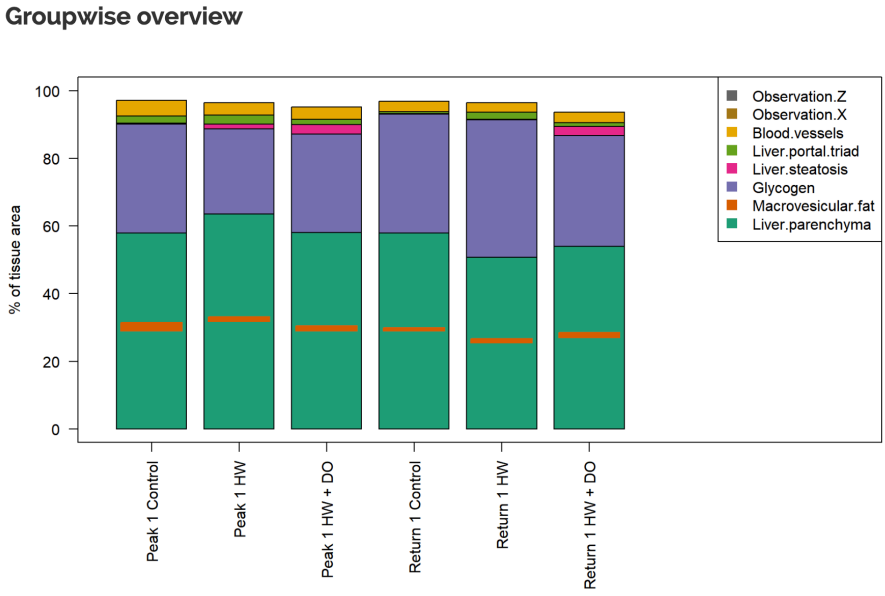

Figure 53: Groupwise overview of the distribution of the different components. Data from AI V5, second run. Observation Z = melanin.

A trend in steatosis within treatment (P=0,081) was observed (figure 54), where HW+DO had higher values than Control and/or HW+DO. In liver portal triad (figure 55), there was a trend to higher values at Peak in comparison to Return (P=0,079). In addition, HW had higher values than Control and/or HW+DO (P=0,069), and the lowest value was within Return Control.

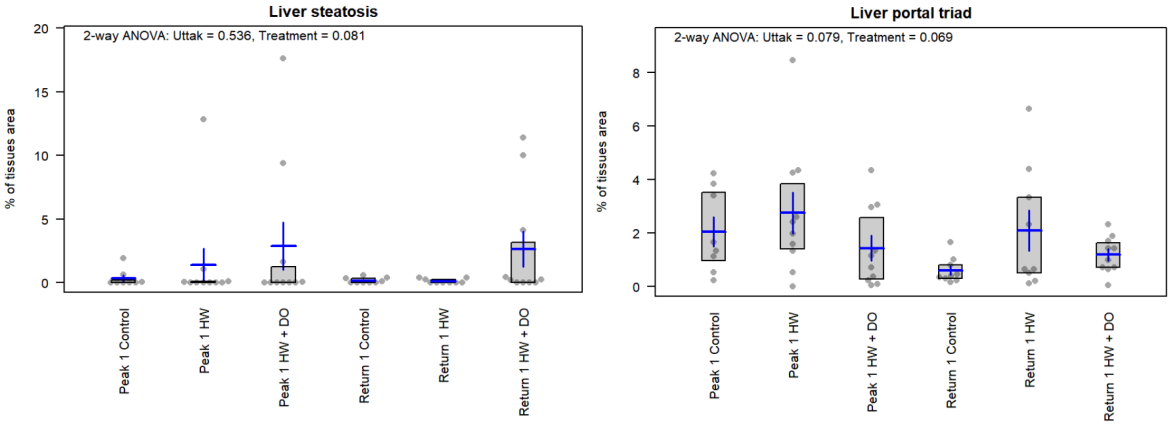

Figure 54 and 55: The data results from AI, second run, presented as mean, ±std, and outside values. Figure 54 shows liver steatosis, while figure 55 shows liver portal triad.

3.3 qPCR

All the data from the qPCR are calculated with nine fish within Return Control and eight fish within Return HW, due to invalid ct-results.

3.3.1 Genes involved in metabolism

Genes connected to metabolic processes in Atlantic salmon, *ndufa1* (figure 56), *ndufa4* (figure 57), *pdk3* (figure 58) and *pk* (figure 59), all exhibited results with significant differences, except *ndufa4* (P=>0,05). *Ndufa1* had significant difference within Return, between Control and HW (P=0,005), and between HW+DO and HW (P=0,035). The expression of both *pdk3* and *pk* between Peak and Return in the HW group was significantly different (*pdk*: P=<0,001 and *pk*: P=0,005). *Pk* had significant difference within Peak, between Control and HW+DO (P=0,002). Within Return, *pk* had significant difference between Control and HW (P=0,011).

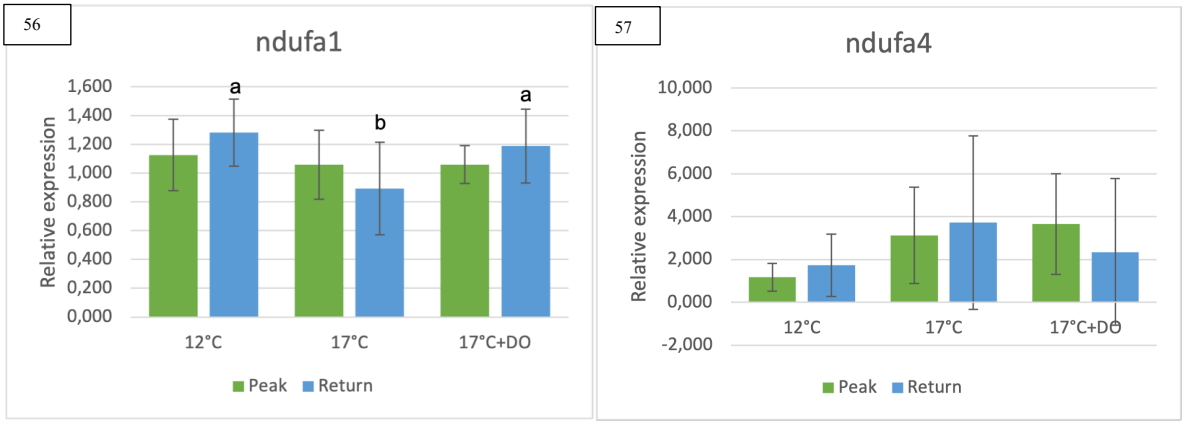

Figure 56 and 57: Relative expression of genes. 56: ndufa1, 57: ndufa4. Results presented as mean and ±std. The significant difference between the three treatment groups, within Return, is denoted by different letters (a, b).

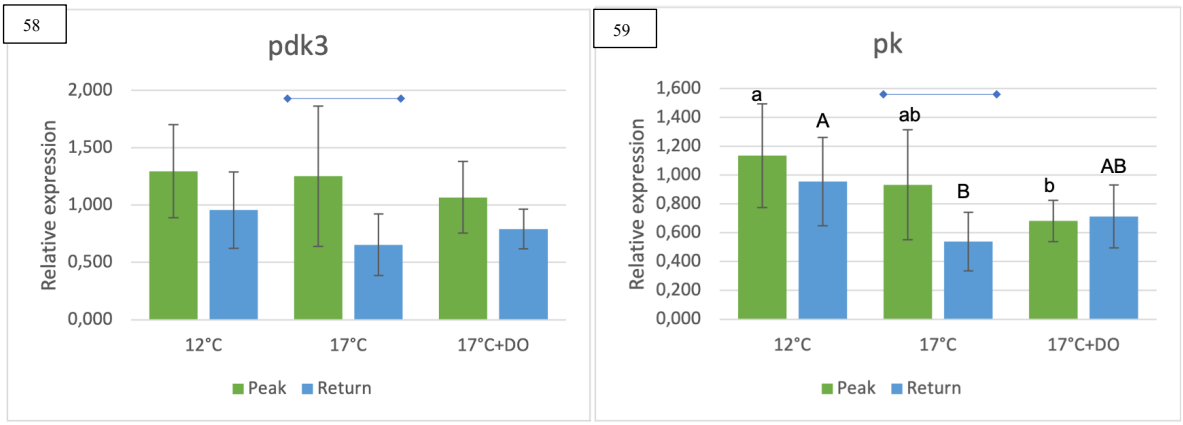

Figure 58 and 59: Relative expression of genes. 58: pdk3, 59: pk. Results presented as mean and ±std. The significant difference between the three treatment groups is denoted by different letters (lowercase: within Peak; uppercase: within Return). Significant differences within treatment group are presented with blue line.

3.3.2 Genes involved in stress response

Genes connected to stress, *Hsp70* (figure 60), *gp* (figure 61), *cat* (figure 62), *mnsod* (figure 63) and *Cu_Zn sod* (figure 64), were included to evaluate how the different treatments affected stress levels. *Gp* and *cat* had results with significant difference. The expression of *gp* between Peak and Return in the Control group was significantly different (P=0,022). At Return, the expression of *cat* among treatments groups showed significant difference where the levels in both HW and HW+DO were significantly lower than Control (P=0,005, P=0,016). Within *mnsod* a trend was exhibited within Return, where HW+DO differentiated from Control and HW with an increase in expression.

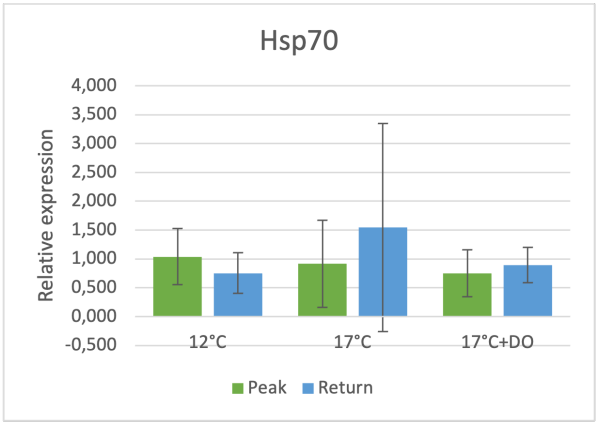

Figure 60: Relative expression of gene Hsp70. Results presented as mean and ±std.

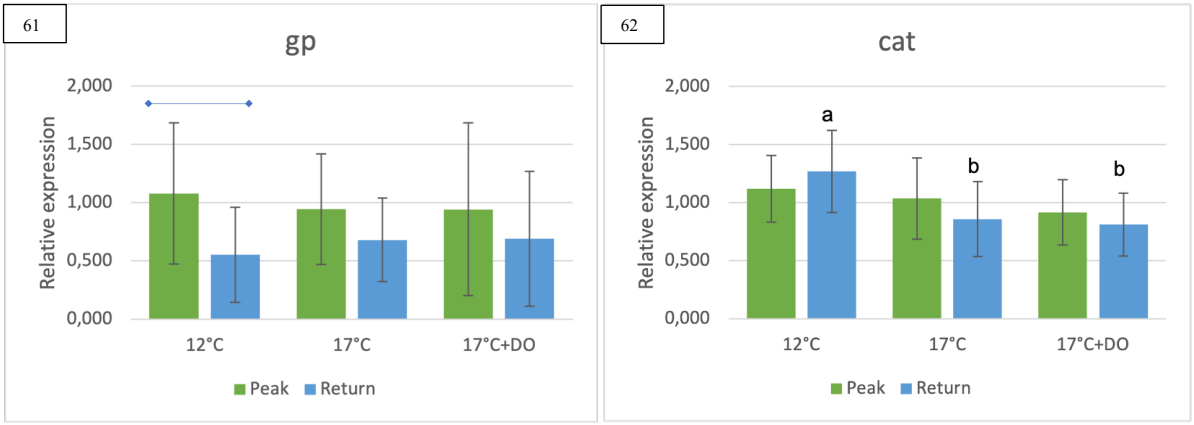

Figure 61 and 62: Relative expression of genes. 61: gp, 62: cat. Results presented as mean and ±std. The significant difference between the three treatment groups, within Return, is denoted by different letters (a, b). Significant differences within treatment group are presented with blue line.

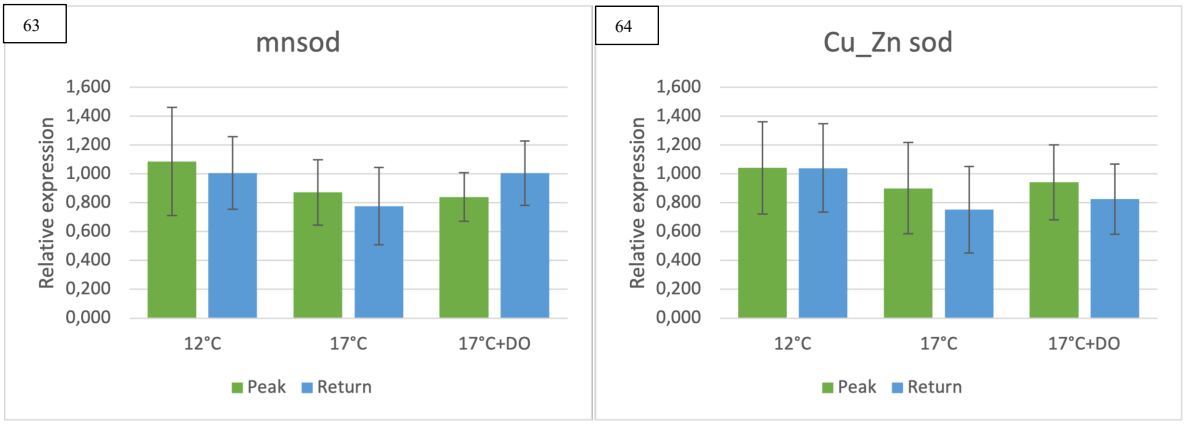

Figure 63 and 64: Relative expression of genes. 63: mnsod, 64: Cu_Zn sod. Results presented as mean and ±std.

3.3.3 Genes involved in apoptosis

Genes connected to apoptosis were included to evaluate tissue damage, *bax* (figure 65) and *casp3a* (figure 66). *Casp3a* showed significant difference within Peak, between Control and HW (P=0,006). The expression of *casp3a* between Peak and Return within both HW and HW+DO, was significantly different (HW: P=<0,001, HW+DO: P=0,033). There was a trend within *bax*, where Control showed higher expression than both HW and HW+DO within both timepoints.

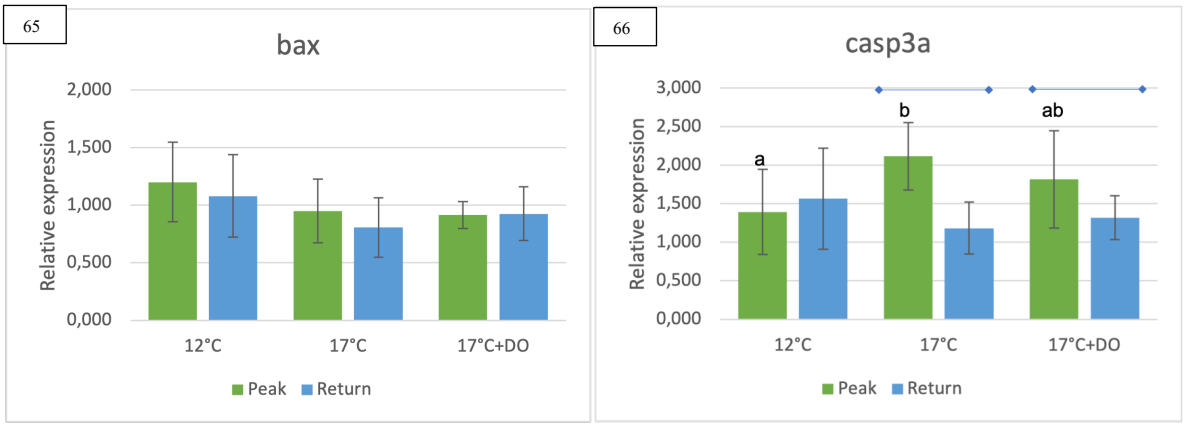

Figure 65 and 66: Relative expression of genes. 65: bax, 66: casp3a. Results presented as mean and ±std. The significant difference between the three treatment groups, within Return, is denoted by different letters (a, b). Significant differences within treatment group are presented with blue line.

3.3.4 Gene involved in the immune system

One gene involved in the immune system was included, *il8* (figure 67). The expression of this gene showed no significant difference within both treatment and timepoint.

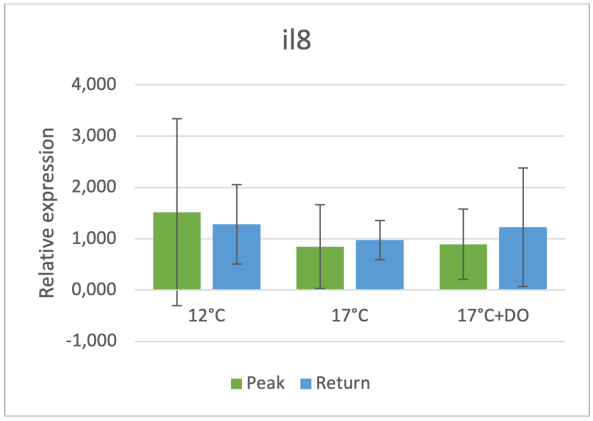

Figure 67: Relative expression of gene il8. Results presented as mean and ±std.

The transcriptional changes were summarized in table 8, with an overview of changes in expression of the genes, from Peak to Return, within each treatment group. Up-regulation from Peak to Return is presented as green arrow pointing up, while down-regulation is presented as blue arrow pointing down. No change between Peak and Return is exhibited as a horizontal red arrow. The groups which showed significant difference within timepoint and/or treatment are marked with a star.

Table 8: Overview of changes in expression of genes. Within each treatment, from Peak to Return; green arrow up indicates upregulation, blue arrow down indicates downregulation, red horizontal arrow indicates no change. Standard deviation was not considered. A star indicates significant difference. In left column, each grey-tone contains genes with same area of function.

	Control	HW	HW+DO
Ndufa1	↑ ★	↓ ★	↑
Ndufa4	↑	↑	↓
Pdk3	↓	↓ ★	↓
pk	↓ ★	↓ ★	→ ★
Hsp70	↓	↑	↑
gp	↓ ★	↓	↓
cat	↑ ★	↓ ★	↓ ★
mnSOD	↓ ★	↓ ★	↑
Cu_znSOD	→	↓	↓
bax	↓ ★	↓ ★	→ ★
Casp3a	↑ ★	↓ ★	↓ ★
Il8	↓	↑	↑

4 Discussion

The aim of this study was to evaluate how elevated temperature in combination with reduced oxygen affected Atlantic salmon liver. Atlantic salmon has an predicted optimal growth around 14°C (Handeland et al., 2008; Hevrøy et al., 2013; Hevrøy et al., 2012), and growth is expected to be reduced if temperature increase above 17°C (Handeland et al., 2000; Kullgren et al., 2013). However, there is uncertainty regarding the preferred thermal range for post smolts (table 4.1.1-1 in (Noble et al., 2018)). In addition, the growth rate of Atlantic salmon may be further reduced if exposed to multiple stressors and compounding factors, such as production procedures like crowding and chasing (McCormick et al., 1998), and reduced oxygen (Olsvik et al., 2013). When fish experience hypoxia, literature shows that this firstly affects the food consumption and the growth of the fish, and later the fish need to proceed anaerobe metabolism. The fish will also experience stress in this situation, and the health- and welfare of the fish might be drastically reduced (Remen et al., 2013). This is in line with our study, where the fish exposed to multiple stressors, high temperature and reduced dissolved oxygen, had the lowest growth-related results. Further, results showed morphological and cellular changes in the liver that may affect the homeostatic balance in the fish, thus might cause reduced health and welfare.

4.1 Operational welfare indicators

Fish from both Control and HW showed a significant difference in average individual weight over time. Fish from the HW+DO regime had the lowest average weight and length compared to the other treatments and no significant increase in weight was recorded after temperature was reduced to 12ºC.

Thermal physiologists have concluded that higher temperatures can result in an increased oxygen demand (Clarke, 2003). This is linked to an increase in the basic maintenance cost, which further reduces the total scope for aerobic performance, thereunder an increase in energic needs for survival (Johansen & Jones, 2011; Pörtner & Farrell, 2008). Additionally, this can result in reduced metabolic performance, such as growth, reproduction and immune functions, due to lack of energy caused by reallocation of energy (Pörtner & Farrell, 2008). Since fish

from the HW group, exposed to the same temperature as HW+DO, showed a significant increase in both weight and length after temperature was changed, it could be possible that the weight gain in HW+DO may be hampered by increased demand for oxygen. However, there was no significant differences between treatments at each time point, that can be caused by a variance in individual weight recorded for all groups. If the trial was held over a longer period (exposure to several HWs) and/or weight of more fish was included in the study, the negative effects of combined HW+DO might become visible. Further, the trends observed in this study could indicate that salmon can maintain growth during short periods of increased temperatures to 17 °C, but that growth may be hampered if additional stressors take place. Impaired growth can indicate an unbalance in the physiological demands of the fish, which is interesting in evaluating how combined stressors might affect the fish health- and welfare.

Evaluating the OWIs, fish from the HW+DO group had the highest scores indicating presence of more damage for all parameters measured, scale loss and gills. OWIs may give an indication on the fish welfare (Noble et al., 2018). A high score on skin loss indicates large areas of scale loss on the fish (Noble et al., 2018), and may indicate reduced welfare. Skin is the first line of defense systems in fish, and it is important that this barrier is intact (Sveen et al., 2020). Skin also has nociceptors, suggesting that skin damage may cause pain (Noble et al., 2018). Gills are highly important in maintaining optimal physiological conditions and health for the salmon, as well as their role in the immune system (Veterinærinstituttet, 2023). Reduced gill health may affect the entire physiology of the fish, due to the organ's role in gas exchange, osmoregulation, and excretion. A reduction in the effect of these functions, thus might lead to reduction in overall fish welfare- and health (Noble et al., 2018; Veterinærinstituttet, 2023).

4.2 Metabolism

In the scoring of histological sections, several morphological deviations were observed in liver from fish within the different temperature regimes. Fish within Control group had had the highest score for vacuolization within both Peak and Return. A high amount of vacuoles indicate the presence of adipocytes in liver tissue, further indicating higher presence of fat lipids in the tissue. Higher amount of fat lipids in liver might imply an excess/balance in energy supply, so that storing of fat can be proceeded. Earlier studies on liver exposed to elevated

temperatures has shown increased lipolysis in liver (Sur et al., 2019). This might explain the reduction in vacuoles between Peak HW+DO and Return HW+DO, where the fish were exposed to environmental stressors, thereunder increased temperature, further might resulting in increased metabolic rates (Hvas et al., 2017). The algorithm made in Aiforia® was not able to detect all vacuoles in the different sections and could therefore not confirm these results. There is a need for more training of the AI model before it can be used to detect liver vacuolization, including adding sections with different shades for AB/PAS staining, as well as different sizes of fish and different areas of the liver.

Detection of steatosis by the AI model showed significant difference within Return, where liver from the Control fish had decreased steatosis, while fish from HW and HW+DO showed increased level of steatosis. HW+DO seemingly had the most occurrence of steatosis. These results were supported in the second run using the AI model. In the second AI run, the four fish with drastically high level of steatosis were excluded to bring forward the differences within the other samples. Further, the results from the manual scoring of steatosis also exhibited results with significant difference within Return, where Control differed from HW and HW+DO with a lower average score. An earlier study done on human liver showed that some autoimmune liver diseases may lead to steatosis (Chentoufi et al., 2014). This provides important information that steatosis can develop correlated with disease, further, as indicated in our studies, steatosis might be stressed induced as well. The gene transcription provided results on genes connected to metabolism, but none of these where directly connected to lipolysis. In further evaluation of responses in liver to elevated temperatures, transcription of genes involved in lipolysis should be included.

The expression of genes connected to metabolism, thereunder *ndufa1, pdk3* and *pk*, resulted in significant differences. *Ndufa1* was significantly downregulated within Return HW compared to Control, which might indicate shortage of needed oxygen within HW. This, because of the role of *ndufa1* in the mitochondrial electron transport chain (Au et al., 1999). The gene ndufa1 codes for a subunit in Complex I of the electron transport chain, thus reduced expression of this gene indicates reduction in oxidative phosphorylating, further implying reduced level of oxygen, since the electron transport chain demands oxygen (Au et al., 1999; Boyer et al., 1977). Contrary, HW+DO had an upregulation of this gene from Peak to Return. *Pdk3* was in earlier studies upregulated in fish exposed to warm and normoxic environment, not in warm and hypoxic (Beemelmanns, Zanuzzo, Xue, et al., 2021). In contrary, another study gave upregulated expression of *Pdk3* within a fish group exposed to warm and hypoxic, compared

to control (Beemelmanns, Zanuzzo, Sandrelli, et al., 2021). Common for both is the upregulation in conjunction with fish exposed to higher temperatures. In this study, HW showed a downregulation in the expression of *Pdk3* from Peak to Return. *Pdk3* is a protein kinase, involved in glycolysis (ATP-dependent metabolic circle), which indicates a higher access to ATP within Peak. On the other hand, there was also a significant difference in expression of *pk*, within timepoint HW, might indicating lack of oxygen. *Pk* is a cAMP dependent kinase, thus a product of ATP converted to cyclic AMP (cAMP), further synthesis of ATP is dependent of oxidative phosphorylation (Ferguson & Boutilier, 1988; Hemmer et al., 1997). In Return, the fish had a significant decrease in expression of this gene. Contradictory, in Return the fish was no longer exposed to elevated temperature. Thus, the reduction could indicate stress response and problems with recovery after being exposed to an environmental stressor, and maybe the fish proceeded anaerobe metabolism. This is reflected by the significant difference within Return, between Control and HW. Control also was significantly different from HW+DO, where the expression of *pk* was lower in HW+DO. This reflects the reduced oxygen level in the environment of the fish, further imply that the fish experiences hypoxia. There was no significant difference within HW+DO between Peak and Return, but there is a slight increase of expression in Return, which can indicate some recovery.

There was no manual scoring done on glycogen and the detection of glycogen by the Aiforia® algorithm showed no significant differences. In an earlier study, increased levels of glycogen was observed when the fish was exposed to environmental stressors (Cardoso et al., 2019). Training the algorithm further to have more precise detection of glycogen may provide a better tool for understanding how the environmental stressors effect metabolism in salmon, since variation in the level of glycogen could be affected by elevated temperature.

4.3 Stress

In ectotherms, higher temperatures can increase the mitochondrial respiration, further resulting in accelerated mitochondrial ROS (reactive oxygen species) formation, which can lead to oxidative stress (Beemelmanns, Zanuzzo, Xue, et al., 2021). The expression of the genes involved in oxidative and cellular stress responses (*gp* and *cat*) showed significant difference in expression. *Catalase* (*Cat*) is an antioxidant enzyme, removing oxyradicals (ROS),

thereunder hydrogen peroxide, thus an important enzyme connected to oxidative stress as it is involved in maintenance of the redox balance in the immune system (Livingstone et al., 1993; Wang et al., 2012). *Cat* showed lower transcription at Return within HW and HW+DO compared to Control. Up- and down-regulations of *cat* can induce biological processes, since hydrogen peroxide are involved in sensing and signaling of several biological events, such as apoptosis (Matés et al., 1999; Wang et al., 2012). An earlier study on Atlantic salmon in marine water showed no results on expression of *cat* between control (12°C) and warm (20°C, 4 weeks exposure) (Beemelmanns, Zanuzzo, Sandrelli, et al., 2021), while another study done on *Onychostoma macrolepis* gave increased expression of *cat* when exposed to thermal stress (30°C) (Yu et al., 2017). *Glutathione peroxidase* (*gp*) had a significant difference within Control, with a decrease in expression from Peak to Return. The same pattern seemed to occur within HW and HW+DO. *Gp* codes for a major peroxide scavenging enzyme and is thus involved in prevention of oxidative stress (Miyamoto et al., 2003). The reduced expression in Control could indicate reduced oxidative stress in the liver, indicating internal balance between ROS and antioxidants that scavenge them. An earlier study on fish blood exhibited results on increased peroxidase activity when exposed to 12h of thermal stress (23°C) (Roche & Gérard, 1996). On the other hand, studies on some pathological animal models, for example rats, have shown an decreased GP activity in tissues were oxidative stress occurred (Miyamoto et al., 2003). Thus, the reduction in expression within Return HW and HW+DO do not necessarily indicate reduction in oxidative stress, however, may suggest an imbalance in the liver. Transcription of *mitochondrial superoxide dismutase* (*mnsod*) showed a trend within treatments between Control and HW, with a higher expression in Control. Fish from both Control and HW had a reduced expression of *mnsod* between Peak and Return, while HW+DO showed increased expression from Peak to Return. Activation of *mnsod* is important to prevent oxidative stress (Ozden et al., 2011), since the enzyme converts superoxide to hydrogen peroxide, which later can be converted to water by catalase and peroxidase. *Copper/zinc superoxide dismutase* (*Cu_Zn sod*) is another marker for oxidative stress response, specific for intracellular cytoplasmic compartments or extracellular elements (Zelko et al., 2002). Transcription levels of this gene showed no significant differences. Results from salmon exposed to chronic higher temperature (19°C, 45 days) showed a down-regulation in expression of both *mnsod* and *Cu_Zn sod* (Olsvik et al., 2013). This result was explained by the fact that higher temperature might reduce the overall metabolism, thereunder mitochondrial ROS production. Elevated temperature often increase oxygen consumption, further leading to increased ROS production,

which might result in oxidative stress (Heise et al., 2006; Olsvik et al., 2013). Transcription of genes involved in stress-responses are complex. For example, in this trial, fish exposed to thermal stress as single factor and fish exposed to combined stressors, had different regulation of several genes related to stress.

Transcription of *hsp70*, had a minor up-regulated trend at Return in both HW and HW+DO. In the regulation of cellular stress response in aquatic animals, HSPs are essential, as they play an important role in health, such as their function as molecular chaperones in maintenance of cell homeostasis (Basu et al., 2002; Roberts et al., 2010). They are involved in not only thermal stress, but also a high variety of other stressors, such as hypoxia. In an earlier study, Atlantic salmon exposed to 20°C and hypoxic conditions (~70% oxygen content in air) for three days, showed increased expression of *hsp70*, further might indicating increased level of cellular stress (Beemelmanns, Zanuzzo, Sandrelli, et al., 2021). The results within this trial imply the same trend, due to the increase within Return HW and Return HW+DO. Further, there was a decrease within Return Control, showing a trend where fish exposed to environmental stressors might experience imbalance within cell homeostasis.

The scoring of connective tissue exhibited results with significant difference within Return, between all three groups. Highest amount of connective tissue was observed in liver within HW and HW+DO, might indicating a beginning phase of *fibrosis*. *Fibrosis* is defined as an accumulation of connective tissue, such as overgrowth and hardening, and occurs in conjunction with chronic inflammation (Wynn, 2008). It is describes as a "wound-healing" reaction, and it is implied that oxidative stress can have impact on hepatic fibrogenesis (Poli, 2000). There are knowledge gaps when it comes to occurrence and development of fibrosis in Atlantic salmon liver. In rainbow trout, decreased connective tissue was found in hearts from fish at low temperatures (Vornanen et al., 2005), and increased connective tissue has been associated with chronic liver diseases in humans (Rauterberg et al., 1981). Within this trial, HW+DO had most detected connective tissue, followed by fish from the HW groups. Oxidative stress might have an impact on development of connective tissue (Poli, 2000), hence fish exposed to combined stressors might have increased chance of experience fibrosis. Thus, the increased connective tissue found in this study may reflect important mechanisms in the liver caused by stress and elevated temperatures.

4.4 Apoptosis

Programmed cell death, *apoptosis*, is an important regulation of the homeostatic balance and normal development of all multicellular organisms, where redundant or abnormal cells that are threatening to other cells can, with this type of cell suicide, be removed without affecting the neighbor cells (reviewed in (Takle & Andersen, 2007)). Caspases (cysteine-dependent aspartate proteases) are the key apoptotic factor, because they can cleave several vital cell-substrates (Cohen, 1997). *Casp3a* showed significant difference within Peak, between Control and HW, where HW had highest expression. HW+DO also had higher expression within Peak compared to Control. Increased transcription of *casp3* may indicate increased apoptotic activity when exposed to environmental stressors. The observed significant decreased transcription in both HW and HW+DO, from Peak to Return, might reflect a recovery of homeostatic balance. On the other hand, *bax* showed a trend within treatment, where Control had the highest expression in comparison with HW and HW+DO. *Bax* is involved in the modulation phase of apoptosis, and is a pro-apoptotic protein essential for completion of the apoptosis (Kanzler & Galle, 2000; Lalier et al., 2007). Contrasting with the results on expression of *casp3a*, this might indicate reduced apoptotic activity within the treatment groups HW and HW+DO, further might indicate homeostatic balance. Alternately, the fish experienced homeostatic imbalance, but the apoptotic activity was not prioritized as the exposure to thermal stress maybe increased the basic maintenance cost (Johansen & Jones, 2011; Pörtner & Farrell, 2008).

4.5 Melanin as an indicator of the immune system

There was no significant difference for the manual scoring of melanin, but the trend showed more melanin in livers from HW and HW+DO. This contrast between the two groups (HW, HW+DO) and Control might indicate differences connected to the immune response (Steinel & Bolnick, 2017). The digital scoring of melanin showed significant difference, supporting the trend from the manual scoring. This illustrates one of the benefits using digital detection in histology, digitalization may substantiate differences, especially when it comes to features that may be difficult to quantify manually. An overall view on the digital scoring exhibit highest score for HW (at both Peak and Return) and for HW+DO (Peak only). Fish exposed to chronic

heat stress have shown increased melanomacrophages in liver tissue (Hernández-López et al., 2018). Further, an increase of melanin within wounds and wound-healing, have been previously shown in comparative studies, like wound healing studies in Zebrafish (*Danio rerio*) (Lévesque et al., 2013). This builds on the connection between reduced fish health- and welfare and formation of melanin. Melanomacrophage centers contain a variety of highly pigmented phagocytes, such as melanin, that can neutralize free radicals and cation activity associated with oxidizing conditions (Bruno et al., 2013). In the presence of cachectic disease and injury, an increase in accumulation of melanin have been documented (Bruno et al., 2013). Melanomacrophages often gather in chronic, granulomatous inflammation, and their number might increase connected to chronic infection in fish, thus they are commonly used as a histological biomarker in fish immune response (Steinel & Bolnick, 2017). On the other hand, the role of melanomacrophages connected to modulating infections and the role in fish immunity is speculative, and its role in the adaptive immune system is still not confirmed (Bruno et al., 2013; Steinel & Bolnick, 2017). In this study, the highest detection of melanin spots in HW and HW+DO may indicate changes in the immune system and increased presence of melanomacrophages due to stress.

In this trial, one gene involved in the immune response, *il8*, was ran, but there was no significant difference within these results. In a study where Atlantic salmon, post-smolts, were exposed to elevated temperature and hypoxia, genes involved in immune response was not greatly affected until temperature reached 20°C (Beemelmanns, Zanuzzo, Sandrelli, et al., 2021). Including other immune-related genes could contribute to building further on the results from the histology.

4.6 Method

In this trial, a new digital algorithm was developed to detect the different components in liver tissue. Results from the final version developed showed several errors, indicating that the algorithm needs additional training. For example, the program had problems detecting micro vesicular fat and glycogen. Liver is a homogenous tissue that might result in difficulties for the algorithm in separating the different components, and differences between the staining on the slides (expression of color) and variation between tissues (etc. steatosis) makes the process in

developing a well working algorithm more difficult. Failure to detect these features may lead to uncertainties in the AI-results. On the other hand, the errors done by the algorithm may be similar through all slides, thus provide a correct indication of ratio and difference between the slides. For some features, such as melanin, there were no errors in detection. More training of the algorithm led to higher accuracy on all components, and further training that includes liver from e.g., other fish trials, fish size etc., will lead to a higher accuracy. In this trial, approximately 80 hours of drawing was done in the training of the liver algorithm, and the training exhibited results in the accuracy in detecting the different components. However, detailed data on tissue components, such as amount, ratio and correlation, can be accessed through this digital scoring. As shown here, digital histology can provide studies with a high level of information on liver. Tools like this may be useful in the evaluation on how climate change effect the liver of the fish, as changes may be difficult to observe using traditional histology.

4.7 Conclusion and further research

This trial provided insight on the effect climate related environmental stressors have on salmon liver. External signs, thereunder growth and OWIs, implied reduced fish welfare within the group HW+DO. The vital functions in liver, such as metabolism, stress-response, apoptosis, and immune-response, showed variation in response when exposed to the different stressors. Fish exposed to fluctuating temperature as a single stressor and fish exposed to combined stressors differed from the Control group in several of the approaches used in the trial.

There were signs of imbalance in the metabolism of the fish in HW and HW+DO, with decreased expression of several genes involved in metabolism, as well as lower level of vacuoles, while the level of steatosis was increased. Regarding stress-response, there was no clear trends within the expressions of the different stress-related genes, but the general trend was highest expression in Control. This might be explained by a general down-regulation of genes in fish exposed to thermal stress, thereunder metabolic processes within the mitochondria, that further might result in reduced level of oxidative stress. Additionally, the difference within amount of connective tissue between Control and the two other groups (HW and HW+DO), reflects a reaction in liver exposed to environmental stressors, outside the

normal. Increased production of connective tissue can indicate imbalance within the fish, as a protective mechanism in order to maintain homeostatic balance. The significant difference between HW and HW+DO regarding connective tissue, provides important data showing dissimilarities between liver exposed to a single stressor and those exposed to combined stressors. The results connected to apoptotic response had contrasts that brought uncertainty, but there were results indicating increased activity within the groups exposed to environmental stress. Further, the results showed a potential recovery within these groups. The highest detection of melanomacrophages were within HW and HW+DO, which might indicate changes in the immune system, as well their role as antioxidants connected to oxidative stress, of fish exposed to environmental stressors.

Involving transcription of other genes, as well as adding histopathologic scorings, such as necrosis and immune cells, can provide further insight on how environmental stressors affect the vital functions in the liver. Additionally, implementing other analysis methods, such as microarray and/or RNA sequencing, can contribute to a greater understanding of all transcripts. Continuing the development of the liver algorithm in the Aiforia® platform, can result in a highly useful tool in further evaluation on how climate change, and other treatments and stressors, affects the Atlantis salmon liver.

In conclusion, exposing fish to thermal stress, as well as lowered level of dissolved oxygen, resulted in cellular differences and morphological changes in the liver of Atlantic salmon. It is shown that fluctuating temperature and reduced oxygen levels had compounding effects on the Atlantic salmon, thereunder holistically signs of reduced fish health- and welfare. There is a need for further studies in order to generate more knowledge on how climate related stressor effect the Atlantic salmon, and to understand the biological effects of the changes observed in this study.

References

(IPCC), I. P. o. C. C. (2023). AR6 Synthesis Report - Climate Change 2023. https://report.ipcc.ch/ar6syr/pdf/IPCC_AR6_SYR_LongerReport.pdf

Adams, A. (2019). Progress, challenges and opportunities in fish vaccine development. *Fish and Shellfish Immunology*, 210-214. https://doi.org/10.1016/j.fsi.2019.04.066

Agius, C., & Roberts, R. (2003). Melano‐macrophage centres and their role in fish pathology. *Journal of fish diseases*, *26*(9), 499-509.

aiforia.com. *aiforia*. https://www.aiforia.com

Au, H. C., Seo, B. B., Matsuno-Yagi, A., Yagi, T., & Scheffler, I. E. (1999). The NDUFA1 gene product (MWFE protein) is essential for activity of complex I in mammalian mitochondria. *Biochemistry*, *96*, 4354-4359. https://doi.org/10.1073/pnas.96.8.4354

Bancroft, J. D., & Stevens, A. (1990). *Theory and Practice of Histological Techniques*.

Bankhead, P., Loughrey, M. B., FERNÁNDEZ, J. A., DOMBROWSKI, Y., MCART, D. G., DUNNE, P. D., MCQUAID, S., GRAY, R. T., MURRAY, L. J., COLEMAN, H. G., JAMES, J. A., SALTO-TELLEZ, M., & HAMILTON, P. W. (2017). *QuPath: Open source software for digital pathology image analysis.* . In Scientific Reports.

Basu, N., Todgham, A. E., Ackerman, P. A., Bibeau, M. R., Nakano, K., Schulte, P. M., & Iwama, G. K. (2002). Heat shock protein genes and their functional significance in fish. *An international journal on genes and genomes*, *295*, 173-183. https://doi.org/10.1016/S0378-1119(02)00687-X

Beemelmanns, A., Zanuzzo, F. S., Sandrelli, R. M., Rise, M. L., & Gamperl, A. K. (2021). The Atlantic salmon´s stress- and immune-related transcriptional responses to moderate hypoxia, an incremental temperature increase, and these challenges combined. *G3*, *11*(7). https://doi.org/10.1093/g3journal/jkab102

Beemelmanns, A., Zanuzzo, F. S., Xue, X., Sandrelli, R. M., Risa, M. L., & Gamperl, A. K. (2021). The transcriptomic responses of Atlantic salmon (Salmo salar) to high temperature stress alone, and in combination with moderate hypoxia. *BMC genomics*. https://doi.org/10.1186/s12864-021-07464-x

Boyer, P. D., Chance, B., Ernster, L., Mitchell, P., Racker, E., & Slater, E. C. (1977). Oxidative phosphorylation and photophosphorylation. *Annual review of biochemistry*, *46*, 955-966. https://doi.org/10.1146/annurev.bi.46.070177.004515

Breitburg, D., Levin, L. A., Oschlies, A., Grégorie, M., Chavez, F. P., Conley, D. J., Garcon, V., Gilbert, D., Gutiérrez, D., Isensee, K., Jacinto, G. S., Limburg, K. E., Montes, I., Naqvi, S. W. A., Pitcher, G. C., Rabalais, N. N., Roman, M. R., Rose, K. A., Seibel, B. A., . . . Zhang, J. (2018). Declining oxygen in the global ocean and coastal waters. *Breitburg et al., Science*, *359*(6371). https://doi.org/10.1126/science.aam7240

Bruno, D. W., Noguera, P. A., & Poppe, T. T. (2013). *A Colour Atlas of Salmonid Diseases* (Second edition ed.). Springer.

Bruslé, J., & Anadon, G. G. i. (1996). The Structure and Function of Fish Liver. In *Fish Morphology*.

Burge, C. A., Eakin, C. M., Friedman, C. S., Froelich, B., Hershberger, P. K., Hofmann, E. E., Petes, L. E., Prager, K. C., Weil, E., Willis, B. L., Ford, S. E., & Harvell, C. D. (2014). Climate Change influendes on Marine Infectious Diseases: Implications for Management and Society. *Annual Review of Marine Science 6*, 249-277. https://doi.org/10.1146/annurev-marine-010213-135029

Cardoso, P. G., Resende-de-Oliveira, R., & Rocha, E. (2019). Combined effects of increased temperature and levonorgestrel exposure on zebrafish female liver, using stereology and immunohistochemistry against catalase, CYP1A, HSP90 and vitellogenin. *Environmental Pollution*, *252*, 1059-1067. https://doi.org/10.1016/j.envpol.2019.06.058

Chentoufi, A. A., Serov, Y. A., Alazmi, M., & Baba, K. (2014). Immune Components of liver Damage Associated with Connective Tissue Diseases. *Journal of Clinical and Translational Hepatology*, 37-44. https://doi.org/10.14218%2FJCTH.2014.00001

Chiang, J. Y. L. (2009). Bile acids: regulation of synthesis. *Journal of Lipid Research*, *50*. https://doi.org/10.1194/jlr.R900010-JLR200

Clarke, A. (2003). Costs and consequences of evolutionary temperature adaption *TRENDS in Ecology and Evolution*, *18*. https://doi.org/0.1016/j.tree.2003.08.007

Cohen, G. M. (1997). Caspases: the executioners of apoptosis. *Biochemical Journal*, *326*, 1-16.

Emhoff, C.-A. W., Messonnier, L. A., Horning, M. A., Fattor, J. A., Carlson, T. J., & Brooks, G. A. (2013). Gluconeogenesis and hepatic glycogenolysis during exercise at the lactate threshold. 297-428. https://doi.org/10.1152/japplphysiol.01202.2012

Exton, J. H. (1972). Gluconeogenesis. *Metabolism*, *21*(10), 945-990. https://doi.org/10.1016/0026-0495(72)90028-5

Falconer, L., Telfer, T. C., Angus, G., Hermansen, Ø., Mikkelsen, E., Hjøllo, S. S., McAdam, B. J., & Ytteborg, E. (2022). Insight into real-world complexities is required to enable effective response from the aquaculture sector to climate change. https://doi.org/10.1371/journal.

FAO. (2020). *The State of World Fisheries and Aquaculture 2020, sustainbility in action* https://doi.org/10.4060/ca9229en

FAO. (2021). *FAO´s work on climate change - Fisheries and aquaculture 2020* https://doi.org/10.4060/cb3414en

Ferguson, R. A., & Boutilier, R. G. (1988). Metabolic energy production during adrenergic pH regulation in red cells of the Atlantic salmon, Salmo salar. *Respiration Physiology*, *74*(1), 65-75. https://doi.org/10.1016/0034-5687(88)90141-7

Frölicher, T. L., Fischer, E. M., & Gruber, N. (2018). Marine heatwaves under global warming. *Springer Nature Limited*, *560*. https://doi.org/10.1038/s41586-018-0383-9

Grefsrud, E. S., Andersen, L. B., Bjørn, P. A., Grøsvik, B. E., Hansen, P. K., Husa, V., Karlsen, Ø., Kvamme, B. O., Samuelsen, O. B., & Sandlund, N. (2022). Risikorapport norsk fiskeoppdrett 2022-risikovurdering—Effekter på miljø og dyrevelferd i norsk fiskeoppdrett. *Rapport fra havforskningen*.

Guillot, A., & Tacke, F. (2019). Liver Macrophages: Old Dogmas and New Insight. *Hepatology communications*, *3*. https://doi.org/10.1002/hep4.1356

Handeland, S. O., Berge, Å., Björnsson, B. T., Lie, Ø., & Stefansson, S. O. (2000). Seawater adaption by out-of-season Atlantic salmon (Salmo salar L.) smolts at different temperatures. *Aquaculture*, *181*, 377-396. https://doi.org/10.1016/S0044-8486(99)00241-0

Handeland, S. O., Imsland, A. K., & Stefansson, S. O. (2008). The effect of temperature and fish size on growth, feed intake, food conversion efficiency and stomack evacuation rate of Atlantic salmon post-smolts. *Aquaculture*, *283*, 36-42. https://doi.org/10.1016/j.aquaculture.2008.06.042

Heise, K., Puntarulo, S., Nikinmaa, M., Abele, D., & Pörter, H.-O. (2006). Oxidative stress during stressful heat exposure and recovery in the North Sea eelpout Zoarces viviparus L. *Journal of Experimental Biology 209*(2), 353-363. https://doi.org/10.1242/jeb.01977

Hemmer, W., McGlone, M., Tsigelny, I., & Taylor, S. S. (1997). Role of the Glycine Triad in the ATP-binding Site of cAMP-dependent Protein Kinase. *Protein Chemistry and Structure*, *272*(27). https://doi.org/10.1074/jbc.272.27.16946

Hernández-López, J. R., Hernández-Rodríguez, Rivas-Manzano, P., & Bückle-Ramirez, L. F. (2018). Thermal Effect of Acute and Chronic Stress on Hepatic and Renal Tissue of the Pacific Sardine, Sardinops sagax caeruleus. *International Journal of Morphology*, *36*(1), 212-220.

Hevrøy, E. M., Hunskår, C., Gelder, S. d., Shimizu, M., Waagbø, R., Breck, O., Takle, H., Sussort, S., & Hansen, T. (2013). GH-IGF system of attenuated muscle growth and lipolysis in Atlantic salmon reared at elevated sea temperatures. *J Comp Physiol B*, *183*, 243-259. https://doi.org/10.1007/s00360-012-0704-5

Hevrøy, E. M., Waagbø, R., Torstensen, B. E., Takle, H., Stubhaug, I., Jørgensen, S. M., Torgersen, T., Tvenning, L., Susort, S., Breck, O., & Hansen, T. (2012). Ghrelin is involved in voluntary anorexia in Atlantic salmon raised at elevated sea temperatures. *General and Comparative Endocrinology*, *175*, 118-134. https://doi.org/10.1016/j.ygcen.2011.10.007

Hvas, M., Folkedal, O., Imsland, A., & Oppedal, F. (2017). The effect of thermal acclimation on aerobic scope and critical swimming speed in Atlantic salmon, Salmo salar. *Journal of Experimantal Biology*, *220*, 2757-2764. https://doi.org/10.1242/jeb.154021

Iversen, A., Asche, F., Hermansen, Ø., & Nystøyl, R. (2020). Production cost and competitivitiveness in major salmon farming countries 2003-2018. *Aquaculture*, *522*. https://doi.org/10.1016/j.aquaculture.2020.735089

Jin, Y., Chen, R., Liu, W., & Fu, Z. (2010). Effect of endocrine disrupting chemicals on the transcription of genes related to the innate immune system in the early developmental stage of zebrafish (Danio rerio). *Fish & Shellfish Immunology*, *28*(5-6), 854-861. https://doi.org/10.1016/j.fsi.2010.02.009

Johansen, J. L., & Jones, G. P. (2011). Increasing ocean temperature reduces the metabolic performance and swimming ability of coral refef samselfishes. *Global Change Biology*, *17*(9), 2971-2979. https://doi.org/https://doi.org/10.1111/j.1365-2486.2011.02436.x

Kanzler, S., & Galle, P. R. (2000). Apoptosis and the liver *Cancer Biology*, *10*, 173-184. https://doi.org/10.1006/scbi.2000.0318

Kiron, V. (2011). Fish immune system and its nutritional modulation to preventive health care. *Animal Feed Science and Technology*, 111-133. https://doi.org/10.1016/j.anifeedsci.2011.12.015

Kristjánsson, Ó. H., Gjerde, B., Ødegård, J., & Lillehammer, M. (2020). Quantitative Genetics of Growth Rate and Filet Quality Traits in Atlantic Salmon Inferred From a Longitudinal Bayesian Model for the Lefs-Censored Gaussian Trait Growth Rate. *Frontiers in Genetics*, *11*. https://doi.org/10.3389/fgene.2020.573265

Kryvi, H., & Poppe, T. (2016). *Fiskeanatomi*. Fagbokforlaget.

Kullgren, A., Jutfelt, F., Fontanillas, R., Sundell, K., Samuelsson, L., Wiklander, K., Kling, P., Koppe, W., Larsson, D. G. J., Björnsson, B. T., & Jönsson, E. (2013). The impact of temperature on the metabolome and endocrine metabolic signals in Atlantic salmon (Salmo salar). *Comparative Biochemistry and Physiology*, *164*, 44-53. https://doi.org/10.1016/j.cbpa.2012.10.005

Lalier, L., Cartron, P.-F., Juin, P., Nedelkina, S., Manon, S., Bechinger, B., & Vallette, F. M. (2007). Bax activation and mitochondrial insertion during apoptosis. *Apoptosis*, *12*, 887-896. https://doi.org/10.1007/s10495-007-0749-1

Lévesque, M., Heng, Y., Jones, R. A., & Martin, P. (2013). Inflammation drives wound hyperpigmentation in zebrafish by recruiting pigment cells to sites of tissue damage. *Disease Models & Mechanisms*, *6*, 508-515. https://doi.org/10.1242%2Fdmm.010371

Livingstone, D. R., Lemaire, P., Matthews, A., Peters, L., Bucke, D., & Law, R. J. (1993). Pro-oxidant, Antioxidant and 7-Ethoxyresorufin O-Deethylase (EROD) Activity Responses in Liver of Dab (Limanda limanda) Exposed to Sediment Contaminated with Hydrocarbons and Other Chemicals. *Marine Pollution Bulletin*, *26*, 602-606. https://doi.org/10.1016/0025-326x(93)90498-9

Matés, J. M., Pérez-Gómez, C., & Castro, I. N. D. (1999). Antioxidant Enzymes and Human Diseases. *Clinical Biochemistry*, *32*, 595-603. https://doi.org/10.1016/S0009-9120(99)00075-2

McBryan, T. L., Anttila, K., Healy, T. M., & Schulte, P. M. (2013). Responses to Temperature and Hypoxia as Interacting Stressors in Fish: Implications for Adaptation to Environmental Change. *Integrative and Comparative Biology*, *53*, 648-659. https://doi.org/10.1093/icb/ict066

McCormick, S. D., Shrimpton, J. M., Carey, J. B., O´Dea, M. F., Sloan, K. E., Moriyama, S., & Björnsson, B. T. (1998). Repeated acute stress reduces growth rate of Atlantic salmon parr and alters plasma levels of growth hormone, insuline-like growth factor I and cortisol. *Aquaculture*, *168*, 221-235. https://doi.org/10.1016/S0044-8486(98)00351-2

Mills, K. E., Pershing, A. J., Brown, C. J., Chen, Y., Chiang, F.-S., Holland, D. S., Lehuta, S., Nye, J. A., Sun, J. C., Thomas, A. C., & Wahle, R. A. (2023). Fisheries Management in a Changing Climate: Lessons from the 2012 Ocean Heat Wave in the Northwest Atlantic. *Oceanography Society*, *26*, 191-195. https://doi.org/10.5670/oceanog.2013.27

Miyamoto, Y., Koh, Y. H., Park, Y. S., Fujiwara, N., Sakiyama, H., Misonou, Y., Ookawara, T., Suzuki, K., Honke, K., & Taniguchi, N. (2003). Oxidative Stress Caused by Inactivation of Glutathione Peroxidase and Adaptive Responses. *Biological Chemistry*, *384*, 567-574. https://doi.org/10.1515/BC.2003.064

Newfoundland, F. a. M. I. o. M. U. o. (2020). A Review of the 2019 Newfoundland and Labrador South Coast Cultured Atlantic Salmon Mortality Event. https://www.gov.nl.ca/ffa/files/publications-pdf-2019-salmon-review-final-report.pdf

Nilsson, J., Gismervik, K., Nielsen, K. V., Iversen, M. H., Noble, C., Kolarevic, J., Frotjold, H., Nilsen, K., Wilkinson, E., Klakegg, B., Hauge, H. S., Sæther, P. A., Kristiansen, T., & Stien, l. H. (2022). *LAKSVEL - Standardisert operasjonell velferdsovervåking for laks i matfiskanlegg* (Rapport fra havforskningen, Issue.

Noble, C., Gismervik, K., Iversen, M. H., Kolarevic, J., Nilsson, J., Stien, L. H., & Turnbull, J. F. (2018). *Welfare Indicators for farmed Atlantic salmon: tools for assessing fish welfare*

Nuez-Ortín, W. G., Carter, C. G., Nichols, P. D., Cooke, I. R., & Wilson, R. (2018). Liver proteome response of pre-harvest Atlantic salmon following exposure to elevated temperature. *BMC genomics*, *19*(1), 1-13. https://doi.org/10.1186/s12864-018-4517-0

Oliver, E. C. J., Benthuysen, J. A., Darmaraki, S., Donat, M. G., Hobday, A. J., Holbrook, N. J., Schlegel, R. W., & Gupta, A. S. (2021). Marine Heatwaves. *Annual Review of marine Science*, *13:313-342*. https://doi.org/10.1146/annurev-marine-032720-095144

Oliver, E. C. J., Donat, M. G., Burrows, M. T., Moore, P. J., Smale, D. A., Alexander, L. V., Bnthuysen, J. A., Feng, M., Gupta, A. S., Hobday, A. J., Holbrook, N. J., Perkins-Kirkpatrick, S. E., Scannell, H. A., Straub, S. C., & Wernberg, T. (2018). Longer and more frequent marine heatwaves over the past century. https://doi.org/10.1038/s41467-018-03732-9

Olsvik, P. A., Vikeså, V., Lie, K. K., & Hevrøy, E. M. (2013). Transcriptional responses to temperature and low oxygen stress in Atlantic salmon studied with next-generation sequencing technology. *BMC genomics*. https://doi.org/10.1186/1471-2164-14-817
Ozden, O., Park, S.-H., Kim, H.-S., Jiang, H., Coleman, M. C., Spitz, D. R., & Gius, D. (2011). Acetylation of MnSOD directs enzymatic activity responding to cellular nutrient status or oxidative stress. *Aging (Albany NY)*, *3*, 102-107. https://doi.org/10.18632%2Faging.100291
Paulsen, S. M., Lunde, H., Engstad, R., E., & Robertsen, B. (2003). In vivo effects of B-glucan and LPS on regulation of

lysozyme activity and mRNA expression in Atlantic

salmon (Salmo salar L.). *Fish & Shellfish Immunology*, *14*, 39-54. https://doi.org/10.1006/fsim.2002.0416
Pitcher, T. J., & Lam, M. E. (2015). Fish commoditization and the historical origins of catching fish for profit. https://doi.org/10.1186/s40152-014-0014-5 (Springer)
Poli, G. (2000). Pathogenesis of liver fibrosis: role of oxidative stress. *Molecuar Aspects of Medicine*, *21*(3), 49-98. https://doi.org/10.1016/S0098-2997(00)00004-2
Pörtner, H. O., & Farrell, A. P. (2008). Physiology and Climate Change. *Science*, *322*(5902), 690-692. https://doi.org/10.1126/science.1163156
Rabalais, N. N., Cai, W.-J., Carstensen, J., Conley, D. J., Fry, B., Hu, X., Quiñones-Rivera, Z., Rosenberg, R., Slomp, C. P., Turner, R. E., Voss, M., Wissel, B., & Zhang, J. (2014). Eutrophication-Driven Deoxygenation in the Coastal Ocean. *The official magazine of the oceanography society, Oceanography*, *27*, 172-183. https://doi.org/10.5670/oceanog.2014.21
Raina, S., Sachar, A., & Gupta, K. (2015). Temperature fluctuations induced histopathological alterations in the liver of fish, Labeo boga inhabiting Jammu waters. *International Journal of Fisheries and Aquatic Studies*, *2*, 12-16. https://www.fisheriesjournal.com/archives/2015/vol2issue4/PartA/2-3-60.pdf
Rauterberg, J., Voss, B., Pott, G., & Gerlach, U. (1981). Connective Tissue Components of the Normal and Fibrotic Liver. *Klin Wochenschr*, *59*, 767-779. https://doi.org/10.1007/bf01724682
Rembold, C. M. (2004). The Health benefits of Eating Salmon. *305*(5683). https://doi.org/10.1126/science.305.5683.475b
Remen, M., Oppedal, F., Stien, L. H., Torgersen, T., & Olsen, R. E. (2013). Får oppdrettslaks nok oksygen?
Richards, J. G. (2009). Chapter 10 Metabolic and Molecular Responses of Fish to Hypoxia In *Fish Physiology: Hypoxia* (Vol. 27, pp. 443-485). https://doi.org/10.1016/S1546-5098(08)00010-1
Roberts, R. J., Agius, C., Saliba, C., Bossier, P., & Sung, Y. Y. (2010). Heat shock proteins (chaperones) in fish and shellfish and their potential role in relation to fish health: a review. *Journal of fish diseases*, *33*(10), 789-801. https://doi.org/10.1111/j.1365-2761.2010.01183.x
Roche, H. e., & Gérard, B. (1996). Fish Blood Parameters as a Potential Tool for Identification of Stress Caused by Environmental Factors and Chemical Intoxication. *Marine Environmental Research*, *41*, 27-43. https://doi.org/10.1016/0141-1136(95)00015-1
Saurabh, S., & Sahoo, P. K. (2008). Lysozyme: an important defence molecule of fish innate immune system. *Aquaculture Research*, *39*, 223-239. https://doi.org/10.1111/j.1365-2109.2007.01883.x

Scheffers, B. R., De Meester, L., Bridge, T. C., Hoffmann, A. A., Pandolfi, J. M., Corlett, R. T., Butchart, S. H., Pearce-Kelly, P., Kovacs, K. M., & Dudgeon, D. (2016). The broad footprint of climate change from genes to biomes to people. *Science*, *354*(6313), aaf7671. https://doi.org/10.1126/science.aaf7671

Selmi, C., Mackay, I. R., & Gershwin, M. E. (2007). The Immunological Milieu of the Liver. *Seminars in Liver Disease*, *27*(2), 129-139. https://doi.org/10.1055/s-2007-979466

Shi, K.-P., Dong, S.-L., Yan-Gen, Z., Li, Y., Gao, Q.-F., & Sun, D.-J. (2019). RNA-seq reveals temporal differences in the transcriptome response to acute heat stress in the Atlantic salmon (Salmo salar). *Comparative Biochemistry and Physiology - Part D*, *30*. https://doi.org/10.1016/j.cbd.2018.12.011

Sjømatråd, N. (2021). *Markedsinnsikt*. https://seafood.no/markedsinnsikt/nokkeltall/

Steinel, N. C., & Bolnick, D. I. (2017). Melanomacrophage Centers As a Histological Indicator of Immune Function in Fish and Other Poikilotherms. *frontiers in Immunology*, *8*. https://doi.org/10.3389/fimmu.2017.00827

Sur, S., Sharma, A., Trivedi, A. K., Bhardwaj, S. K., & Kumar, V. (2019). Temperature affects liver and muscle metabolism in photostimulated migratory redheaded buntings (Emberiza bruniceps). *Journal of Comparative Physiology B*. https://doi.org/10.1007/s00360-019-01229-5

Sveen, L., Karlsen, C., & Ytteborg, E. (2020). Mechanical induced wounds in fish - a review on models and healing mechanisms. *Reviews in Aquaculture*, *12*(4), 2446-2465. https://doi.org/10.1111/raq.12443

Sveen, L., Timmerhaus, G., Johansen, L.-H., & Ytteborg, E. (2021). Deep neural network analysis - a paradigm shift for histological examination of health and welfare of farmed fish. *Aquaculture*, *532*. https://doi.org/10.1016/j.aquaculture.2020.736024

Takle, H., & Andersen, Ø. (2007). Caspases and apoptosis in fish. *Journal of Fish Biology*, *71*, 326-349. https://doi.org/10.1111/j.1095-8649.2007.01665.x

Thorstad, E. B., Bliss, D., Breau, C., Damon-Randall, K., Sundt-Hansen, L. E., Hatfield, E. M. C., Horsburgh, G., Hansen, H., Maoiléidigh, N. Ó., Sheehan, T., & Sutton, S. G. (2021). Atlantic salmon in a rapidly changing environment- Facing the challanges of reduced marine survival and climate change. https://doi.org/10.1002/aqc.3624

Tilseth, S., Hansen, T., & Møller, D. (1991). Historical development of salmon culture. *Aquaculture*, *98*(1-3), 1-9. https://doi.org/10.1016/0044-8486(91)90367-G

Verspoor, E., Strandmeyer, L., & Nielsen, J. L. (2007). *The Atlantic Salmon*

Genetics, Conservation and Management. Blackwell Publishing Ltd. https://doi.org/10.1002/9780470995846

Veterinærinstituttet. *Lakelus*. https://www.vetinst.no/sykdom-og-agens/lakselus

Veterinærinstituttet. (2023). Fiskehelserapporten 2022.

Vornanen, M., Hassinen, M., Koskinen, H., & Krasnov, A. (2005). Steady-state effects of temperature acclimation on the transcriptome of the rainbow trout heart. *American Journal of Physiology- Regulatory, Integrative and Comparative Physiology*, *289*(4), R913-R1231. https://doi.org/10.1152/ajpregu.00157.2005

Wake, K., & Sato, T. (2015). «The Sinusoid» in the Liver: Lessons Learned from the Original Definition by Charles Sedwick Minot (1900). *The Anatomical Record 298*(12), C1, 1969-2150. https://doi.org/10.1002/ar.23263

Wang, C., Yue, X., Lu, X., & Liu, B. (2012). The role of catalase in the immune respomse to oxidative stress and pathogen challenge in the clam Meretrix meretrix. *Fish & Shellfish Immunology*, *34*, 91-99. https://doi.org/10.1016/j.fsi.2012.10.013

Webb, J., Verspoor, E., Aubin-Horth, N., Romakkaniemi, A., & Amiro, P. (2007). The Atlantic salmon. In *The Atlantic salmon: genetics, conservation and management* (Vol. 1, pp. 17-56). https://doi.org/10.1002/9780470995846.ch2

Wynn, T. (2008). Cellular and molecular mechanisms of fibrosis. *The Journal of Pathology*, *214*(2), 199-210. https://doi.org/10.1002/path.2277

Yu, H., Deng, W., Zhang, D., Gao, Y., Yang, Z., Shi, X., Sun, J., Zhou, J., & Ji, H. (2017). Antioxidant defenses of Onychostoma macrolepis in response to thermal stress: Insight from mRNA expression and activity of superoxide dismutase and catalase. *Fish & Shellfish Immunology*, *66*, 50-61. https://doi.org/10.1016/j.fsi.2017.04.027

Zechner, R., Strauss, J. G., Haemmerle, G., Achim, L., & Zimmermann, R. (2005). Lipolysis: pathway under construction. *Lipid metabolism*, 333-340. https://doi.org/10.1097/01.mol.0000169354.20395.1c

Zelko, I. N., Maiani, T. J., & Folz, R. J. (2002). Superoxide dismutase multigene family: a comparison of the Cu-Zn-SOD (SOD1), Mn-SOD (SOD2), and EC-SOD (SOD3) gene structures, evolution and expression. *Free Radical Biology and Medicine*, *33*(3), 337-349. https://doi.org/10.1016/S0891-5849(02)00905-X